

Institut für Theoretische Physik
Fachrichtung Physik
Fakultät Mathematik und Naturwissenschaften
der Technischen Universität Dresden

**Quasiparticle description of QCD
thermodynamics:
effects of finite widths, Landau damping
and collective excitations**

Diplomarbeit
zur Erlangung des akademischen Grades
Diplom-Physiker

vorgelegt von
Robert Schulze
geboren am 15. Oktober 1981 in Dresden

Dresden 2007



Eingereicht am 29.06.2007

1. Gutachter: Prof. Dr. R. Schmidt
2. Gutachter: Prof. Dr. B. Kämpfer

Kurzfassung:

Die Beschreibung der thermodynamischen Eigenschaften eines heißen Plasmas stark wechselwirkender Materie ist von großer Bedeutung in verschiedenen Feldern der Physik, wie der Astrophysik, der Kosmologie und der Physik der Schwerionenkollisionen. Das Quasiteilchenmodell, welches auf Quark- und Gluonfreiheitsgraden basiert, wurde entwickelt, um die Thermodynamik eines solchen Plasmas zu beschreiben.

In dieser Diplomarbeit wird das Quasiteilchenmodell mit Hilfe des CJT-Formalismus mit einem Zwei-Loop-Funktional Γ_2 systematisch unter Einbeziehung von Effekten endlicher Breiten, Dämpfungsmechanismen, insbesondere Landau-Dämpfung, und kollektiver Moden abgeleitet. Die Resultate werden mit QCD-Gitterrechnungen für das reine SU(3)- und das Quark-Gluon-Plasma mit 2 und 2+1 Quarkflavors bei endlichen Temperaturen und endlichem chemischen Potential verglichen.

Abstract:

The description of the thermodynamic properties of a hot plasma of strongly interacting matter is of importance in various fields of physics such as astrophysics, cosmology and relativistic heavy-ion collisions. The quasiparticle model, which is based on quark and gluon degrees of freedom, was developed in order to describe the thermodynamics of such a plasma.

In the present thesis, the quasiparticle model is systematically derived from the CJT formalism with a 2-loop functional Γ_2 in order to take into account effects of finite particle widths, damping mechanisms with emphasis on Landau damping and collective excitations. The results are compared to QCD lattice calculations at finite temperature and chemical potential for the pure SU(3) and the quark-gluon plasma with 2 and 2 + 1 quark flavors.

Contents

1	Introduction	7
1.1	Standard model of particle physics	7
1.2	Quantum Chromodynamics	8
1.3	The quark-gluon plasma	10
1.4	Heavy ion collisions and quasiparticles	12
1.5	Outline of the work	13
2	Derivation of the QCD plasma entropy density	15
2.1	Self-consistent approximations of many-body systems	15
2.2	Evaluation of the traces	17
2.3	Application to QCD	18
2.4	Properties of the HTL self-energies; Landau damping	20
2.5	Investigation of the dispersion relations	22
2.6	The HTL grand canonical potential	25
2.7	Effective coupling	26
2.8	The entropy density	26
2.9	Lattice QCD	28
3	The effective quasiparticle model	31
3.1	Necessary approximations	31
3.2	Outline of the model	33
3.3	Extension of the model to $\mu > 0$	34
3.4	The pressure correction Taylor expansion coefficients	35
3.5	Extension of the model below the critical temperature	36
3.6	Alternative parametrizations of the effective coupling	36
4	The distributed quasiparticle model	39
4.1	Outline of the model	39
4.2	Test of the model at $\mu = 0$	40
4.3	General discussion of the ansatz	41
4.4	Extension to non-vanishing chemical potential	43
4.4.1	The flow equation	43
4.4.2	Taylor coefficients of the pressure expansion	43
4.5	The effective QPM as limit of the dQP	47
4.6	Temperature dependent widths	48
5	Improved quasiparticle models	51
5.1	An universal expression for the QPM entropy density	51
5.2	Lorentz widths improved quasiparticle model	52
5.3	Landau damping improved quasiparticle model	54

6 Full HTL quasiparticle model	59
6.1 Outline of the model	59
6.2 Comparison with lattice data at $\mu = 0$	60
6.3 Extension of the full HTL QPM to nonzero chemical potential	62
7 Conclusion and Outlook	65
A Evaluation of Matsubara sums	67
B Mathematical relations	69
B.1 Imaginary part of the logarithm	69
B.2 Derivative of Arg and arctan	69
C List of derivatives	71
C.1 Derivatives of the HTL thermal masses	71
C.2 Derivatives of the Breit-Wigner distribution	72
D Coefficients of the flow equations	73
D.1 Effective and distributed quasiparticle models	73
D.2 Full HTL model	74
Bibliography	81

1 Introduction

1.1 Standard model of particle physics

According to the standard model of particle physics, the essential building blocks of matter consist of two classes of fundamental particles: leptons and quarks (and their corresponding antiparticles), see Figure 1.1. These spin-1/2 particles (fermions) interact via four fundamental forces: gravity, weak, electromagnetic and strong interaction - in order of rising strength.

Except for gravity, the interactions can be described by *gauge field theories*. Within these theories an interaction is described through the exchange of gauge bosons (particles with integer spin, here spin-1). The quantum field theoretical treatment of gravity has not yet reached a satisfying level to be included into the standard model - but quite a few proposals (M-theory, loop quantum gravity, etc.) exist. Another area of large interest is the search for the still missing Higgs boson, which is supposed to generate the masses of weak gauge bosons and also part of the fermion masses.

The strength of an interaction is given by its *coupling constant*. It turns out, that this quantity is not constant at all, but depends on the distance of the interacting particles. This is due to the vacuum not being empty either, but instead consisting of quantum fluctuations allowed by Heisenberg's uncertainty principle [Hei27]. In the case of Quantum Electrodynamics (QED) they mainly consist of electron-positron pairs which depict virtual dipoles. They increasingly screen the charged particles with growing distance (or, analogously, small momentum transfer) leading to a decreasing coupling "constant" α_{em} .

At very high energies ($\sim 10^{15}$ GeV), the coupling constants of weak, strong and electromagnetic interaction seem to merge. This gives rise to the hope that all fundamental forces can be unified into one which was split during the first moments after the Big Bang. With the exception of the electroweak interaction as unification of electromagnetic and weak forces, this has yet to be achieved.

Fermions				Bosons	
Quarks	$2/3e$	u up	c charm	t top	γ photon
	$-1/3e$	d down	s strange	b bottom	
Leptons	0	ν_e electron neutrino	ν_μ muon neutrino	ν_τ tau neutrino	W W boson
	$-1e$	e electron	μ muon	τ tau	

Figure 1.1: Elementary particles according to the standard model (Higgs and antiparticles omitted).

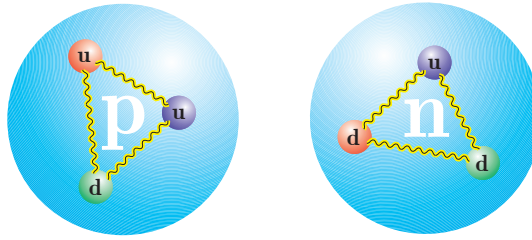


Figure 1.2: Naive pictorial representation of a proton (p) and a neutron (n) as composites of up (u) and down (d) quarks. Wiggly lines schematically indicate gluons as carriers of the strong force. Derived from [KSS06].

The focus of the work is the description of properties of strongly interacting matter. The corresponding gauge field theory is called Quantum Chromodynamics (QCD).

1.2 Quantum Chromodynamics

In analogy to QED, which very accurately describes electromagnetic interactions as exchange of photons between electrically charged particles, strong interactions arise from an exchange of gluons between quarks that carry an additional “color charge”. While the electrical charge can be described in terms of an elementary charge e , the color charge of quarks has three possible values which are illustrated as colors (thus the prefix *chromo*).

Quarks of different colors are attracted to each other just as particles of different electrical charges are - which means that only “white” (neutral color charge) particles are stable. Employing the notion of constituent¹ quarks, this can be achieved either by a quark-antiquark pair with opposite colors (called *meson*, e.g. composed of a red and an anti-red quark) or three quarks of a different color each (called *baryon*, e.g. composed of one red, one green and one blue quark). Our surrounding matter is essentially made of protons, neutrons and electrons. While the electron is one of the leptons and therefore fundamental, the proton and the neutron are baryons composed of *up* and *down* constituent quarks (Figure 1.2).

While QED has a simple gauge group structure, namely $U(1)$, leading to only one gauge boson (the photon), the non-Abelian $SU(3)$ gauge group of QCD contains eight gluons, each carrying a unique color-anticolor combination (except white). In this way, the gluons are color-charged particles themselves and consequently interact not only among each other by exchanging further gluons - which in turn interact via even more gluons - but also with the virtual quarks and gluons of the vacuum.

As a consequence, the strong coupling strength g small for short quark distances (or high momentum transfers) and increases with growing distance (or decreasing momentum transfer leading to gluon “inflation” and antiscreening of the quarks). This effect is called *asymptotic freedom*.²

¹The constituent quarks used to understand hadron spectra have to be distinguished from the current quarks of the gauge theory. Although they carry the same quantum numbers such as isospin, strangeness, etc., their masses may differ by several orders of magnitude.

²For the discovery of this phenomenon in 1973 - which led to the widespread acceptance of the non-Abelian QCD in the following years - D. Gross, D. Politzer and F. Wilczek have been awarded the Nobel prize in 2004. Asymptotic freedom has been verified, e.g. in deep inelastic scattering experiments. It is due to this effect that, rather than coupling strength, the notion *running coupling* is more accurately being employed for g .

Even though a mathematical proof is still required, it is assumed that quarks and gluons can never be observed as isolated particles. The energy spent for the separation of two color-charged particles leads to another pair being created in between, thus leaving the experimentalist with two pairs.

The mathematical description of QCD is based on the classical Lagrangian (cf. [PDG06], p. 110 and p. 319)

$$\mathcal{L}_{\text{QCD}} = \sum_q \bar{\psi}_q^i (i\gamma^\mu (D_\mu)_{ij} - \delta_{ij} m_q) \psi_q^j - \frac{1}{4} F_{\mu\nu}^a F_a^{\mu\nu} + \mathcal{L}_{\text{gauge}} + \mathcal{L}_{\text{FP}}, \quad (1.1)$$

where $\mu, \nu = 0 \dots 3$ are Lorentz indices, $i, j = 1 \dots 4$ are Dirac spinor indices, and $a = 1 \dots 8$ is the adjoint color index counting the gluon color states. The sum over all quark flavors $q \in \{u, d, c, s, t, b\}$ is given explicitly; for the remaining indices the Einstein sum convention has to be followed.

The quark fields ψ_q (color triplets) refer to current quarks. They are coupled minimally to the gauge sector by the covariant derivative

$$(D_\mu)_{ij} = \delta_{ij} \partial_\mu + ig \frac{(\lambda_a)_{ij}}{2} A_\mu^a, \quad (1.2)$$

where the A_μ^a represent the gauge fields (gluons) and the λ_a are the generators of the local $SU(3)$ gauge group in the fundamental representation.³

The pure Yang-Mills term $\mathcal{L}_{\text{YM}} := -\frac{1}{4} F_{\mu\nu}^a F_a^{\mu\nu}$ describes the gluons just as any other gauge boson. For the gluons the field strength tensor is given by

$$F_a^{\mu\nu} = \underbrace{\partial^\mu A_a^\nu - \partial^\nu A_a^\mu}_{\text{in analogy to QED}} + \underbrace{gf_{abc} A^{b\mu} A^{c\nu}}_{\text{gluon-gluon interaction}}. \quad (1.3)$$

As a result of the additional terms, \mathcal{L}_{YM} contains expressions trilinear and quadri-linear in the gluon fields A_a^μ leading to three- and four-gluon interactions.

The contribution $\mathcal{L}_{\text{gauge}}$ fixes the still remaining gauge degree of freedom and \mathcal{L}_{FP} takes care of possibly occurring unphysical degrees of freedom by introducing Fadeev-Popov ghost fields. A very insightful, deeper look at those phenomena is given by [GTP11].

The current quark masses m_q and the coupling strength g have to be adjusted to physical observables. Due to renormalization within the quantized theory, the quantities m_q and g entering the classical Lagrangian (1.1) become subject to a redefinition resulting in a scale dependence. The same holds for matter and gauge sector fields.

By performing an expansion in terms of its small coupling constant ($\alpha_{em} \approx 1/137$ at asymptotically small energy scales), the equations for QED scattering processes, for instance, can be solved up to a certain energy scale, where it diverges [PS95]. Due to asymptotic freedom, the situation is reversed for the QCD running coupling g which is smaller than unity only at very high energy or momentum scales. For larger g , non-perturbative methods are needed in order to solve the QCD field equations. One way is to discretize space and time and apply Monte Carlo sampling methods. This approach is called lattice QCD. As an abbreviation, the results of such methods are dubbed “lattice data”.

³The standard representation of λ_a are the Gell-Mann matrices. They are the three-dimensional extension of the Pauli matrices. They form the Lie algebra of $SU(3)$ with commutation relations $[\lambda_a, \lambda_b] = 2if_{abc}\lambda^c$, where f_{abc} are the fully antisymmetric structure constants.

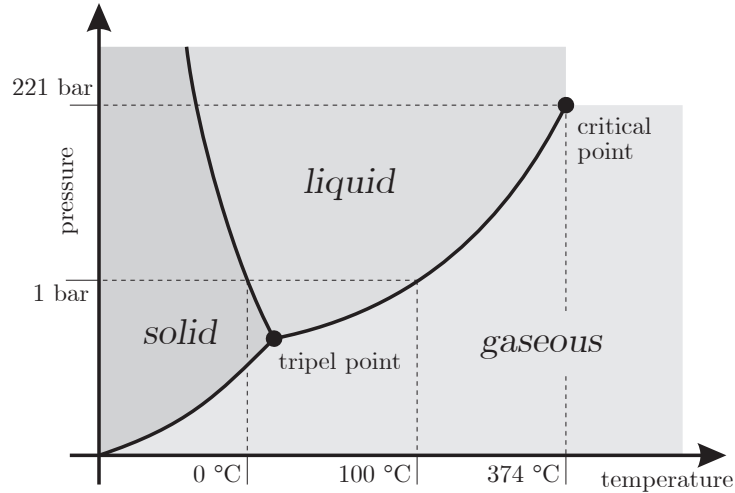


Figure 1.3: A part of the phase diagram of water, showing its three major phases and the phase transitions. (*source*: www public domain)

For vanishing quark masses the QCD Lagrangian (1.1) is chirally symmetric, meaning that both left and right handed world are fully decoupled. Lattice data is often obtained using unphysically large quark masses and therefore needs to be extrapolated towards the *chiral limit*, i.e. the physical mass scales.

Even for small values of g , perturbation theory for a strongly interacting system can fail at nonzero temperature T despite the use of modern expansion methods [CH98]. This is due to the energy scale introduced by the temperature which leads to expansion terms $\sim gT/p$ [BP90a, BP90b]. These are no longer of order g , but can be of order unity for a typical momentum scale p of particles in a heat bath of temperature T . The usual relation of the order of the loop expansion and powers of g is lost: effects of leading order in g arise from every order in the loop expansion and one cannot arrange different contributions according to powers of g anymore. Consequently, in order to still be able to apply perturbative methods, all these terms need to be taken into account which can be done by resummation techniques.

1.3 The quark-gluon plasma

We experience matter in three different phases: solid, fluid and gaseous. But certain materials have a much richer phase structure. For instance water can assume twelve or more different ice phases [LFK98], the usual fluid form or become vapor. These phases transform into each other with the change of exterior conditions such as pressure and temperature as depicted in Figure 1.3. These phase transitions are often combined with tremendous changes in material properties like compressibility, transparency or electrical conductivity.

If water is brought to sufficiently high temperatures it turns into yet another state: a plasma consisting of ions and quasifree electrons. Since the transition happens slowly through ionization of single molecules by collisions it is not considered a phase change. Still a plasma shows new collective effects such as screening and plasma oscillations and is therefore often considered as fourth state of matter.

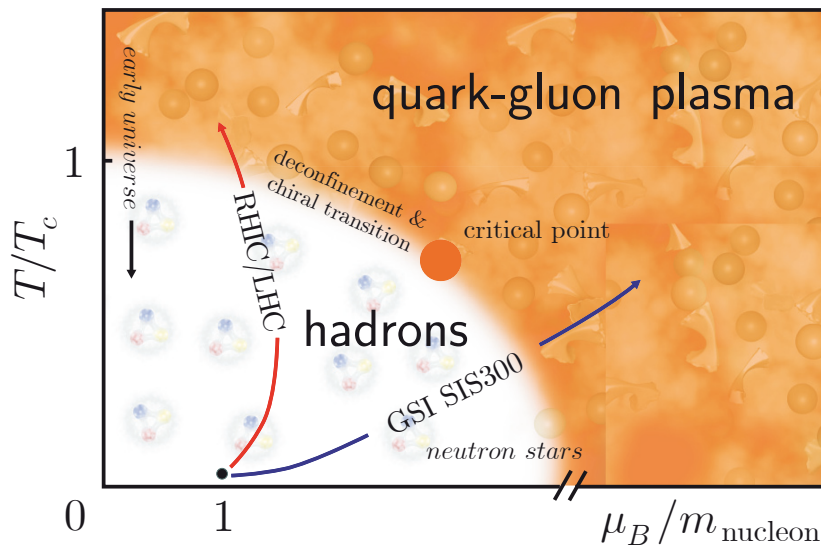


Figure 1.4: Schematic plot of the phase diagram of strongly interacting matter for constant volume V and variable net baryon density or baryo-chemical potential μ_B scaled by a typical nucleon mass and temperature T scaled by the transition temperature at $\mu_B = 0$. The white region for low μ_B and T represents the hadronic regime, the red region the quark-gluon plasma with the deconfinement and chiral transition in between. The arrows depict areas accessible to current and future experiments and the evolutionary path of the universe. Neutron star matter occupies the region of low temperature and large baryon density (*source: GSI*)

The plasma phase can also be reached through compression, by which electrons are released from their orbitals and form a degenerate quantum plasma. This transition is a real phase change (an insulator-metal transition) and is observed e.g. when a star collapses into a White Dwarf (which often cannot further collapse because of the sufficiently large degeneracy pressure of the electrons).

The nuclei of water molecules consist of protons and neutrons which are again formed by constituent quark triplets (Figure 1.2) interacting through an exchange of gluons. Quarks and gluons are confined within the nucleons. Just as - after heating and compressing it sufficiently - the constituents of water molecules form a plasma, this strongly interacting matter is presumed to deconfine, i.e. transit into a phase with much less correlation, often assuming quarks and gluons as freely roaming. This phase is called the *quark-gluon plasma* (QGP). Note that although the question about the nature of the transition (first/second order phase transition or just a crossover) actually depends on the number of active quark flavors N_f as well as their masses, the use of the terminology “transition” is widely accepted.

Figure 1.4 shows the presumed phase diagram of strongly interacting matter. The red region is occupied by deconfined matter, where quarks and gluons are thought to represent the relevant degrees of freedom. The white region represents hadronic matter. At the common boundary, strongly interacting matter undergoes the deconfinement transition.

For small chemical potential and $N_f = 2, 2 + 1$ the deconfinement transition is a simple crossover. At the critical point it becomes a real phase transition of second order turning into first order for larger values of μ_B . The critical temperature at vanishing chemical potential is called T_c . The common starting point of the experiments marks hadrons or nuclei in our environment. Not shown is a possible

triple point with the color superconducting phase predicted by some authors [RW00].

The arrows indicate the scope of some present and future experiments outlined within the following chapter.

1.4 Heavy ion collisions and quasiparticles

In order to investigate the properties of deconfined matter, enormous energy scales are necessary. While they cannot be provided by current technology on a continuous basis, it is possible to accelerate nuclei to relativistic velocities and let them collide. Such experiments, aimed at producing deconfined matter, have been performed at the Alternating Gradient Synchrotron (AGS) and Relativistic Heavy Ion Collider (RHIC) at Brookhaven National Laboratories (BNL) as well as the the Super Proton Synchrotron (SPS) at CERN in Geneva. Two future experiments are indicated in Figure 1.4. LHC means the Large Hadron Collider under construction at CERN in Geneva; GSI SIS300 is related to the FAIR project proposed at GSI in Darmstadt. The latter is aimed to investigate the region of high baryon densities at rather low temperatures.

After the collision of the nuclei, the quarks and gluons of the emerging fireball become deconfined and can be described as QGP, i.e. as a fluid or plasma or gas with features to be specified. In order to predict the dynamics of the fireball during this phase and assuming a thermally equilibrated system, hydrodynamics can be employed. This means to solve the equations of energy-momentum and current conservation [LL06]

$$T^{\mu\nu}{}_{;\mu} = 0 \quad \text{and} \quad (nu^\mu)_{;\mu} = 0 \quad (1.4)$$

with the energy-momentum tensor $T^{\mu\nu} = (e + p)u^\mu u^\nu - pg^{\mu\nu}$, energy density e , pressure p and the metric tensor $g^{\mu\nu} = \text{diag}(1, -1, -1, -1)$; u^μ is the 4-velocity and n is the net density of baryons of the respective matter emerging from hadrons at the deconfinement transition. The semicolon denotes the covariant derivative.

The problem is under-determined. Therefore, as one important input for the hydrodynamic description, an interrelation among the state quantities e , p and n , for instance of the form $e = e(p, n)$, i.e. the equation of state (EOS) of strongly interacting matter, in particular the quark-gluon plasma, is needed. As the thermodynamical potential contains all of the information of bulk properties of matter in local equilibrium, our ultimate goal is to find an expression for, e.g., the grand canonical potential Ω from the Lagrangian \mathcal{L} and its associated Feynman rules (i.e. propagators, self-energies, etc.). It can then provide us with the EOS of the QGP.

Given the problems in solving the QCD equations of motion by perturbation theory and lattice calculations especially in the region of high baryon densities as mentioned in section 1.2, a different ansatz is needed. The interpretation of the QGP constituents as noninteracting quasiparticles using effective masses is one approach to a solution of the problem.

The concept of quasiparticles is one of the few known ways of simplifying the quantum mechanical many-body problem. It has proven to be very successful within the field of condensed matter physics but its scope of application is not limited to it. This work makes use of quasiparticle excitations in order to describe the thermodynamics of the quark-gluon plasma.

A quasiparticle is an elementary excitation of a system. If chosen in a sensible way, other excitations of the system can be described by the presence of multiple

quasiparticles. In certain limits the interaction between multiple quasiparticle species can turn out to become negligible, giving the possibility to investigate properties of the many-body system by examining properties of the individual species.

As for most many-body systems, the QGP is expected to possess two classes of quasiparticles: the first one corresponds to actual, single particles, the motions of which are modified by the interactions within the plasma. The other class represents collective excitation modes of the system. For the QGP, the longitudinal gluon (or plasmon) mode and the plasminos are such collective excitations.

1.5 Outline of the work

Up to now, damping and width effects of the QGP were usually neglected when deriving an expression for the thermodynamic potential of the QGP. Nevertheless, the treatment of these effects constitutes the key to the calculation of transport coefficients of the QGP. Therefore, it is the goal of this work to include finite widths and collective damping into the quasiparticle model (QPM) [Pes00, Pes02, Blu04].

In chapter 2 the thermodynamic potential of 2-loop QCD is systematically derived using two (equivalent) formalisms. Assuming internal momenta of order T and a parametrization of the QCD coupling an entropy density expression of strongly interacting matter is found. Using certain approximations, the existing effective quasiparticle model (eQP) is derived from this expression in chapter 3. The principles of extending a QPM to nonzero chemical potential and below the pseudocritical temperature are demonstrated and some problems of the model are pointed out. An investigation of several alternative parametrizations of the strong coupling closes the chapter.

In chapter 4 an ansatz including quasiparticle temperature dependent and independent widths into the eQP by allowing for statistically distributed masses is presented. The resulting model is tested at vanishing chemical potential and extended to nonzero values. The procedure to retrieve the eQP expressions in the limit of vanishing width is shown in detail.

Returning to the exact 1-loop entropy density expression of chapter 2 a reformulation is presented in chapter 5 allowing for a description of quasiparticle widths in a more systematic way than the ansatz of chapter 4. While applying the expression to Lorentz widths in order to review a proposal from [Pes04], a verification for the distributed mass ansatz is found. Additionally, the effects of Landau damping for the QPM are investigated.

Chapter 6 concentrates on the formulation of a QPM based on the full entropy density expression. The resulting model is investigated at vanishing and at nonzero chemical potential. Details of the extension to nonzero μ are given in Appendix 6.3.

In chapter 7 gives a compact presentation of the results. The work is summarized and ends with an outlook.

2 Derivation of the QCD plasma entropy density

2.1 Self-consistent approximations of many-body systems

In current research essentially two formalisms are frequently used to determine the thermodynamic potential of a relativistic many-body system from its excitation spectrum (i.e. its dispersion relation) in a thermodynamically consistent way. As demonstrated in the following both are equivalent given certain assumptions.

The first one is based on a proposal of Luttinger and Ward [LW60] to derive the thermodynamic potential of non-relativistic, fermionic systems from Feynman graphs, i.e. using propagator expressions. As such this formalism is only a translation of a stationarity theorem by Lee and Yang [LY60b] - which expresses the thermodynamic potential Ω in terms of mean occupation numbers - into propagator language.¹ Since then, the formalism has been extended to bosonic [GW65, FW71] and, important for us, relativistic systems [NC75, VB98].

The expression for the thermodynamic potential reads [BIR01]

$$\Omega[D, S] = T \left\{ \frac{1}{2} \text{Tr} [\ln D^{-1} - \Pi D] - \text{Tr} [\ln S^{-1} - \Sigma S] \right\} + T\Phi[D, S], \quad (2.1)$$

where D and S are dressed bosonic and fermionic propagators with respective self-energies Π and Σ , and $-\Phi$ is the sum of all two particle irreducible (2PI) skeleton diagrams (i.e. diagrams without external lines which do not become disconnected upon cutting two propagator lines) with full propagators. Tr denotes the trace in configuration space, containing integrations over the four phase space dimensions and sums over all discrete indices (color, flavor, spin, etc.) denoted by tr . Since this work uses the Coulomb gauge, there is no contribution from Faddeev-Popov ghost fields.

The self-energies are defined by Dyson's equations

$$\Pi[D] := D^{-1} - D_0^{-1} \quad \text{and} \quad \Sigma[S] := S^{-1} - S_0^{-1}, \quad (2.2)$$

where D_0 and S_0 are the bare propagators, so that

$$\Omega[D, S] = T \left\{ \frac{1}{2} \text{Tr} [\ln D^{-1} + D_0^{-1} D - 1] - \text{Tr} [\ln S^{-1} + S_0^{-1} S - 1] \right\} + T\Phi[D, S]. \quad (2.3)$$

In thermodynamic equilibrium the thermodynamic potential has to be stationary with respect to functional variations of the physical propagators D and S

$$\frac{\delta\Omega}{\delta D} = \frac{\delta\Omega}{\delta S} = 0 \quad (2.4)$$

¹In fact, it can even be reformulated to use any subset of n -point amplitudes with $n \leq 4$ [dDM64, NC75, Kle82, Car04, Ber04].

yielding

$$0 = -D^{-1} + D_0^{-1} + 2\frac{\delta\Phi}{\delta D} \quad \text{and} \quad 0 = S^{-1} - S_0^{-1} + \frac{\delta\Phi}{\delta S}. \quad (2.5)$$

Comparison with the definitions in (2.2) leads to

$$\Pi = 2\frac{\delta\Phi}{\delta D} \quad \text{and} \quad \Sigma = -\frac{\delta\Phi}{\delta S}, \quad (2.6)$$

which are dubbed ‘‘gap equations’’. Note that, on account of its stationarity, Ω is formally gauge independent, even though the propagators may be not.

Since Φ is an infinite sum, these gap equations can presently only be solved approximately by selecting a subset of the skeleton diagrams in Φ . The truncated self-energies are then found from (2.6) in an elegant way: The functional derivative with respect to the propagators is graphically represented by simply cutting one propagator line in the skeleton diagrams, keeping in mind all the symmetry factors. From the truncated self-energies, the corresponding truncated dressed propagators follow self-consistently from Dyson’s equations

$$D = \frac{1}{D_0^{-1} + \Pi[D]} \quad \text{and} \quad S = \frac{1}{S_0^{-1} + \Sigma[S]}. \quad (2.7)$$

Even though truncation introduces approximations, they were shown to obey the fundamental physical laws such as number, energy and momentum conservation [BK61, Bay62]. Therefore, this approach is often called conservation law preserving or symmetry conserving self-consistent approximation scheme. Baym also introduced the notion *Φ -derivable approximations* due to eq. (2.6).

Only a few years after Luttinger and Ward [LW60], it was Jona-Lasinio [Jon64], who emphasized the importance of the *effective action* for discussions of spontaneous symmetry breaking in relativistic particle theory. Consequently, Jona-Lasinio, Dahmen and Tarski [DJ67, DJ69, DJT72] presented a variational formulation of relativistic quantum field theory based on combinatorial analysis.

It was reformulated using functional methods and presented with some example applications in a review paper by Cornwall, Jackiw and Tomboulis [CJT74] which was widely referenced, leading to the term *CJT formalism*.² Essentially, the CJT formalism is the result of the generalization of the LW formalism. In the following, this relation is elaborated.

As opposed to the thermodynamic potential of the LW formalism, the starting point of the CJT formalism is the *effective action*³ Γ [Ris03]

$$\begin{aligned} \Gamma[D, S] = I - \frac{1}{2} \{ & \text{Tr} [\ln D^{-1}] + \text{Tr} [D_0^{-1}D - 1] \} \\ & + \{ \text{Tr} [\ln S^{-1}] + \text{Tr} [S_0^{-1}S - 1] \} + \Gamma_2[D, S], \end{aligned} \quad (2.8)$$

where I is the classical action of the system and $-\Gamma_2$ corresponds to the LW-functional Φ , i.e. it represents the sum over all 2PI diagrams without external lines and internal lines given by the full propagators.

²In that way, both the CJT and the LW formalism are named after the translators rather than the inventors. They might as well be called DJT and LY formalism, respectively. In fact, the CJT formalism could also be named after A. N. Vasil’ev and A. K. Kazanskii, who developed it independently within the Soviet science community [VK72, VK73a, VK73b].

³For more on the concept of the effective action in the framework of symmetry breaking, the interested reader is referred to [PS95] and [Riv88].

The effective action is subject to stationarity conditions

$$\frac{\delta\Gamma}{\delta D} = \frac{\delta\Gamma}{\delta S} = 0 \quad (2.9)$$

which, in a similar manner as in (2.6), yield

$$\Pi = -2\frac{\delta\Gamma_2}{\delta D} \quad \text{and} \quad \Sigma = \frac{\delta\Gamma_2}{\delta S}. \quad (2.10)$$

For translationally invariant systems, where an arbitrary propagator fulfills $\Delta_{(0)}(x, y) = \Delta_{(0)}(x - y)$, an overall factor of the four-dimensional space T/V can be extracted from the trace integrals in (2.8) and it suffices to consider the *effective potential*

$$V_{\text{eff}}[D, S] = -\frac{T}{V} \Gamma[D, S] \quad (2.11)$$

instead of the effective action [CJT74, Ris03, Bec05, Roe05]. At the stationary point V_{eff} is connected to the grand canonical potential via (see [Bro92], p. 104, or [Riv88])

$$\frac{\Omega}{V} = V_{\text{eff}}. \quad (2.12)$$

The classical action I can also be replaced by a classical potential $U = -IT/V$, which describes the broken symmetries of the system. If no broken symmetries are considered, U can be set to zero and one obtains exactly the LW expression (2.3).

We can conclude that for *translationally invariant systems without broken symmetries* CJT and LW formalism describe the same stationarity principle. In the following the CJT formalism is used assuming these premises.

2.2 Evaluation of the traces

In the expressions above, Tr contains a trace tr over the discrete indices as well as an integration over the four-dimensional phase space. In order to take effects of finite temperature into account, the energy integration has to be performed using the imaginary time formalism (see [LeB96, Kap89, YHM95] for an introduction). This is done by performing a sum over the discrete Matsubara frequencies

$$i\omega_n = \begin{cases} 2ni\pi T & \text{for bosons,} \\ (2n+1)i\pi T + \mu & \text{for fermions,} \end{cases} \quad (2.13)$$

where μ denotes the one independent chemical potential⁴ of the system. Since the expression for the thermodynamic potential depends on the three-momentum quadratically only, i.e. it is rotationally invariant, the momentum integral $(2\pi)^{-3} \int d^3k$ reduces to $(2\pi^2)^{-1} \int dk k^2$. Translation invariance gives an overall factor of the three-volume V of the system yielding

$$\text{Tr} \longrightarrow \frac{V}{2\pi^2} \text{tr} \sum_n \int dk k^2. \quad (2.14)$$

⁴Considering the case of $N_f = 2$ dynamical quark flavors and assuming zero net electric charge and equal u and d quark masses, the isospin chemical potential $\mu_I = (\mu_u - \mu_d)/2$ vanishes. Therefore, there is only one independent chemical potential $\mu = \mu_q = \mu_u = \mu_d = \mu_B/3$, where μ_B is the baryo-chemical potential.

The Matsubara sum can be performed using standard contour integration techniques. This is shown explicitly in Appendix A. Applying the found result

$$T \sum_{n=-\infty}^{+\infty} f(p_0 = i\omega_n) = - \int_{-\infty}^{+\infty} \frac{d\omega}{\pi} n_B(\omega) \text{Im}(f(\omega + i\varepsilon)), \quad (2.15)$$

where $n_B = (\exp(\beta\omega) - 1)^{-1}$ with $\beta = 1/T$ is the Bose-Einstein statistical distribution function, and an analogous expression for fermions with the Fermi-Dirac distribution $n_F = (\exp(\beta(\omega - \mu)) + 1)^{-1}$ and opposite sign, yields the following expression for the thermodynamic potential from eq. (2.3):

$$\begin{aligned} \frac{\Omega}{V} &= \text{tr} \int \frac{d^4k}{(2\pi)^4} n_B(\omega) \text{Im}(\ln D^{-1} - \Pi D) \\ &+ 2 \text{tr} \int \frac{d^4k}{(2\pi)^4} n_F(\omega) \text{Im}(\ln S^{-1} - \Sigma S) - \frac{T}{V} \Gamma_2, \end{aligned} \quad (2.16)$$

where the propagators D and S now represent the retarded bosonic and fermionic propagators, respectively. Thus, in the following only retarded propagators and corresponding self-energies are used.

2.3 Application to QCD

The presentation in this section is based on work done by Peshier [Pes01] and Blaizot, Iancu and Rebhan [BIR01], who used the Luttinger-Ward formalism presented in section 2.1.

Because Γ_2 is an infinite sum, it is not (yet) possible to solve the problem exactly and the sum has to be truncated. Since Γ_2 contains two-particle irreducible diagrams only, there are no 1-loop contributions and the first non-trivial contribution is encountered at 2-loop order. The corresponding contributions to Γ_2 are shown in Figure 2.1.

$$\Gamma_2 = \frac{1}{12} \text{diagram}_1 + \frac{1}{8} \text{diagram}_2 - \frac{1}{2} \text{diagram}_3 \quad (2.17)$$

Figure 2.1: Contributions to Γ_2 at 2-loop order; wiggly lines are gluons, solid lines represent quarks. Due to the chosen gauge (Coulomb), ghost contributions are not needed.

Despite the truncation, a self-consistent approximate solution which conserves particle number, energy and momentum can be obtained [Bay62]. This is achieved by first calculating both quark and gluon self-energies using the gap equations, i.e. performing a functional variation of Γ_2 with respect to the propagators. In a graphical sense this can be interpreted as cutting one propagator line within the Feynman graphs. Taking the prefactors and symmetries into account, the 2-loop contributions to Γ_2 lead to the 1-loop self-energies shown in Figure 2.2.

$$\Pi = \frac{1}{2} \text{diagram}_1 + \frac{1}{2} \text{diagram}_2 - \text{diagram}_3 \quad (2.18)$$

$$\Sigma = \text{diagram}_4 \quad (2.19)$$

Figure 2.2: The 1-loop QCD self-energies derived from Γ_2 at 2-loop order.

Although, as a consequence of the truncation, gauge invariance is lost, it can be restored by assuming soft external momenta or equivalently Hard Thermal Loops (HTL) in the propagator and self-energy expressions. For 1-loop QCD in the chiral limit⁵ the HTL approximation provides gauge invariant self-energies [BP90b]. We follow the conventions of [BIR01] and use the HTL self-energies and propagators for gluons and massless quarks given therein:

$$\begin{aligned} \Pi_{\mu\nu} &= \Pi_T(\omega, k) \left(\Lambda_T(\vec{k}) \right)_{\mu\nu} - \Pi_L(\omega, k) \left(\Lambda_L(\vec{k}) \right)_{\mu\nu}, \\ \gamma_0 \Sigma &= \Sigma_+(\omega, k) \Lambda_+(\vec{k}) - \Sigma_-(\omega, k) \Lambda_-(\vec{k}) \end{aligned} \quad (2.20)$$

with the scalar self-energies

$$\begin{aligned} \Pi_T(\omega, k) &= \frac{m_D^2}{2} \left(1 + \frac{\omega^2 - k^2}{k^2} \Pi_L(\omega, k) \right), \\ \Pi_L(\omega, k) &= m_D^2 \left(1 - \frac{\omega}{2k} \ln \frac{\omega + k}{\omega - k} \right), \\ \Sigma_{\pm}(\omega, k) &= \frac{\hat{M}^2}{k} \left(1 - \frac{\omega \mp k}{2k} \ln \frac{\omega + k}{\omega - k} \right), \end{aligned} \quad (2.21)$$

where $\hat{M} = \hat{M}(T, \mu, g^2)$ is the thermal fermion mass or plasma frequency and $m_D = m_D(T, \mu, g^2)$ is the Debye mass. They read

$$\begin{aligned} m_D^2 &= \underbrace{\left(\frac{C_b}{3} T^2 + \frac{N_c N_f}{6\pi^2} \mu^2 \right)}_{2\tilde{C}_b} G^2, \\ \hat{M}^2 &= \underbrace{\frac{C_f}{8} \left(T^2 + \frac{\mu^2}{\pi^2} \right)}_{\tilde{C}_f} G^2, \end{aligned} \quad (2.22)$$

where $C_f = \frac{N_c^2 - 1}{2N_c}$ and $C_b = \left[N_c + \frac{N_q + N_h}{2} \right]$. In this work the number of colors N_c is fixed at 3. N_q is the number of light quark flavors (up and down) while N_h is the number of heavy quark flavors (e.g. strange) with $N_f = N_q + N_h$. Note that \hat{M}^2 is sometimes denoted \hat{M}_q^2 for the light quark flavors in order to contrast $\hat{M}_s^2 = \hat{M}^2|_{\mu=0}$ of the heavy quark flavor. The explicit form of the projectors Λ_i can be found in [BIR01]. In contrast to the vacuum case, the longitudinal gluon mode, which at zero temperature is a static mode producing the familiar Coulomb interaction, propagates for nonzero temperature and has to be taken into account.

⁵For nonzero quark masses, the quark self-energy is no longer gauge invariant (cf. [Sei07]).

Since the additional HTL approximation impairs self-consistency, the term ‘‘approximately self-consistent approximation’’ has been established. It is worth mentioning that, since only undressed vertices are used, the Ward identities are obviously violated. According to [BIR01] vertex corrections can be implemented self-consistently but are negligible at 2-loop order.

Finally Dyson’s equations (2.7) are used to self-consistently determine the dressed propagators

$$\begin{aligned} D_T^{-1} &= -\omega^2 + k^2 + \Pi_T, \\ D_L^{-1} &= -k^2 - \Pi_L, \\ S_{\pm}^{-1} &= -\omega \pm (k + \Sigma_{\pm}). \end{aligned} \quad (2.23)$$

2.4 Properties of the HTL self-energies; Landau damping

This section deals with symmetries and other properties of the real and imaginary parts of the retarded self-energies as knowledge about these proves useful further below.

The real and the imaginary parts of the HTL self-energies (2.21) are found to be⁶

$$\begin{aligned} \text{Re}\Pi_T &= \frac{1}{2}m_D^2 \left(\frac{\omega^2}{k^2} - \frac{\omega^2 - k^2}{k^2} \frac{\omega}{2k} \ln \left| \frac{\omega + k}{\omega - k} \right| \right), \\ \text{Re}\Pi_L &= m_D^2 \left(1 - \frac{\omega}{2k} \ln \left| \frac{\omega + k}{\omega - k} \right| \right), \\ \text{Re}\Sigma_{\pm} &= \frac{\hat{M}^2}{k} \left(1 - \frac{\omega \mp k}{2k} \ln \left| \frac{\omega + k}{\omega - k} \right| \right), \\ \text{Im}\Pi_T &= \frac{1}{2}m_D^2 \frac{\omega^2 - k^2}{k^2} \frac{\omega}{2k} \pi \Theta(k^2 - \omega^2) \varepsilon(k), \\ \text{Im}\Pi_L &= m_D^2 \frac{\omega}{2k} \pi \Theta(k^2 - \omega^2) \varepsilon(k), \\ \text{Im}\Sigma_{\pm} &= \frac{\hat{M}^2}{k} \frac{\omega \mp k}{2k} \pi \Theta(k^2 - \omega^2) \varepsilon(k), \end{aligned} \quad (2.26)$$

where $\varepsilon(k)$ is the sign function. The gluon self-energies show the symmetries

$$\begin{aligned} \text{Re}\Pi_i(-\omega) &= \text{Re}\Pi_i(\omega), \\ \text{Im}\Pi_i(-\omega) &= -\text{Im}\Pi_i(\omega), \end{aligned} \quad (2.28)$$

i.e. the real parts are symmetric and the imaginary parts are antisymmetric with respect to the energy ω . This can explicitly be seen for a momentum of $k = 0.5T$ in

⁶The complexity of the self-energies is due to the logarithmic term. It therefore suffices to find real and imaginary parts of the logarithm of $z = (\omega + k)/(\omega - k)$. For the latter, retardation

$$z(\omega + i\varepsilon) = \frac{\omega + i\varepsilon + k}{\omega + i\varepsilon - k} = \frac{\omega + k}{\omega - k} - i\varepsilon \frac{2k}{(\omega - k)^2}. \quad (2.24)$$

plays the decisive role as applying the infinitesimally small imaginary part of $z(\omega + i\varepsilon)$ to eq. (B.3) gives

$$\text{Im} \ln \frac{\omega + k}{\omega - k} = \pi \varepsilon(-k) \Theta\left(-\frac{\omega + k}{\omega - k}\right) = -\pi \Theta(k^2 - \omega^2) \varepsilon(k) \quad (2.25)$$

while it would be zero for non-retarded z .

The real part of the logarithm $\ln(z)$ is $\ln|z|$.

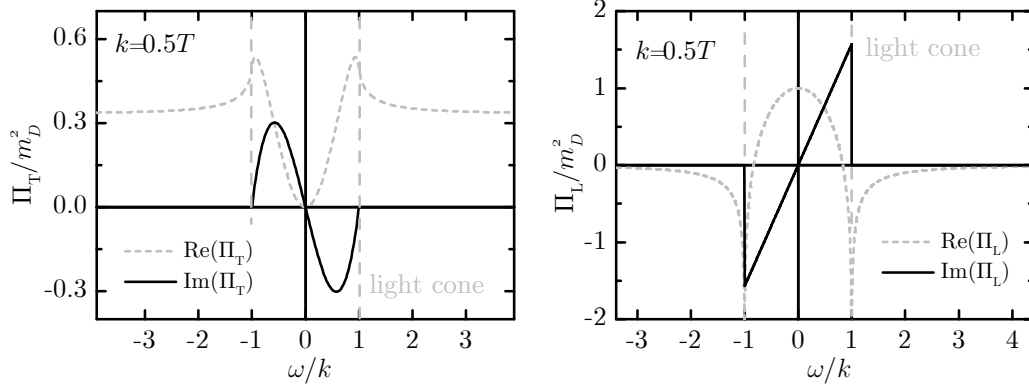


Figure 2.3: The real and imaginary parts of the retarded transverse (left) and longitudinal (right) gluon self-energies scaled by the Debye mass squared are shown as functions of the energy ω scaled by the momentum k which is fixed at $k = 0.5T$. The real parts are symmetric with respect to ω , while the imaginary parts are antisymmetric and differ from zero only below the light cone $|\omega| = k$.

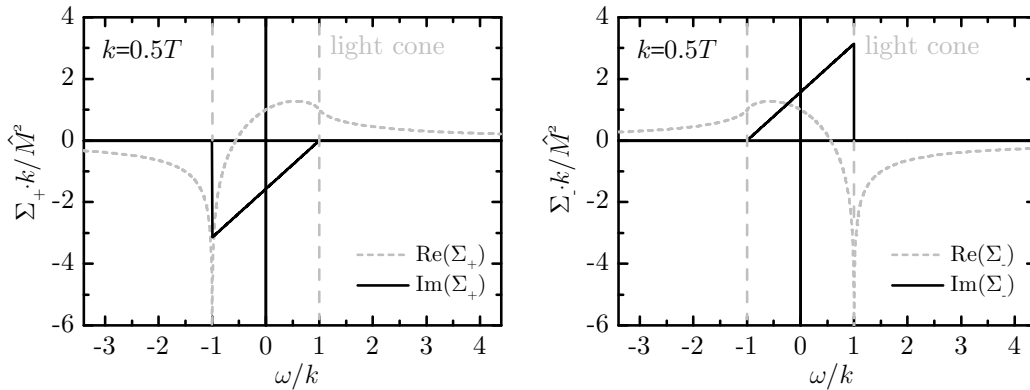


Figure 2.4: The real and imaginary parts of the retarded quark self-energies for the normal (left) and abnormal branch (right) scaled by the plasma frequency squared are shown as functions of the energy ω scaled by the momentum k which is fixed at $k = 0.5T$. They fulfill the parity relations $\text{Re}\Sigma_+(-\omega) = \text{Re}\Sigma_-(\omega)$ and $\text{Im}\Sigma_+(-\omega) = -\text{Im}\Sigma_-(\omega)$. The imaginary parts of the self-energy are nonzero only below the light cone.

Figure 2.3. Analogously, the quark self-energies fulfill the parity relations

$$\begin{aligned} \text{Re}\Sigma_+(-\omega) &= \text{Re}\Sigma_-(\omega), \\ \text{Im}\Sigma_+(-\omega) &= -\text{Im}\Sigma_-(\omega) \end{aligned} \quad (2.29)$$

as shown for $k = 0.5T$ in Figure 2.4.

The HTL self-energies do not account for quasiparticle widths, as there is no imaginary part at the poles of the propagator. The nonzero imaginary parts of the self-energies below the light cone are due to *Landau damping* (LD). LD is a collective effect caused by energy transfer between the gauge field and plasma particles with velocities close to the phase velocity (“resonant particles”). As this resonance would be spoiled by collisions in a normal fluid, it is a unique feature of collisionless plasmas [ONC99].

Consider particles whose velocity is slightly higher than ω/k prior to an energy transfer. If they gain energy from the gauge field they leave the area of resonance, while, if losing energy to the gauge field, they approach the resonant velocity even

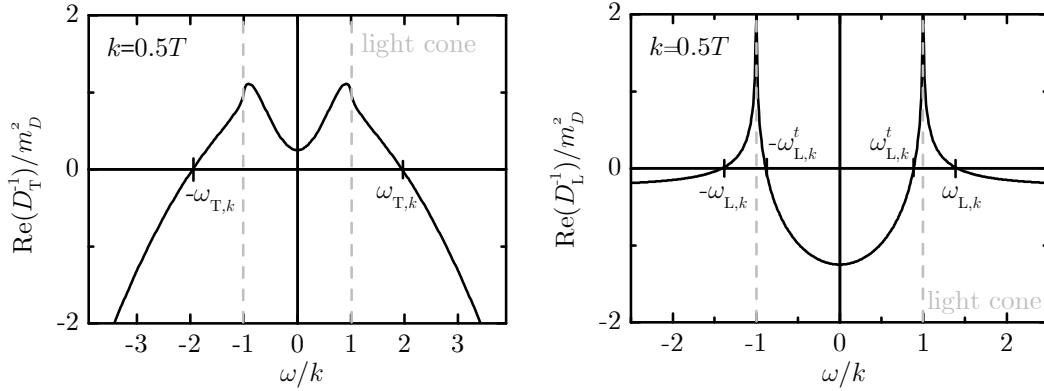


Figure 2.5: The real parts of the inverse gluon propagators $D_{T,L}^{-1}$ scaled by the Debye mass squared are shown as functions of the energy ω scaled by the momentum k which is fixed at $k = 0.5T$. Both are symmetric with respect to ω . The zero of $\text{Re}D_T^{-1}$ determines the dispersion relation $\omega_{T,k}$ for transverse gluons. The zero of $\text{Re}D_L^{-1}$ above the light cone indicates the dispersion relation $\omega_{L,k}$ of longitudinal gluons, while the tachyonic dispersion relation $\omega_{L,k}^t$ (below the light cone) is due to Landau damping.

closer and can again interact with the gauge field. These particles would effectively lose energy to the gauge field.

In the opposite case, particles with velocity slightly below ω/k effectively gain energy from the gauge field. Since physical distributions favor states of lower energy, the states of energy loss are usually less populated than the ones which gain energy. Therefore, a net energy transfer to the particles takes place, damping the gauge field.⁷

Even though the imaginary parts are formally nonzero only below the light cone, retardation leads to an infinitely small contribution even above the light cone, giving a definite sign to the self-energies for all ω :

$$\begin{aligned}\varepsilon(\text{Im}\Pi_T(\omega)) &= -\varepsilon(\omega), \\ \varepsilon(\text{Im}\Pi_L(\omega)) &= +\varepsilon(\omega), \\ \varepsilon(\text{Im}\Sigma_{\pm}(\omega)) &\equiv \mp 1.\end{aligned}\tag{2.30}$$

Note that the sign of the imaginary parts above the light cone is solely due to retardation and not related to Landau damping which is found below the light cone only.

2.5 Investigation of the dispersion relations

On-shell (quasi)particles satisfy a dispersion relation determined by $\text{Re}D^{-1} = 0$, where D denotes the propagator of the particles. It is therefore useful to first investigate the real part of the inverse retarded HTL propagators.

Both inverse gluon propagators $D_{T,L}^{-1}$ are symmetric in the energy domain and have just one positive energy dispersion relation above the light cone: $\omega_{T,k}$ and $\omega_{L,k}$, respectively. This means that - up to the sign - transverse and longitudinal gluons have the same dispersion relations as their anti(quasi)particle counterparts. The

⁷Thus, Landau damping prevents the collisionless plasma from becoming unstable. In contrast, Cherenkov instabilities, i.e. the gauge field gaining energy from the particles, may occur in some non-Maxwellian plasmas where states of higher energy are more populated than states of lower energy, e.g. a beam-plasma system. [TL97]

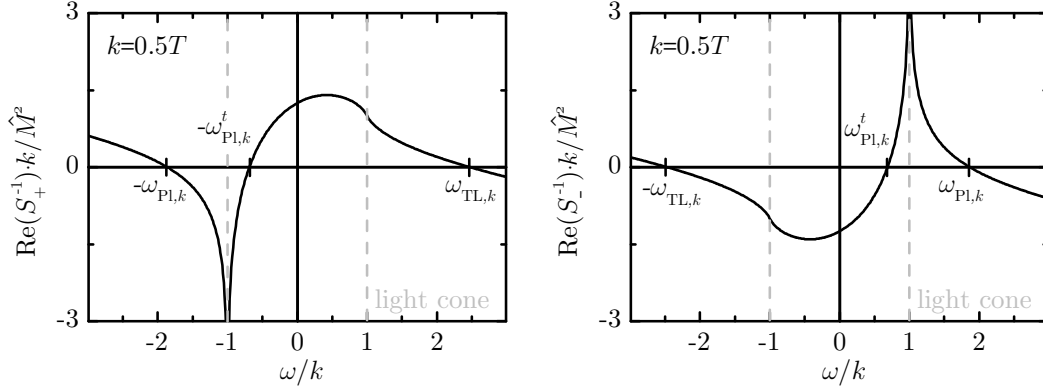


Figure 2.6: The real parts of the inverse quark propagators S_{\pm}^{-1} scaled by the fermionic mass parameter squared are shown as functions of the energy ω scaled by the momentum k which is fixed at $k = 0.5T$. The real part of neither inverse quark propagator shows any symmetry with respect to ω . However, there a parity relation $\text{Re}S_{+}^{-1}(-\omega) = -\text{Re}S_{-}^{-1}(\omega)$ between the two holds. The tachyonic dispersion relation $\omega_{PI,k}^t$ is due to Landau damping.

additional tachyonic dispersion relation for longitudinal gluons is related to Landau damping. Figure 2.5 explicitly shows the real parts for fixed momentum $k = 0.5T$.

The inverse quark propagators are not symmetric for themselves but, as a consequence of (2.29), satisfy the parity property (cf. Figure 2.6)

$$\text{Re}S_{+}^{-1}(-\omega) = -\text{Re}S_{-}^{-1}(\omega). \quad (2.31)$$

This is a sign of the intricate nature of both propagators: quarks are described by the positive energy dispersion relation of S_{+}^{-1} , while the dispersion relation of antiquarks is found from the negative energy solution of $\text{Re}S_{-}^{-1} = 0$. The remaining two dispersion relations represent collective quark excitations: the positive energy dispersion relation of S_{-}^{-1} describes the plasminos, while the negative energy solution of $\text{Re}S_{+}^{-1} = 0$ represents antiplasminos. Again, a tachyonic solution appears within the regime of Landau damping.

The evolution of the zeros of the real part of the inverse retarded propagators as a function of the momentum k gives the dispersion relations $\omega_{i,k}$. It is one of the difficulties of the subject at hand that these dispersion relations cannot be expressed as analytic functions $\omega(k)$: $\text{Re}D_i^{-1}(\omega, k, \Pi_i(\omega, k)) = 0$ and $\text{Re}S_i^{-1}(\omega, k, \Sigma_i(\omega, k)) = 0$ lead to transcendental equations since the self-energies cannot analytically be resolved for ω . Instead, they have to be solved numerically.

The results are shown in Figures 2.7 and 2.8. Due to the parity property (2.31) quarks and antiquarks obey identical dispersion relations up to the sign as do plasminos and antiplasminos.

Asymptotic dispersion relations and quark restmasses

It turns out useful to have explicit dispersion relations $\omega_i(k)$ in order to acquire simple analytic expressions for the thermodynamic variables by using asymptotic dispersion relations near the light cone instead of the full HTL dispersion relations. For transverse gluons, where $\text{Re}D_T^{-1} = -\omega_{T,k}^2 + k^2 + \text{Re}\Pi_T(\omega_{T,k}, k) \stackrel{!}{=} 0$, this is done by a first order iterative approximation

$$\omega_{T,k}^2 = k^2 + \text{Re}\Pi_T(\omega_{T,k}, k) \approx k^2 + \text{Re}\Pi_T(k, k) \quad (2.32)$$

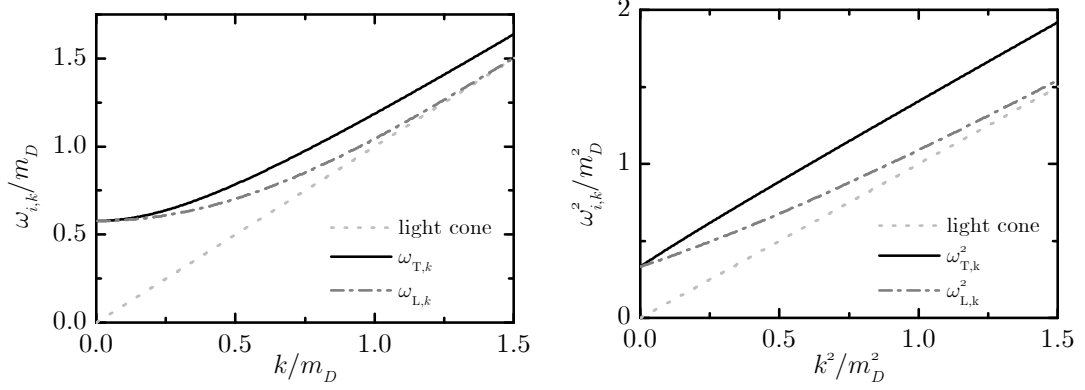


Figure 2.7: The dispersion relations $\omega_{T,k}$ of transverse and $\omega_{L,k}$ of longitudinal gluon modes scaled by the Debye mass are shown as functions of the momentum k scaled by the Debye mass in linear (left) and quadratic (right) scales.

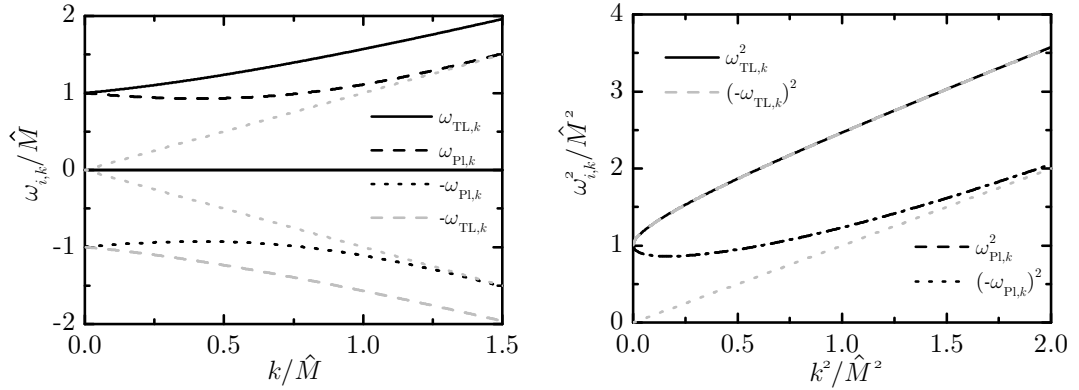


Figure 2.8: The dispersion relations $\omega_{i,k}$ of quarks (solid black), antiquarks (dashed grey), plasminos (black dashes) and antiplasminos (black points) scaled by the fermionic mass parameter are shown as functions of the momentum k scaled by the fermionic mass parameter in linear (left) and quadratic (right) scales. The dispersion relations of quarks and antiquarks as well as of plasminos and antiplasminos are equal up to the sign.

which gives a simple dispersion relation of the form

$$\omega_T^2(k) = k^2 + m_{g,\infty}^2 \quad (2.33)$$

with the asymptotic gluon mass $m_{g,\infty}^2 := \text{Re}\Pi_T(k, k) = m_D^2/2$, which is independent of both energy and momentum.

In order to derive the asymptotic dispersion relation for quarks from $\text{Re}S_+^{-1} = -\omega + k + \text{Re}\Sigma_+(\omega, k) \stackrel{!}{=} 0$ a factor k and some zeros are introduced:

$$0 = -\omega k + k^2 + \text{Re}\Sigma_+ k + \omega^2 - \omega^2 + \omega k - \omega k$$

which leads to

$$\omega^2 = (\omega - k)^2 + \text{Re}\Sigma_+ k + (k + \text{Re}\Sigma_+)k.$$

The difference $(\omega - k)^2$ can be neglected near the light cone and $\text{Re}\Sigma_+(\omega, k)$ is again approximated by its first order iteration $\text{Re}\Sigma_+(k, k)$. If ω is positive, the result

$$\omega_{TL}^2(k) = k^2 + m_{q,\infty}^2 \quad (2.34)$$

is the asymptotic dispersion relation for quarks with the asymptotic quark mass $m_{q,\infty}^2 := 2\text{Re}\Sigma_+(k,k)k = 2\hat{M}^2$. Even more, due to the fact that the squared dispersion relations of quarks and antiquarks are identical, this is also the asymptotic dispersion relation of antiquarks for negative ω .

The quality of the approximations is best estimated by a direct comparison of full and asymptotic dispersion relations, as done in Figure 2.9. For $k > m_D$ or $2\hat{M}$ both dispersion relations are virtually indistinguishable. Since the main contributions to thermodynamic integrals are found at momenta k of order T , while m_D and M are of order gT (eq. (2.22)), the asymptotic dispersion relations are good approximations of the full dispersion relations.

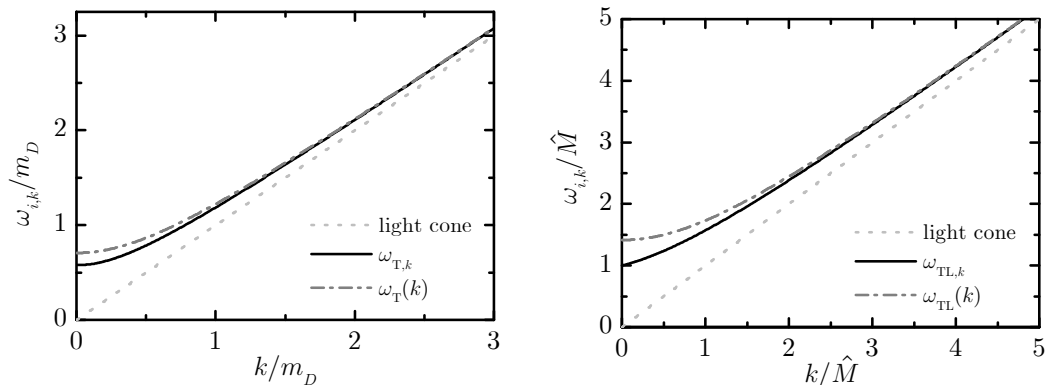


Figure 2.9: The full (solid lines) and asymptotic (dash dotted lines) dispersion relations for transverse gluons (left) and quarks (right) scaled by their respective mass parameters are shown as functions of the momentum k also scaled by the respective mass parameter. For large momenta (near the light cone) the asymptotic expressions prove to be good approximations of the full dispersion relations $\omega_{i,k}$.

These results are obtained and valid for the chiral limit. In order to compare with lattice calculations of quarks with nonzero quark rest masses they need to be modified. Assuming a current quark rest mass m_q in the order of the thermal quark mass $\sim gT$ or lower, this can be done by introducing additional terms related to the rest mass into the asymptotic mass [Pes98, Pis89b, Blu04]⁸

$$\tilde{m}_{i,\infty}^2 = m_i^2 + 2m_i m_{i,\infty} + 2m_{i,\infty}^2. \quad (2.35)$$

The index i denotes either light quarks q with $m_{q,\infty}^2 = 2\hat{M}_q^2 = 2\hat{M}^2$, strange quarks s with $m_{s,\infty}^2 = 2\hat{M}_s^2 = 2\hat{M}^2|_{\mu=0}$ or gluons g , where $m_g = 0$ and therefore $\tilde{m}_{g,\infty}^2 := m_{g,\infty}^2 = m_D^2/2$.

2.6 The HTL grand canonical potential

Given the explicit form of the HTL self-energies and the respective propagators, the remaining traces tr in eq. (2.16) can be evaluated. Taking the trace in Minkowski space, the gluonic part decomposes into three contributions for one longitudinal and two (equivalent) transverse polarizations, while the quark contribution becomes the sum of the normal and the abnormal quark branch (positive and negative chirality

⁸It has recently been pointed out [Sei07] that this treatment might be valid at zero momentum only and that the term linear in the rest mass should be omitted. Since this still remains to be confirmed and only minimal deviations are expected, this work continues to use the established procedure also used in [KBS06, BKS06, BKS07a, BKS07b].

over helicity ratio, respectively) when taking the Dirac trace. The remaining traces are simple, as they only give overall factors: the color trace ($N_c^2 - 1$) for the gluons and N_c for the quarks, and the flavor and spin traces for quarks an additional $2N_f$. Therefore, we define the prefactors $d_g = N_c^2 - 1$ and $d_q = 2N_c N_f$.

For brevity we introduce the abbreviation $\int_{d^4k} = \int d^4k/(2\pi)^4$. The HTL grand canonical potential then reads (cf. [BIR01])

$$\begin{aligned} \frac{\Omega}{V} &= d_g \int_{d^4k} n_B \left\{ 2\text{Im}(\ln D_T^{-1} - D_T \Pi_T) + \text{Im}(\ln(-D_L^{-1}) + D_L \Pi_L) \right\} \\ &\quad + 2d_q \int_{d^4k} n_F \left\{ \text{Im}(\ln S_+^{-1} - S_+ \Sigma_+) + \text{Im}(\ln(-S_-^{-1}) + S_- \Sigma_-) \right\} - \frac{T}{V} \Gamma_2. \end{aligned} \quad (2.36)$$

2.7 Effective coupling

Obviously, 2-loop QCD is only a crude approximation of the full theory. In order to accommodate further non-perturbative effects within the quasiparticle model, we introduce some flexibility by parameterizing the QCD coupling constant g^2 in a physically motivated way.

In doing so we utilize the renormalized coupling [PDG06] at truncated (i.e. neglecting a term involving $\ln^{-2}(\bar{\mu}^2/\Lambda^2)$ which is only a small correction for $\bar{\mu}^2 \approx \Lambda^2$) 2-loop order:

$$g^2(\bar{\mu}) = \frac{16\pi^2}{\beta_0 \ln(\bar{\mu}^2/\Lambda^2)} \left(1 - \frac{2\beta_1}{\beta_0^2} \frac{\ln[\ln(\bar{\mu}^2/\Lambda^2)]}{\ln(\bar{\mu}^2/\Lambda^2)} \right), \quad (2.37)$$

where $\beta_0 = 11/3 - 2N_f/3$ and $\beta_1 = 51 - 19N_f/3$. It depends on the ratio of the renormalization scale $\bar{\mu}$ and the QCD scale parameter Λ . The first one is usually taken to be the first Matsubara frequency $2\pi T$, while the latter one is just a parameter to be adjusted using experimental data. Introducing the pseudocritical temperature of QCD matter at vanishing net baryon density T_c and substituting $\Lambda \rightarrow 2\pi T_c/\lambda$, we arrive at another valid parametrization, where the ratio $\bar{\mu}/\Lambda$ becomes $\lambda T/T_c$.

In order to avoid the Landau pole of $g^2(T/T_c)$ at T_c , the QCD coupling is substituted by an *effective coupling* $G^2(T)$ which is shifted by a temperature T_s

$$G^2(T \geq T_c, \mu = 0) = \frac{16\pi^2}{\beta_0 \ln\left(\frac{T-T_s}{T_c/\lambda}\right)^2} \left(1 - \frac{4\beta_1}{\beta_0^2} \frac{\ln\left[\ln\left(\frac{T-T_s}{T_c/\lambda}\right)^2\right]}{\ln\left(\frac{T-T_s}{T_c/\lambda}\right)^2} \right). \quad (2.38)$$

While G^2 behaves well within the plasma phase, it is still infrared (IR) divergent within the hadronic phase. This is remedied by introducing a phenomenological IR regulator (cf. section 3.2).

2.8 The entropy density

Differentiating the thermodynamic potential with respect to the temperature at constant chemical potential gives the entropy as one of the state variables of the QGP. In contrast to the pressure, which is influenced by vacuum fluctuations, the entropy is sensitive to thermal excitations only and therefore manifestly ultraviolet (UV) finite. As such, it is ideally suited to investigate the properties of the QGP.

Due to the stationarity of the thermodynamic potential with respect to the full propagators, only the statistical distribution functions that explicitly depend on the temperature need to be differentiated, i.e.

$$\frac{\partial \Omega}{\partial T} = \frac{\partial \Omega}{\partial T} \Big|_{\text{expl.}} + \underbrace{\frac{\delta \Omega}{\delta D_i}}_0 \frac{\partial D_i}{\partial T} + \frac{\delta \Omega}{\delta D_{0,i}} \underbrace{\frac{\partial D_{0,i}}{\partial T}}_0. \quad (2.39)$$

Using $\text{Im}(D_T \Pi_T) = \text{Re} D_T \text{Im} \Pi_T + \text{Im} D_T \text{Re} \Pi_T$, the entropy density can be written as

$$s := -\frac{1}{V} \frac{\partial \Omega}{\partial T} \Big|_{\mu} = s_{g,T} + s_{g,L} + s_{q,+} + s_{q,-} + s' \quad (2.40)$$

with

$$\begin{aligned} s_{g,T} &= -2d_g \int \frac{d^4 k}{(2\pi)^4} \frac{\partial n_B(\omega)}{\partial T} \left\{ \text{Im} \ln(+D_T^{-1}) - \text{Re} D_T \text{Im} \Pi_T \right\}, \\ s_{g,L} &= -d_g \int \frac{d^4 k}{(2\pi)^4} \frac{\partial n_B(\omega)}{\partial T} \left\{ \text{Im} \ln(-D_L^{-1}) + \text{Re} D_L \text{Im} \Pi_L \right\}, \\ s_{q,\pm} &= -2d_q \int \frac{d^4 k}{(2\pi)^4} \frac{\partial n_F(\omega)}{\partial T} \left\{ \text{Im} \ln(\pm S_{\pm}^{-1}) \mp \text{Re} S_{\pm} \text{Im} \Sigma_{\pm} \right\} \end{aligned} \quad (2.41)$$

and a residual entropy density s' . While each of the first four terms in (2.40) describes the entropy density of one particle species in the absence of the others, s' can be interpreted as the interaction entropy density between the different contributions. It contains the terms of the form $\text{Im} D_T \text{Re} \Pi_T$ and the derivative of $\Gamma_2 T$ with respect to the temperature. At 2-loop order, these terms exactly cancel each other and thus $s' = 0$ [BIR01]. In fact, this seems to be a topological feature [CP75] which has explicitly been proven for QED [VB98] and Φ^4 theory [Pes01] too. The conclusion is that there is no interaction between the four constituents of the quark-gluon plasma at 2-loop order, and it is justified to speak of quasiparticles.

We now focus on the terms $\text{Im} \ln(\pm D_{T,L}^{-1})$ and $\text{Im} \ln(\pm S_{\pm}^{-1})$, which equal the argument of the respective inverse propagators (Appendix B.1), and proceed by substituting the argument by the arc tangent (Appendix B.1), giving rise to an additional term compensating for its periodicity:

$$\text{Im}(\ln D_T^{-1}) = \arctan\left(\frac{\text{Im} D_T^{-1}}{\text{Re} D_T^{-1}}\right) + \pi \varepsilon(\text{Im} D_T^{-1}) \Theta(-\text{Re} D_T^{-1}), \quad (2.42)$$

$$\text{Im}(\ln(-D_L^{-1})) = \arctan\left(\frac{\text{Im} D_L^{-1}}{\text{Re} D_L^{-1}}\right) - \pi \varepsilon(\text{Im} D_L^{-1}) \Theta(+\text{Re} D_L^{-1}). \quad (2.43)$$

Similar expressions apply for the two quark propagators: one has to substitute S_+^{-1} for D_T^{-1} in (2.42) and S_-^{-1} for D_L^{-1} in (2.43).

From the properties of the imaginary parts of the self-energies (2.30), we find $\varepsilon(\text{Im} D_i^{-1}(\omega)) = -\varepsilon(\omega)$ for the gluons and $\varepsilon(\text{Im} S_{\pm}(\omega)) \equiv -1$ for the normal and

abnormal quark branches. We end up with

$$\begin{aligned}
s_{g,T} &= +2d_g \int_{d^4k} \frac{\partial n_B}{\partial T} \left\{ \pi \varepsilon(\omega) \Theta(-\text{Re}D_T^{-1}) - \arctan \frac{\text{Im}\Pi_T}{\text{Re}D_T^{-1}} + \text{Re}D_T \text{Im}\Pi_T \right\}, \\
s_{g,L} &= -d_g \int_{d^4k} \frac{\partial n_B}{\partial T} \left\{ \pi \varepsilon(\omega) \Theta(+\text{Re}D_L^{-1}) - \arctan \frac{\text{Im}\Pi_L}{\text{Re}D_L^{-1}} + \text{Re}D_L \text{Im}\Pi_L \right\}, \\
s_{q,\pm} &= \pm 2d_q \int_{d^4k} \frac{\partial n_F}{\partial T} \left\{ \pi \Theta(\mp \text{Re}S_{\pm}^{-1}) - \arctan \frac{\text{Im}\Sigma_{\pm}}{\text{Re}S_{\pm}^{-1}} + \text{Re}S_{\pm} \text{Im}\Sigma_{\pm} \right\}.
\end{aligned} \tag{2.44}$$

The partial entropy densities (2.44) and therefore the whole entropy density expression are independent of possible renormalization factors. As required, the expression is also explicitly UV finite, as the derivatives of the distribution functions soften the UV behavior.

The quark entropy density $s_q = s_{q,+} + s_{q,-}$ can be simplified by utilizing the parity properties for quark propagators (2.31) and self-energies (2.29). Introducing the distribution function of antiparticles

$$n_F^A = \frac{1}{e^{\beta(\omega+\mu)} + 1} \tag{2.45}$$

with

$$\frac{\partial n_F(-\omega)}{\partial \omega} = -\frac{\partial n_F^A(\omega)}{\partial \omega} \tag{2.46}$$

and substituting $\omega \rightarrow -\omega$ within $s_{q,-}$, we find

$$s_q = 2d_q \int_{d^4k} \left(\frac{\partial n_F}{\partial T} + \frac{\partial n_F^A}{\partial T} \right) \left\{ \pi \Theta(-\text{Re}S_+^{-1}) - \arctan \left(\frac{\text{Im}\Sigma_+}{\text{Re}S_+^{-1}} \right) + \text{Re}S_+ \text{Im}\Sigma_+ \right\}. \tag{2.47}$$

Regarding the quasiparticle pole term $\pi \Theta(-\text{Re}S_+^{-1})$, the energy integration from $-\infty$ to 0 gives the (anti)plasmino contribution, the integration from 0 to $+\infty$ the contributions of the (anti)particles to the entropy density. Isolating both parts of the spectrum by applying the parity properties once more gives the explicit expressions

$$\begin{aligned}
s_{q,TL} &= 2d_q \int_{d^3k} \int_0^{\infty} \frac{d\omega}{2\pi} () \left\{ \pi \Theta(-\text{Re}S_+^{-1}) - \arctan \left(\frac{\text{Im}\Sigma_+}{\text{Re}S_+^{-1}} \right) + \text{Re}S_+ \text{Im}\Sigma_+ \right\}, \\
s_{q,Pl} &= -2d_q \int_{d^3k} \int_0^{\infty} \frac{d\omega}{2\pi} () \left\{ \pi \Theta(\text{Re}S_-^{-1}) - \arctan \left(\frac{\text{Im}\Sigma_-}{\text{Re}S_-^{-1}} \right) + \text{Re}S_- \text{Im}\Sigma_- \right\},
\end{aligned} \tag{2.48}$$

where the sum of the derivatives of the distribution functions is abbreviated by the parentheses (). While this separation seems straightforward, it has to be handled with care as the Landau damping term within the quark self-energies Σ_{\pm} (see the imaginary parts in Figure 2.4) can in general not be separated into quark and plasmino contributions in this simple way.

2.9 Lattice QCD

Lattice rest masses and critical temperature

Most of the past work on the QPM has been tested against lattice data from [Pei00, KLP00] that used rather large and temperature dependent lattice restmasses

of $m_q = 0.4T$ and $m_s = 1.0T$ ($\sim 0.5 \dots 1$ GeV). These have to be compared to the physical quark masses $m_{u,d} \sim 10$ MeV and $m_s \sim 90 - 150$ MeV [PDG06]. Recently, new lattice data has become available [Kar07], which relies on lattice restmasses much closer to the physical quark masses:

$$m_i = \begin{cases} 0.024T & \text{for } q \\ 0.24T & \text{for } s. \end{cases} \quad (2.49)$$

By using eq. (2.35) they are accommodated in the quasiparticle model. As it turns out, the restmasses are small enough to have negligible influence on the results compared to the influence of the asymptotic approximation of the dispersion relation. Therefore, chapter 6 explores a model using full HTL dispersion relations.

While the lattice data from [Pei00, KLP00] used a critical temperature T_c of 170 MeV, the results within [Kar07] were computed using $T_c = 192$ MeV. Within this work we use lattice data of dimensionless quantities e.g. s/T^3 as a function of dimensionless quantities, e.g. T/T_c . Therefore the uncertainty of the pseudocritical temperature has no effect on the results.

To adjust the QPM to the lattice results, we minimize the expression $\chi_y^2/N := \sum_{i=1}^N (y_i - y_i^{\text{lat}})^2/N$, where y is a dimensionless quantity being compared to the lattice result y^{lat} at N (not necessarily equidistant) points indexed by i .

Continuum extrapolation

Lattice calculations are performed on a finite lattice, while our quasiparticle model is formulated in the thermodynamic limit, i.e. aimed at describing a spatially infinite plasma. In order to compare our model with lattice data, the proper continuum extrapolation of the latter one is required.

A safe continuum extrapolation is a fairly demanding work. Therefore, various estimates have been applied, e.g. simply scaling the lattice results by a factor being strictly valid only for asymptotically high temperatures or for the non-interacting limit. To account for some deficit of such rough continuum estimates of the lattice data we introduce an ad hoc scaling factor d_{lat} .

3 The effective quasiparticle model

3.1 Necessary approximations

In order to derive the effective (or simple) quasiparticle model, several assumptions are made:

1. the quasiparticle widths as well as damping effects (i.e. the imaginary parts of the self-energies) are small and can be ignored,
2. the collective excitations, i.e. plasmons and (anti)plasminos, are exponentially suppressed¹ and can therefore be neglected,
3. the asymptotic dispersion relations $\omega_i^2 = k^2 + \tilde{m}_{i,\infty}^2$ are good approximations of the full HTL dispersion relations for thermallike momenta as relevant in thermodynamic integrals.

Neglecting collective modes and damping effects can be justified phenomenologically. Both are bound to the medium frame of reference and thus show only minimal effects on particles at high momenta.

Starting with the first and second approximation, the quark entropy density becomes

$$s_q^{eQP} = 2d_q \int \frac{d^3k}{(2\pi)^3} \int_0^\infty \frac{d\omega}{2\pi} \left(\frac{\partial n_F(\omega)}{\partial T} + \frac{\partial n_F^A(\omega)}{\partial T} \right) \pi \Theta(-\text{Re}S_+^{-1}), \quad (3.1)$$

where (anti)plasminos have been neglected by changing the lower integration limit from $-\infty$ to 0. We use the label eQP as abbreviation for the effective QPM. For gluons we find

$$s_g^{eQP} = 2d_g \int \frac{d^3k}{(2\pi)^3} \int_{-\infty}^{+\infty} \frac{d\omega}{2\pi} \frac{\partial n_B(\omega)}{\partial T} \pi \varepsilon(\omega) \Theta(-\text{Re}D_T^{-1}), \quad (3.2)$$

where the collective longitudinal excitations have been ignored in line with the second assumption.

In order to arrive at an explicit expression for the quasiparticle entropy density, first the transverse gluon dispersion relation is replaced by its asymptotic equivalent. Using the symmetry of the integrand and defining $\sigma_B(\omega) := \beta\omega n_B(\omega) - \ln(1 - e^{-\beta\omega})$ with

$$\frac{\partial \sigma_B}{\partial \omega} = -\frac{\partial n_B(\omega)}{\partial T} \quad (3.3)$$

¹That is after calculating the propagators using Dyson's relation from the HTL self-energies, the residues of the poles in the spectral density of both plasmon and (anti)plasmino propagators vanish exponentially for momenta $k \sim T, \mu$, which give the dominant main contributions to thermodynamic integrals.

integrations by parts are performed. We start from

$$\begin{aligned}
s_g^{eQP} &= 2d_g \int \frac{d^3k}{(2\pi)^3} \int_0^\infty d\omega \underbrace{\frac{\partial n_B(\omega)}{\partial T}}_{-\frac{\partial \sigma_B}{\partial \omega} = u'} \underbrace{\Theta(-\text{Re}D_T^{-1})}_{\Theta(\omega^2 - \omega_T^2(k))=v}, \\
s_g^{eQP} &= 2d_g \int \frac{d^3k}{(2\pi)^3} \left(- \left[\sigma_B(\omega) \Theta(\omega^2 - \omega_T^2(k)) \right]_0^\infty \right. \\
&\quad \left. + \int_0^\infty d\omega \sigma_B(\omega) \left[\delta(\omega - \omega_T(k)) - \delta(\omega + \omega_T(k)) \right] \right). \tag{3.4}
\end{aligned}$$

The first term does not contribute since $\sigma_B(\omega \rightarrow \infty) = \Theta(0 - \omega_T^2(k)) = 0$ as does $\delta(\omega + \omega_T(k))$ due to the energy integration limits. The final result for the eQP gluon entropy is

$$\begin{aligned}
s_g^{eQP} &= 2d_g \int \frac{d^3k}{(2\pi)^3} \sigma_B|_{\omega_T(k)} \\
&= \frac{d_g}{\pi^2} \int_0^\infty dk k^2 \left\{ \beta \omega_T(k) n_B(\omega) - \ln \left(1 - e^{-\beta \omega_T(k)} \right) \right\} \tag{3.5}
\end{aligned}$$

which formally looks like the ideal gas entropy density of particles with mass $\tilde{m}_{g,\infty}$.

Equivalently, using $\sigma_F^{(A)}(\omega) = \beta(\omega \pm \mu) n_F^{(A)}(\omega) + \ln(1 + \exp(-\beta(\omega \pm \mu)))$ and the asymptotic quark dispersion relation $\omega_{TL}(k)$ instead of the full dispersion relation $\omega_{TL,k}$, the quark entropy density contribution is found to be

$$\begin{aligned}
s_q^{eQP} &= 2d_q \int \frac{d^3k}{(2\pi)^3} \left\{ \sigma_F|_{\omega_{TL}(k)} + \sigma_F^A|_{\omega_{TL}(k)} \right\} \\
&= \frac{d_q}{\pi^2} \int_0^\infty dk k^2 \left\{ \beta(\omega_{TL}(k) - \mu) n_F(\omega_{TL}(k)) + \ln \left(1 + e^{-\beta(\omega_{TL}(k) - \mu)} \right) \right. \\
&\quad \left. + \beta(\omega_{TL}(k) + \mu) n_F^A(\omega_{TL}(k)) + \ln \left(1 + e^{-\beta(\omega_{TL}(k) + \mu)} \right) \right\}. \tag{3.6}
\end{aligned}$$

In order to allow the simultaneous treatment of quark and gluon entropy densities, a short-hand notation of the statistical distribution functions is introduced:

$$\begin{aligned}
f_\pm &:= \frac{1}{e^\mp + S_i}, \\
e^\mp &:= e^{\beta(\omega_i \mp \mu_i)}, \tag{3.7}
\end{aligned}$$

where the spin factor S_i is +1 for quarks and -1 for gluons. The dependence of f_\pm and e^\mp on the quasiparticle species $i = g, q$ is implied. In the limit $\mu = 0$, $e^+ = e^-$ is abbreviated as e and $f_+ = f_-$ as f . Integrating the logarithmic terms in (3.5) and (3.6) by parts gives the common expression

$$s_i^{eQP} = \frac{d_i}{2\pi T} \int_0^\infty dk k^2 \left\{ \frac{\frac{4}{3}k^2 + \tilde{m}_{i,\infty}^2}{\omega_i(k)} [f_+ + f_-] - \mu_i [f_+ - f_-] \right\}. \tag{3.8}$$

For comparison with $N_f = 2 + 1$ lattice data an extension of the QPM to include a third, heavier quark flavor (*strange*) with $\mu_s = 0^2$ is necessary. Equation (3.8), using fermionic spin factor $S_s = +1$, asymptotic mass $\tilde{m}_{s,\infty}^2$ and degeneracy prefactor $d_s = 2N_c N_h$, provides the heavy quark entropy density. The number of heavy quarks N_h is set to 1 if strange quarks represent a relevant degree of freedom.

3.2 Outline of the model

Since the entropy density of the quark-gluon plasma in 2-loop QCD is the sum of the single quasiparticle entropy density contributions, it can be considered as mixture of non-interacting ideal quasiparticle gases. It is natural to assume that the pressure, which follows from the entropy density by integration, consists of single partial pressures, too. Therefore, we use the following expression for the pressure

$$p^{eQP}(T, \mu) = \sum_{g,q,(s)} p_i^{eQP}(T, \mu) - B^{eQP}(\tilde{m}_{j,\infty}(\mu, T)), \quad (3.9)$$

where B^{eQP} is the pressure difference to the vacuum. Since QCD is asymptotically free, B^{eQP} is minimal if the plasma is located within the smallest volume possible - a bag within the vacuum. This is why B is sometimes referred to as *bag pressure*.

The ansatz has to satisfy

$$s_i^{eQP} = \left. \frac{\partial p_i^{eQP}}{\partial T} \right|_{\mu} \quad (3.10)$$

which leads to

$$p_i^{eQP}(T, \mu) = \frac{d_i}{6\pi^2} \int_0^{\infty} dk \frac{k^4}{\omega_i} [f_+ + f_-], \quad (3.11)$$

where the integrability condition

$$\frac{\partial B^{eQP}}{\partial \tilde{m}_{j,\infty}^2} = \frac{\partial p^{eQP}}{\partial \tilde{m}_{j,\infty}^2} \quad (3.12)$$

has to be fulfilled. It also ensures the stationarity of the thermodynamic potential under functional variation with respect to the asymptotic masses [GY95].

The pressure completely defines the model. All thermodynamic quantities can be derived from it, e.g. the net particle density $n^{eQP} = \partial p^{eQP} / \partial \mu|_T = \sum_{g,q,(s)} n_i^{eQP}$ with

$$n_i^{eQP} = \frac{d_i}{2\pi^2} \int_0^{\infty} dk k^2 [f_+ - f_-] \quad (3.13)$$

²Generally, the strange quark chemical potential μ_s also has to be included in the description of the considered plasma. However, if the net strangeness given by a certain initial condition is zero and there is no overall change of net strange quark number (e.g. due to strangeness conservation in strong interaction processes) μ_s vanishes. This constellation with $\mu_s = 0$ is referred to by a flavor number $N_f = 2 + 1$. It is a good approximation e.g. for heavy ion collisions, as proton and neutron are both comprised of u and d quarks only. While $s\bar{s}$ -pairs may appear, strangeness conservation could only be violated by weak interactions for which strong interaction time-scales are too short.

We just mention the case $N_f = 3$, where $\mu_s = \mu_q$ is assumed. Within this thesis μ_s is always zero. Therefore μ_q is the only nonzero chemical potential and is referred to as the quark chemical potential μ .

is found (an additional integration by parts has been performed). As a consequence of the definition of f_{\pm} , the net particle densities vanish for gluons and strange quarks as both should do due to $\mu_g = \mu_s = 0$.

Using the entropy density (3.8) and lattice data from [Kar07] the model parameters are adjusted to $T_s = -0.738T_c$, $\lambda = 5.93$, $\alpha = 0.941$ with $d_{\text{lat}} = 0.954$ (see Figures 4.1 and 4.2 in chapter 4).

3.3 Extension of the model to $\mu > 0$

In section 2.7 the effective coupling G^2 was parametrized for $\mu = 0$ only. In order to apply the eQP for nonzero chemical potential one has to map the coupling to finite μ by using the thermodynamic self-consistency of the model [Pes00]. More specifically this means one has to utilize the Maxwell relation

$$\left. \frac{\partial s}{\partial \mu} \right|_T = \left. \frac{\partial n}{\partial T} \right|_{\mu}. \quad (3.14)$$

The explicit derivatives of the distribution functions do not contribute due to Schwartz's theorem so that only the T and μ dependencies of the asymptotic masses have to be considered:

$$\left. \frac{\partial n_q^{eQP}}{\partial \tilde{m}_{q,\infty}^2} \frac{\partial \tilde{m}_{q,\infty}^2}{\partial T} \right|_{\mu} = \sum_{g,q,(s)} \left. \frac{\partial s_i^{eQP}}{\partial \tilde{m}_{i,\infty}^2} \frac{\partial \tilde{m}_{i,\infty}^2}{\partial \mu} \right|_T. \quad (3.15)$$

The derivatives of the asymptotic masses with respect to T and μ can be found in Appendix C.1. They contain derivatives of the effective coupling G^2 according to which the result is ordered. This leads to the flow equation

$$a_T^{eQP} \frac{\partial G^2}{\partial T} + a_{\mu}^{eQP} \frac{\partial G^2}{\partial \mu} = b^{eQP} \quad (3.16)$$

with the coefficients $a_T^{eQP}(\hat{M}^2(G^2))$, $a_{\mu}^{eQP}(\hat{M}^2(G^2), m_D^2(G^2))$ and $b^{eQP}(G^2, \hat{M}^2(G^2), m_D^2(G^2))$ - which all depend on T and μ explicitly and via the masses - given in Appendix D.

The flow equation is an elliptic quasilinear partial differential equation which is solved by the method of characteristics. A curve parameter x is introduced, assuming that $T = T(x)$, $\mu = \mu(x)$ and $G^2 = G^2(x)$. Then

$$\frac{dG^2}{dx} = G_{,T}^2 \frac{dT}{dx} + G_{,\mu}^2 \frac{d\mu}{dx}, \quad (3.17)$$

and the comparison with the flow equation gives a system of three linear, coupled ordinary differential equations: $G_{,x}^2 = -b^{eQP}$, $T_{,x} = -a_T^{eQP}$ and $\mu_{,x} = -a_{\mu}^{eQP}$. This system can be solved using standard numerical methods. The initial condition for the flow equation is the effective coupling at $\mu = 0$, with model parameters fixed by comparison of the eQP entropy density with lattice results.

From the explicit expressions of the coefficients a set of general properties of the solutions follows

- $a_T^{eQP}(T, \mu \rightarrow 0) = 0$ and $a_{\mu}^{eQP}(\mu, T \rightarrow 0) = 0$ cause the characteristics to approach the T and μ axis perpendicularly,

- $a_\mu^{eQP} < 0$ and $a_T^{eQP} > 0$ indicate that characteristics move in the direction of decreasing temperature and increasing chemical potential and
- $b^{eQP} < 0$ for $\mu \gtrsim 0$ causes an increasing coupling at the beginning of a characteristic, which together with
- $b^{eQP}(T, \mu \rightarrow 0) = 0$ implies that the coupling has a local minimum at $\mu = 0$.

To state this more explicitly

$$\left. \frac{\partial G^2}{\partial \mu} \right|_{\mu=0} = \left(\frac{b^{eQP}}{a_\mu^{eQP}} - \frac{a_T^{eQP}}{a_\mu^{eQP}} \frac{\partial G^2}{\partial T} \right) \Big|_{\mu=0} = 0. \quad (3.18)$$

Previous studies of the flow equation [Pes02, Blu04] have shown that the characteristic curves emerging at $T \approx T_c$ cross each other in some region of finite values of μ for parameters adjusted to lattice QCD results (cf. Figure 4.5 in chapter 4). This unfortunate feature prevents an unambiguous extrapolation of thermodynamic quantities in the full T - μ -plane. In work done by Romatschke [Rom04] it is claimed that these crossings can be avoided by taking into account collective modes and Landau damping.

Using the hint from [Blu04] that the crossings are due to the effective coupling G^2 being too large at the pseudocritical temperature, this can be explained. Since the eQP entropy density increases with decreasing mass parameters m_D^2 and \hat{M}^2 which are proportional to $G^2 T^2$ at $\mu = 0$, the crossings would therefore disappear for a larger eQP entropy density. One way to allow for a larger eQP entropy density is to take into account collective modes. As medium effects indicate correlations between the gas-like constituents of the eQP plasma, taking them into account causes a decrease of overall entropy density. Consequently, the eQP parameters have to change in order to still describe the lattice data causing the entropy density to increase. With the resulting decrease of the effective coupling G^2 the crossings then disappear (cf. chapter 6).

Another degree of freedom which is possibly suitable to decrease overall entropy density is a finite quasiparticle width. Depending on how the widths are introduced into the QPM, the crossings can thus be removed (cf. chapter 4 and section 5.2, respectively).

3.4 The pressure correction Taylor expansion coefficients

For the extension of the pressure to nonzero chemical potential, lattice calculations often use the coefficients of the Taylor series for the pressure correction $\Delta p(T, \mu) = p(T, \mu) - p(T, \mu = 0)$ with respect to μ/T

$$\frac{\Delta p(T, \mu)}{T^4} = \sum_{n=1}^{\infty} c_n(T) \left(\frac{\mu}{T} \right)^n, \quad c_n(T) = \frac{T^{n-4}}{n!} \left(\frac{\partial^n p}{\partial \mu^n} \right) \Big|_{\mu=0}. \quad (3.19)$$

In addition to the comparison with lattice data at $\mu = 0$ we are going to investigate whether alternative parametrizations of the effective coupling can improve the description of c_4 , maintaining the quality of c_2 .³

³As a general feature of the theory, all odd-numbered coefficients vanish in the limit $\mu \rightarrow 0$ due to sign changes of the respective derivatives of statistical distribution functions.

For the eQP the coefficients read as follows

$$\begin{aligned} c_2^{eQP} &= \frac{d_q}{2\pi^2 T^3} \int_0^\infty dk k^2 e f^2, \\ c_4^{eQP} &= \frac{d_q}{24\pi^2 T^3} \int_0^\infty dk k^2 e f^4 \left[3T(1 - e^2) \frac{\partial^2 \omega_{\text{TL}}}{\partial \mu^2} \Big|_{\mu=0} + e^2 - 4e + 1 \right] \end{aligned} \quad (3.20)$$

with

$$\frac{\partial^2 \omega_{\text{TL}}}{\partial \mu^2} \Big|_{\mu=0} = \frac{1}{3\omega_{\text{TL}}} \left[\frac{G^2}{\pi^2} + \frac{3m_q}{\pi^2 T} \sqrt{\frac{G^2}{6}} + \left(\frac{3m_q T}{2\sqrt{6}G^2} + \frac{T^2}{2} \right) \frac{\partial^2 G^2}{\partial \mu^2} \Big|_{\mu=0} \right], \quad (3.21)$$

where $\partial^2 G^2 / \partial \mu^2$ can be found by differentiating the flow equation with respect to μ . In the limit of vanishing chemical potential this leads to

$$\frac{\partial^2 G^2}{\partial \mu^2} \Big|_{\mu=0} = \left(\frac{1}{a_\mu} \frac{\partial b}{\partial \mu} - \frac{1}{a_\mu} \frac{\partial a_T}{\partial \mu} \frac{\partial G^2}{\partial T} \right) \Big|_{\mu=0} \quad (3.22)$$

with the derivatives of the flow equation coefficients given in Appendix D. The first term within c_4^{eQP} featuring the second derivative of the dispersion relation with respect to the chemical potential is responsible for a peak structure of this coefficient.

3.5 Extension of the model below the critical temperature

To prevent the divergence of the coupling G^2 below T_c , a phenomenological infrared cutoff for G^2 has to be applied. There are several possible ways, the most simple being a continuous linearization below the transition temperature [Blu04]

$$G_{\text{IR,lin}}^2(T < T_c, \mu = 0) = \frac{1 - \alpha \frac{T}{T_c}}{1 - \alpha} G^2 \Big|_{T=T_c, \mu=0}, \quad (3.23)$$

where α is the slope parameter.

The eQP model has been successfully tested using lattice data for the entropy density from [Pei00, KLP00] in [Blu04]. For $\mu \gtrsim 0$ the eQP pressure correction coefficients have been calculated and compared to lattice data from [All03] in [Blu04]. While the evolution of the second⁴ Taylor coefficient c_2 could be reproduced using the eQP, only approximate agreement with c_4 was achieved with the same set of parameters (see eQP in Figure 3.1).

3.6 Alternative parametrizations of the effective coupling

Introducing additional parameters into the effective coupling G^2 promises to provide us with a more flexible model. Two alternative parametrizations have been investigated.

Using a quadratic parametrization of the effective coupling

$$G_{\text{IR,quad}}^2(T < T_c, \mu = 0) = a \left(\frac{T^2}{T_c^2} - 1 \right) + b \left(\frac{T}{T_c} - 1 \right) + G^2 \Big|_{T=T_c, \mu=0} \quad (3.24)$$

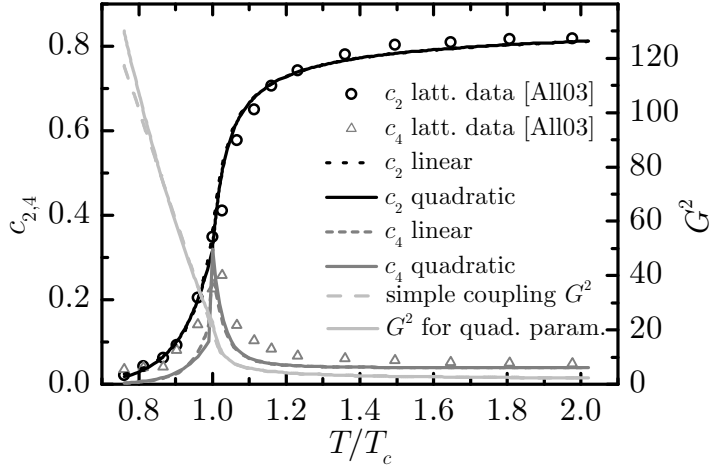


Figure 3.1: Comparison of the pressure correction coefficients c_2 and c_4 according to eq. (3.20) with lattice data from [All03]. The light grey curves exhibit the effective coupling G^2 (right scale). It can be seen that substituting the linear IR regulator ($T_s = -0.87T_c$, $\lambda = 11.9$ and $\alpha = 0.95$ resulting in $\chi^2(c_2)/N = 1.77 \times 10^{-4}$) by a quadratic parametrization ($T_s = -0.87T_c$, $\lambda = 12.1$, $a = 571$ and $b = -1451$ giving $\chi^2(c_2)/N = 1.71 \times 10^{-4}$) results in only minor improvement of the simultaneous description of both coefficients within the hadronic regime. The change in λ above T_c is necessary due to the correlation of the parametrizations by requiring a continuous connection at T_c .

with two parameters a and b below T_c did not significantly improve the quality of the concurrent description within the hadronic regime. As Figure 3.1 shows, the quadratic term does not contribute notably to the coupling.

Substituting

$$\left(\frac{T - T_s}{T_c/\lambda}\right)^2 \rightarrow \left(\frac{T - T_s - \frac{\kappa}{T}}{T_c/\lambda}\right)^2 \quad (3.25)$$

within (2.38) and thus introducing an additional parameter κ in the plasma regime did also not considerably improve the situation above T_c . κ is not the degree of freedom needed to allow for a simultaneously good description of both c_2 and c_4 (see Figure 3.2).

⁴The coefficients c_1 and c_3 are generally zero.

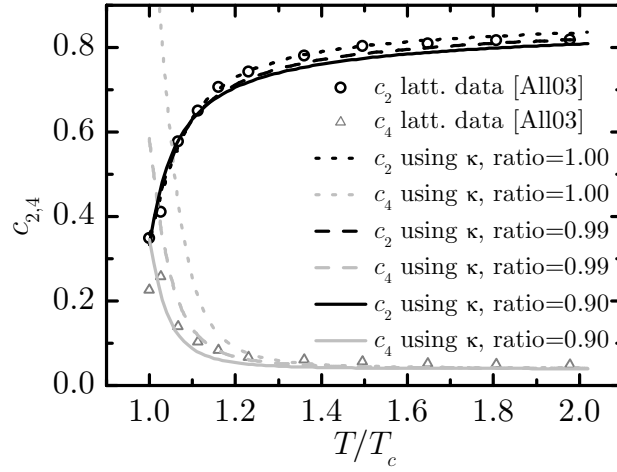


Figure 3.2: As Figure 3.1, but for the alternative parametrization of G^2 given by eq. (3.25). Introducing the additional degree of freedom within the plasma regime does not yield a noticeable improvement for the concurrent description of c_2 and c_4 . Shown are the best adjustments of the model for various ratios $\chi^2(c_2)/\chi^2(c_4)$. The region below T_c remains unchanged.

4 The distributed quasiparticle model

4.1 Outline of the model

One phenomenological method [And06, BB04, Bir06, Bra03] to include finite widths into a model is to convolute appropriate quantities describing the quasiparticles with a probability distribution function. Since the thermal masses of quasiparticles contain the information about the interaction, it is straightforward to choose these to be distributed. As for the eQP they are approximated by the asymptotic masses $\tilde{m}_{i,\infty}$ which for brevity are denoted by m_i . Also, since damping effects in many areas of physics can be described using Breit-Wigner distributions,¹ we choose the following ansatz:

$$\begin{aligned} p^{dQP}(T, \mu) &= \sum_{i=q,s,g} \int_0^\infty dM p_i^{eQP}(T, \mu) \Big|_{m_i \rightarrow M} \text{BW}(m_i, M, \Gamma) - B(m_j) \\ &= \sum_{i=q,s,g} \frac{d_i}{6\pi^2} \int_0^\infty dM \int_0^\infty dk \frac{k^4}{\omega} [f_+ + f_-] \text{BW}(m_i, M, \Gamma) - B(m_j), \end{aligned} \quad (4.1)$$

where

$$\text{BW}_i(m_i, M, \Gamma) = N_i \widetilde{\text{BW}}_i(m_i, M, \Gamma) \quad (4.2)$$

with

$$\widetilde{\text{BW}}_i(m_i, M, \Gamma) = \frac{\Gamma}{[m_i(G^2) - M]^2 + \frac{\Gamma^2}{4}} \quad (4.3)$$

is the Breit-Wigner distribution of the quasiparticle species i . Its shape is governed by the width parameter² Γ , which is assumed to be temperature and particle species independent. As there is only one common width for all particles, this phenomenological extension of the eQP is rather minimalistic. In section 4.6 a possible particle specific temperature dependence of Γ is considered.

The dispersion relation encoded in f_\pm is now given by $\omega^2 = k^2 + M^2$, allowing for off-shell quasiparticles. Since the integrands are continuous with respect to both M and k , the integration order can be interchanged. The normalization N_i of the mass distribution is

$$\begin{aligned} \frac{1}{N_i} &= \int_0^{M_{\max}} \widetilde{\text{BW}}_i dM \\ &= 2 \arctan \left(\frac{2(M_{\max} - m_i)}{\Gamma} \right) + \pi, \end{aligned} \quad (4.4)$$

¹Section 5.1 gives a more formal justification for the ansatz.

²This identification of Γ as the *width* has to be made with some caution. Due to the distribution function being cut off at $M = 0$, its FWHM (the second moment, its *width*) differs to some degree from the distribution parameter Γ . However, for reasonably small Γ the difference is minimal at best and it can safely be called *width*.

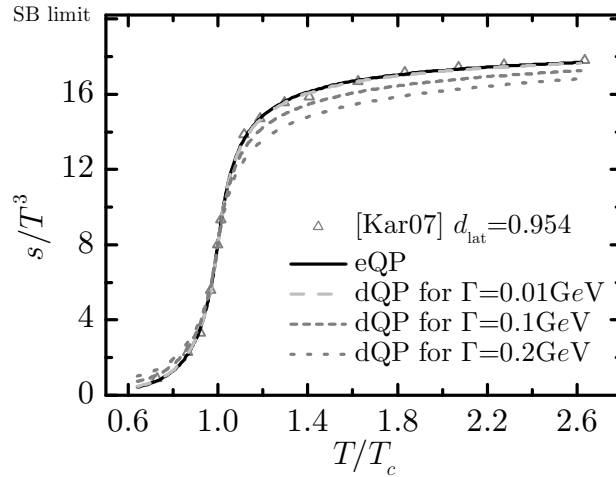


Figure 4.1: Scaled entropy densities s/T^3 of eQP and dQP are shown as functions of the temperature T scaled by the pseudocritical temperature T_c for fixed quasiparticle parameters $T_s = -0.738T_c$, $\lambda = 5.93$, $\alpha = 0.941$ and variable width parameter Γ . For reference, entropy density data from lattice calculations [Kar07] scaled with $d_{\text{lat}} = 0.954$ is indicated by the symbols. For small Γ dQP and eQP results are virtually indistinguishable; with increasing Γ , the dQP entropy density decreases for $T > T_c$ and increases for $T < T_c$.

where M_{max} is the upper limit used in the numeric integration. The normalization N_i explicitly depends on both Γ and the quasiparticle masses m_i and therefore also on the temperature.

Entropy density and particle density follow by differentiating the pressure with respect to the intrinsic quantities (cf. section 3.2). As for the eQP (cf. eq. 3.12), an integrability condition takes care of the derivative of the pressure with respect to the masses $m_i(T, \mu)$. Since the Breit-Wigner distribution does not explicitly depend on T and μ , it is unaffected by the differentiation. Therefore, the expressions of the distributed QPM (dQP) mirror the eQP formulas up to the additional mass distribution integral:

$$n_i^{dQP}(T, \mu) = \frac{d_i}{2\pi^2} \int_0^\infty dk dM k^2 [f_+ - f_-] \text{BW}_i(M) \quad (4.5)$$

and

$$s_i^{dQP}(T, \mu) = \frac{d_i}{2\pi^2 T} \int_0^\infty dk dM k^2 \left\{ \frac{\frac{4}{3}k^2 + M^2}{\omega_i} [f_+ + f_-] - \mu [f_+ - f_-] \right\} \text{BW}_i(M). \quad (4.6)$$

4.2 Test of the model at $\mu = 0$

Taking the limit $\Gamma \rightarrow 0$ leads to $\text{BW}(m, M, \Gamma) \rightarrow \delta(m - M)$ and thus $p^{dQP} \rightarrow p^{eQP}$, $s^{dQP} \rightarrow s^{eQP}$ and $n^{dQP} \rightarrow n^{eQP}$. The dQP exactly gives the eQP in the limit of vanishing width.³

³For further derivatives of the state variables, additional integrations by parts with respect to M may be necessary. As a representative, this is shown for c_2 in section 4.5.

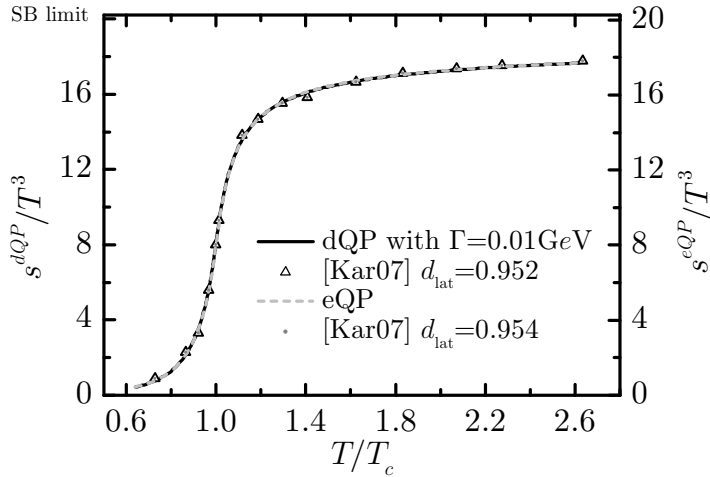


Figure 4.2: As Figure 4.1 but comparing the eQP ($T_s = -0.738T_c$, $\lambda = 5.93$, $\alpha = 0.941$ with $d_{\text{lat}} = 0.954$ resulting in $\chi^2_{s/T^3}/N = 0.0171$) and dQP ($T_s = -0.742T_c$, $\lambda = 6.01$, $\alpha = 0.942$ and $\Gamma = 0.010 \text{ GeV}$ with $d_{\text{lat}} = 0.952$ giving $\chi^2_{s/T^3}/N = 0.0160$) adjustments to lattice data for the entropy density from [Kar07].

Figure 4.1 displays the evolution of the entropy density for increasing values of Γ . Starting from small widths, where the eQP is reproduced, the entropy density steadily decreases for $T > T_c$ and slightly increases for $T < T_c$. The cause of this effect is discussed below in detail.

The adjustment of the dQP at $\mu = 0$ using lattice data (Figure 4.2) shows only a tiny improvement, which comes as no surprise since the data is already described in a close-to-perfect manner by the eQP. The minor decrease of χ^2_{s/T^3} is due to better agreement of the dQP entropy density with the lattice data at and close to T_c . However, due to the steep incline in this area this is visually hardly noticeable.

Note that the continuum extrapolation factor d_{lat} for both models is basically equal. As the same is found for several other models too, $d_{\text{lat}} \sim 0.95$ may be interpreted as a rough estimate of the actual continuum extrapolation factor.

4.3 General discussion of the ansatz

In order to become more acquainted with the dQP, the relation between temperature-independent particle width and particle mass (represented by the coupling G^2 to which the masses are closely related, see eqs. (2.22)) is investigated. In doing so, we require a perfect match with lattice data ([Pei00], $N_f = 2$).⁴ The results are shown in Figure 4.3. In order to understand the behavior we have to inspect the ansatz.

The procedure to introduce widths by convolution with a distribution function can be investigated on very general grounds. Leaving aside any explicit expression for the entropy density $s(M, T)$ and even allowing a possible temperature dependence of the width Γ , some intrinsic features of the ansatz

$$s(m, T) \Rightarrow \int dM s(M, T) BW(M, m, \Gamma) \quad (4.7)$$

⁴As the temperature dependent widths under investigation in section 4.6 depend on G^2 (cf. eq. (4.16)) this can be done for the temperature independent case only.

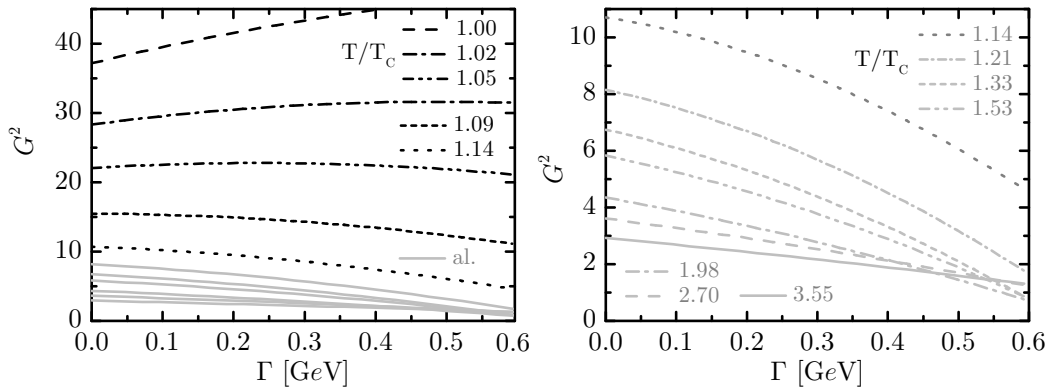


Figure 4.3: Dependence of G^2 on the width Γ of quasiparticles at various temperatures if entropy density data for $N_f = 2$ [Pei00] is to be accurately matched. The right Figure is a zoom into the region below $G^2 = 10$ of the left Figure; the solid grey curves in the left Figure are the curves shown in the right Figure.

can be found.

The entropy density $s(M, T)$ here is a monotonically decreasing but non-negative function of M with its maximum at $M = 0$ (since the phase space continuously grows for decreasing particle masses with zero being the lowest physically possible mass and s being non-negative per definitionem) for arbitrary T . $BW(M, m, \Gamma)$ is symmetric around m and normalized. Let Γ be reasonably smaller than m .

We first consider the case where s is simply inversely proportional to M . The convolution of s and BW is then governed by an increase of the entropy density for $M < m_i$ and an equivalent decrease for $M > m_i$. Since both changes are of the same order, BW keeps its normalization and the integration $\int_{-\infty}^{+\infty} s(M)BW(M, m)dM$ simply gives $s(m)$.

Generally, $s(M, T)$ is of a more involved nature, i.e. $\partial^2 s(M)/\partial M^2 \neq 0$. For those cases the changes of the entropy density above and below m_i do not compensate each other, and the integral $\int_{-\infty}^{+\infty} s(M)BW(M, m)dM$ does not coincide with $s(m)$.

If the second derivative is negative at m the entropy density is smaller than $s(m)$ since the entropy density decreases faster for $M < m_i$ than it increases for $M > m_i$. Analogously, the new entropy density is larger than $s(m)$ if the derivative is positive.

Both cases occur in our model due to the specific form of the entropy density (see Figure 4.4) which has a negative second derivative for rather small masses and a positive one for larger masses. The inflection point that separates both regimes is influenced by the temperature T from the statistical distribution function. It moves towards higher masses for increasing temperature.

Looking at Figure 4.3 while keeping in mind that G^2 is strongly related to our masses we can easily distinguish both cases. For large masses (close to T_c , where they account for the strongly decreasing entropy density, and at large temperatures T , where the effect is subdued by the mentioned increase of the inflection point) the increasing entropy density is compensated by increasing coupling G^2 (i.e. mass). The increase diminishes and is finally stopped because the Breit-Wigner peak stretches more and more into regions with negative second derivative. The opposite happens for small masses.

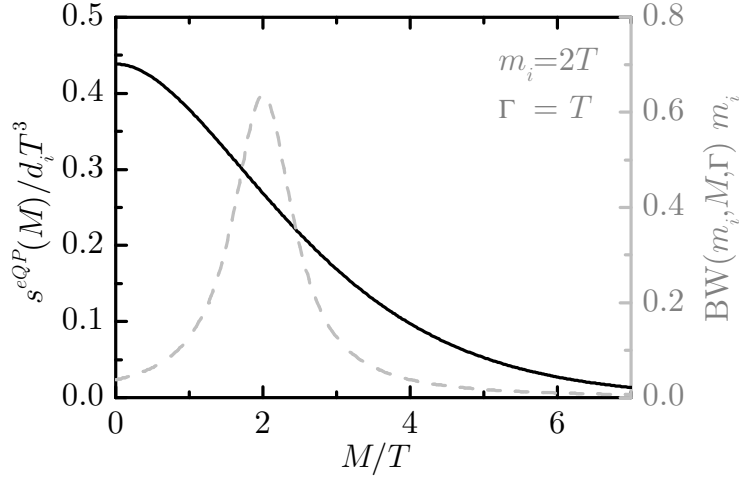


Figure 4.4: The two functions $s^{eQP}(M)$ (left ordinate) and $BW(m, M, \Gamma)$ (right ordinate) as functions of the mass parameter M . All quantities are scaled appropriately.

4.4 Extension to non-vanishing chemical potential

4.4.1 The flow equation

As outlined in section 3.3, a partial differential equation for the effective coupling G^2 can be found by imposing one of Maxwell's relations (cf. eq. (3.14)) on the model. For the dQP again the explicit derivatives cancel due to Schwarz's theorem and the general form of the resulting flow equation

$$a_T^{dQP} \frac{\partial G^2}{\partial T} + a_\mu^{dQP} \frac{\partial G^2}{\partial \mu} = b^{dQP} \quad (4.8)$$

remains unchanged. The new coefficients a_T^{dQP} , a_μ^{dQP} and b^{dQP} can be found in Appendix D. They retain the properties of the eQP flow equation coefficients, so that the characteristics show the same behavior and the effective coupling G^2 evolves in a similar way. The derivative of G^2 with respect to the chemical potential vanishes at $\mu = 0$ as for the dQP.

Solving the flow equation gives the remarkable result that the crossings (cf. section 3.3) disappear with increasing width if the remaining parameters remain fixed (see Figure 4.5).

Unfortunately, the width has to be of the order of 1 GeV to avoid all crossings near to T_c (see Figure 4.6). While widths of this order may be allowed in the transition region, even for extreme values of the remaining dQP parameters, lattice data cannot be described for higher temperatures. This is visualized in Figure 4.7 which shows the best possible adjustment of the dQP for $\Gamma = 1$ GeV.

4.4.2 Taylor coefficients of the pressure expansion

The pressure correction coefficients introduced in section 3.4 constitute another test of the dQP for nonzero quark chemical potential. Applying eq. (3.19) to the

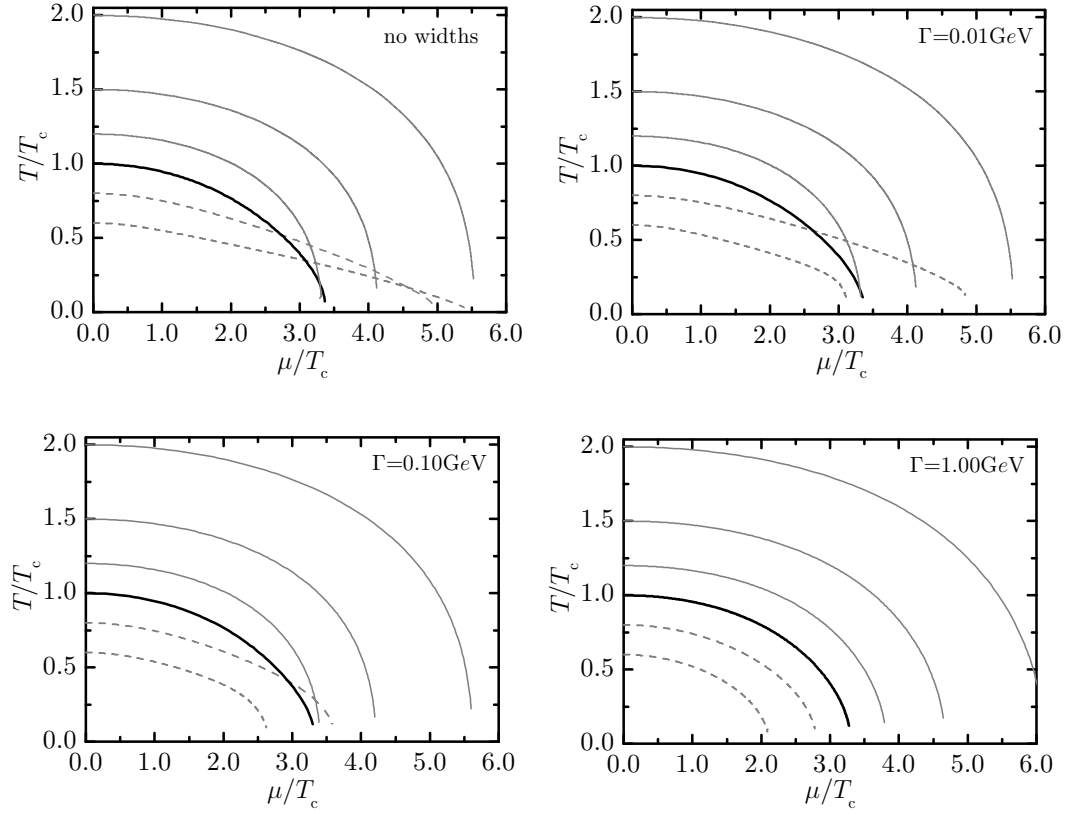


Figure 4.5: Characteristic curves in the T - μ plane. Thick solid curves are characteristics emerging from $T = T_c$ which can be interpreted as an estimate of the phase borderline. Increasing the width parameter Γ , while keeping the other QPM parameters fixed at the values from the adjustment of the eQP ($T_s = -0.738T_c$, $\lambda = 5.93$, $\alpha = 0.941$), removes the ambiguities near the phase transition. Thin solid lines indicate characteristics governed by the parameters T_s and λ , while the dashed characteristics are governed by α .

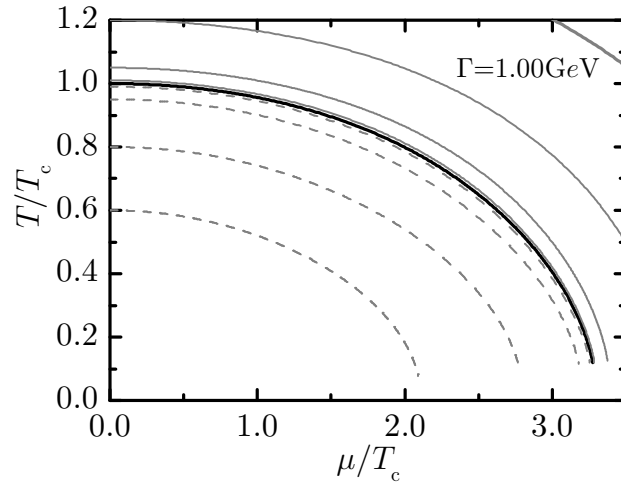


Figure 4.6: As Figure 4.5 (bottom right panel) but depicting a few more characteristic curves emerging from $T \approx T_c$. The crossings have entirely disappeared.

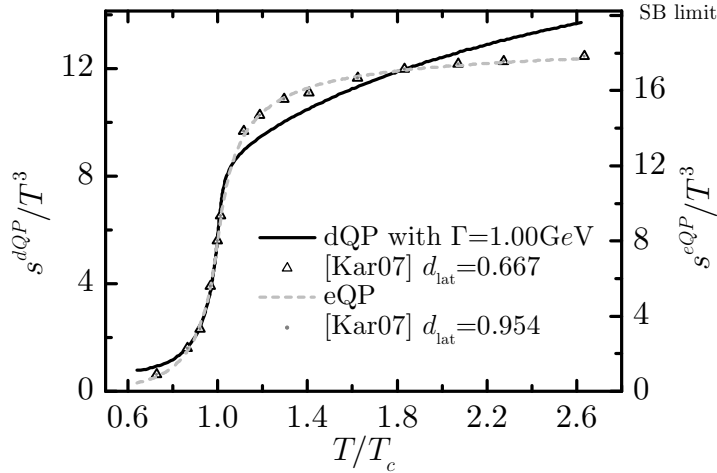


Figure 4.7: The best possible adjustment of the scaled dQP entropy density s/T^3 , using a large width of $\Gamma = 1$ GeV, to lattice data from [Kar07] is shown. The other model parameters are $T_s = -0.91T_c$, $\lambda = 16.6$ and $d_{\text{lat}} = 0.67$. While the region $T \approx T_c$ can be described, the slope introduced by the large width makes an accurate adjustment of lattice data above T_c impossible.

distributed model gives

$$\begin{aligned}
 c_2^{dQP} &= \frac{d_q}{2\pi^2 T^3} \int_0^\infty dk dM k^2 e f^2 \text{BW}, \\
 c_4^{dQP} &= \frac{d_q}{24\pi^2 T^3} \int_0^\infty dk dM k^2 \left\{ [e f^2 - 6e^2 f^3 + 6e^3 f^4] \text{BW} + 3T^2 e f^2 \left. \frac{\partial^2 \text{BW}}{\partial \mu^2} \right|_{\mu=0} \right\},
 \end{aligned} \tag{4.9}$$

where the second derivative of the Breit-Wigner distribution with respect to the chemical potential is given in Appendix C.2.

As for the entropy density and in line with the argument given in section 4.3, the Breit-Wigner distribution within the thermodynamic integral for c_2^{dQP} causes a decrease of the pressure correction coefficient above T_c and an increase below T_c with growing width parameter Γ (see Figure 4.8). The effect on c_4 is similar but subdued. It is only the additional term containing the second derivative of the Breit-Wigner distribution with respect to the chemical potential, being responsible for the peak structure (cf. section 3.4), which shows some width dependence: the peak vanishes for increasing values of Γ .

This is the reason, why the dQP is not able to describe lattice data for the pressure correction coefficients better than the eQP. Both the absolute value of c_2 outside the region around T_c and the peak structure of c_4 at T_c are actually described in a less favorable way if the new degree of freedom - the width - starts to contribute significantly. Therefore, the adjustment of the dQP proves virtually similar to the eQP with almost vanishing width parameter Γ . Details are shown in Figure 4.9.

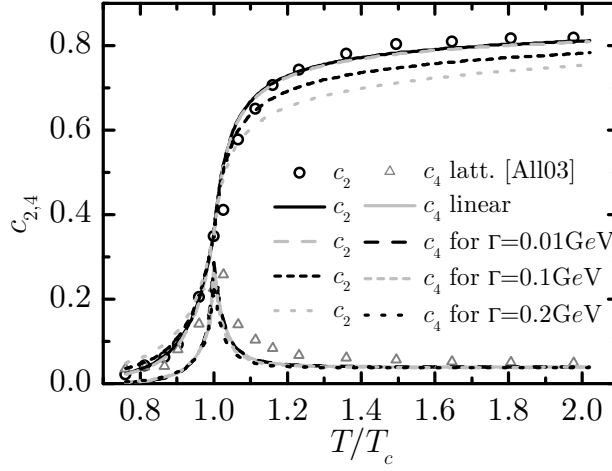


Figure 4.8: The effect of the width parameter Γ on the pressure correction coefficients $c_{2,4}$ as functions of T/T_c is shown. While c_2 is largely affected, c_4 seems to be rather stable with only the peak structure showing some Γ -dependence. Parameters used: $T_s = -0.87T_c$, $\lambda = 12$, $\alpha = 0.95$ as proposed for the eQP in [Blu04].

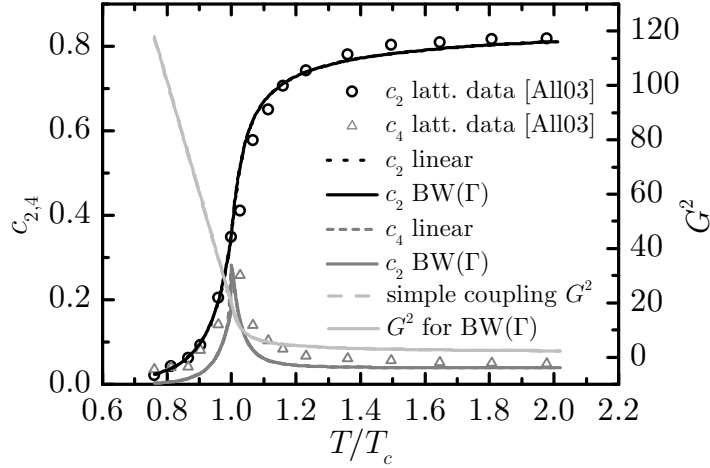


Figure 4.9: The adjustments of both eQP and dQP using lattice data [All03] are all but similar as are the parameters for both models: $T_s = -0.87T_c$, $\lambda = 12$ and $\alpha = 0.95$ with $\Gamma = 0.001$ for the dQP. Only a minor improvement in quality ($\chi_{c_2}^2/N = 1.77 \times 10^{-4}$ vs. $\chi_{c_2}^2/N = 1.53 \times 10^{-4}$) is measurable.

4.5 The effective QPM as limit of the dQP

By going to the limit of vanishing width, where $\text{BW}(m, M, \Gamma) \rightarrow \delta(m - M)$, the dQP turns into the eQP. Due to the integrability condition the state variables contain no derivatives of the distribution function BW and the mass integral containing a delta function can directly be evaluated. This is not the case for further derivatives of the pressure, since $\text{BW} \rightarrow \delta$ in the limit $\Gamma \rightarrow 0$ and the derivative of the Dirac delta distribution (see footnote 1 in Appendix B.2) proves problematic, so that e.g. $\partial \text{BW} / \partial \mu$ is not clearly defined. As long as the remaining integrand is sufficiently differentiable, we can solve the dilemma through an integration by parts, throwing the derivation for BW onto the other part of the integrand.⁵

As an example, the pressure correction coefficient c_4 contains the second derivative of BW with respect to the chemical potential. For brevity assuming $N = (2\pi)^{-1}$ and setting $m^2 = \tilde{m}_{q,\infty}^2$ the concerned part of c_4^{dQP} from eq. (4.9) reads

$$\int_0^\infty dM e f^2 \frac{\partial^2 \text{BW}}{\partial \mu^2} = \int_0^\infty dM e f^2 \left\{ \frac{\partial^2 m^2}{\partial \mu^2} \frac{\partial \text{BW}}{\partial m^2} + \left(\frac{\partial m^2}{\partial \mu} \right) \frac{\partial^2 \text{BW}}{\partial m^2} \right\}. \quad (4.10)$$

It has to be taken at $\mu = 0$, where $\partial G^2 / \partial \mu = 0$ and thus $\partial m / \partial \mu$ (cf. eq. (C.10)) vanishes. The integral $\int_0^\infty dM$ of the derivative of BW with respect to the squared asymptotic quark mass is given by

$$\int_0^\infty dM \frac{\partial \text{BW}}{\partial m^2} = \frac{1}{2m} \int_0^\infty dM \frac{\partial \text{BW}}{\partial m} = -\frac{1}{2m} \int_{-m}^\infty d(M - m) \frac{\partial \text{BW}}{\partial (M - m)} = -\frac{\text{BW}}{2m}. \quad (4.11)$$

The derivative of the remaining part is

$$\frac{\partial}{\partial M} e f^2 \frac{\partial^2 m^2}{\partial \mu^2} = \left(\frac{1}{T} e f^2 - \frac{2}{T} e^2 f^3 \right) \frac{\partial^2 m^2}{\partial \mu^2} \frac{\partial \omega}{\partial M}, \quad (4.12)$$

where here $\omega^2 = k^2 + M^2$.

Performing the partial integration $\int dM u'v = [uv] - \int dM uv'$ and taking the limit $\text{BW} \rightarrow \delta$, $[uv]$ vanishes at the limits as it is directly proportional to BW and the derivative $\partial \omega / \partial M$ becomes $\partial \omega / \partial m$. Since

$$\frac{\partial^2 \omega}{\partial \mu^2} = \frac{\partial^2 m^2}{\partial \mu^2} \frac{1}{2m} \frac{\partial \omega}{\partial m} \quad (4.13)$$

due to $\partial m / \partial \mu$ vanishing at $\mu = 0$ as above, we find

$$\int_0^\infty dM e f^2 \frac{\partial^2 \text{BW}}{\partial \mu^2} \Big|_{\mu=0} = \frac{1}{T} (e f^2 - 2e^2 f^3) \frac{\partial^2 \omega}{\partial \mu^2} \Big|_{\mu=0}. \quad (4.14)$$

⁵This is actually one of the essences of distribution theory. Here, however, it would have to be applied cum grano salis. It is tempting to interpret $\{BW\}(\phi) := \int dM \phi(M) \text{BW}(M, m, \Gamma)$ as regular distribution converging to the irregular distribution δ for $\Gamma \rightarrow 0$, where the remaining integrand ϕ is a test function, and to rely on the framework of distribution theory. While the integrands of thermodynamic integrals usually are ϵC^∞ with respect to the mass parameter M , they do not have compact support. Nevertheless, main contributions are found at $k \sim T$ and vanish exponentially for $k \rightarrow \infty$, so that the general technique still proves fruitful.

Inserting the result into (4.9) finally gives the eQP expression (3.20)

$$\begin{aligned}
c_4^{dQP} \Big|_{\Gamma=0} &= \frac{d_q}{24\pi^2 T^3} \int_0^\infty dk k^2 \left\{ e f^2 - 6e^2 f^3 + 6e^3 f^4 + 3T(e f^2 - 2e^2 f^3) \frac{\partial^2 \omega}{\partial \mu^2} \Big|_{\mu=0} \right\} \\
&= \frac{d_q}{24\pi^2 T^3} \int_0^\infty dk k^2 e f^4 \left\{ (e+1)^2 - 6e(e+1) + 6e^2 \right. \\
&\qquad\qquad\qquad \left. + 3T((e+1)^2 - 2e(e+1)) \frac{\partial^2 \omega}{\partial \mu^2} \Big|_{\mu=0} \right\} \\
&= \frac{d_q}{24\pi^2 T^3} \int_0^\infty dk k^2 e f^4 \left\{ e^2 - 4e + 1 + 3T(1 - e^2) \frac{\partial^2 \omega}{\partial \mu^2} \Big|_{\mu=0} \right\} \\
&= c_4^{eQP}.
\end{aligned} \tag{4.15}$$

This accomplishes our proof that the first Taylor expansion coefficients of the dQP turn into the ones of the eQP for vanishing widths. Using the same procedure, this can be shown for all other thermodynamic quantities of the dQP.

4.6 Temperature dependent widths

One possible way to model the temperature and particle species dependence of the width is to utilize the gluon and quark damping rates from [Pis93], which were also used in [Pes04, Pes05]:

$$\Gamma_i(T) = C_i \frac{G^2 T}{8\pi} \ln \frac{c}{G^2} \tag{4.16}$$

where C_i is the Casimir constant of the respective symmetry groups ($C_g = N_c$ and $C_q = (N_c^2 - 1)/2N_c$) and c is the parameter of the temperature dependent width. In contrast to the width parameter Γ from the preceding sections, c is dimensionless.

Due to the logarithm, there exists a temperature (close to T_c), below which the width becomes negative. That imposes a limit of validity for this ansatz. Consequently, the model can only be compared to lattice data for $T \gtrsim T_c$.

Due to the T -dependence of the width, the Breit-Wigner distribution is also temperature dependent and the expression for the entropy density becomes more involved:

$$\begin{aligned}
s_i^{dQP(T)}(T, \mu) &= \frac{\partial p_i}{\partial T} \Big|_{\mu} \\
&= \frac{\partial p_i}{\partial T} \Big|_{\mu, \text{BW}_i, B} + \frac{\partial p_i}{\partial \text{BW}_i} \frac{\partial \text{BW}_i}{\partial T} \Big|_{\mu} - \frac{\partial B}{\partial T} \Big|_{\mu}.
\end{aligned}$$

As for the eQP, terms arising from the derivative of m_i with respect to T vanish due to the integrability condition. For $\mu = 0$ we are left with

$$s_i^{dQP(T)}(T, 0) = \frac{d_i}{\pi^2 T} \int_0^\infty dk dM k^2 f \left\{ \frac{\frac{4}{3}k^2 + M^2}{\omega} \text{BW}_i + \frac{T}{3} \frac{k^2}{\omega} \frac{\partial \text{BW}_i}{\partial T} \Big|_{m_i} \right\},$$

where

$$\frac{\partial \text{BW}_i}{\partial T} \Big|_{m_i} = \left\{ N_i \frac{\partial \widetilde{\text{BW}}_i}{\partial \Gamma_i} + \frac{\partial N_i}{\partial \Gamma_i} \widetilde{\text{BW}}_i \right\} \frac{\partial \Gamma_i}{\partial T} \tag{4.17}$$

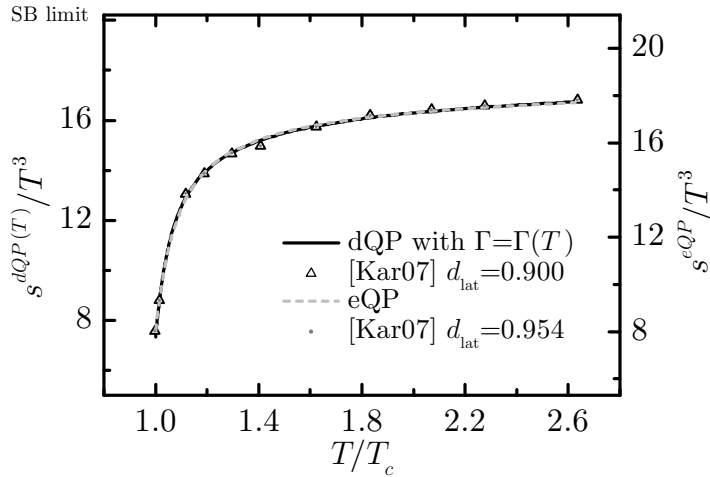


Figure 4.10: At $\mu = 0$ the dQP with temperature dependent widths according to eq. (4.16) ($T_s = -0.833T_c$, $\lambda = 9.259$ and $c = 340.5$ with $d_{\text{lat}} = 0.900$ resulting in $\chi_s^2/T^3 = 0.0104$) shows slightly better agreement with lattice data from [Kar07] than the eQP ($T_s = -0.738T_c$ and $\lambda = 5.93$ with $d_{\text{lat}} = 0.954$ giving $\chi_s^2/T^3/N = 0.0171$).

with

$$\frac{\partial BW_i}{\partial \Gamma_i} = \frac{(m_i - M)^2 - \frac{\Gamma_i^2}{4}}{\left((m_i - M)^2 + \frac{\Gamma_i^2}{4}\right)^2},$$

$$\frac{\partial N_i}{\partial \Gamma_i} = \frac{\partial N_i}{\partial N_i^{-1}} \frac{\partial N_i^{-1}}{\partial \Gamma_i} = -N_i^2 \left[\frac{-m_i}{m_i^2 + \frac{\Gamma_i^2}{4}} - \frac{M_{\text{max}} - m_i}{(M_{\text{max}} - m_i)^2 + \frac{\Gamma_i^2}{4}} \right]$$

and

$$\frac{\partial \Gamma_i}{\partial T} = \frac{C_i}{8\pi} \left\{ G^2 \ln \frac{c}{G^2} + T \left[\ln \frac{c}{G^2} - 1 \right] \frac{\partial G^2}{\partial T} \right\}. \quad (4.18)$$

Adjusting the dQP entropy density for temperature dependent widths at $\mu = 0$ using the same lattice data as for the analysis of temperature independent widths and eQP above some improvement is noticeable (see Figure 4.10). The adjustment quality parameter χ^2 divided by the number of lattice data points N decreases by almost two thirds.

Unfortunately, this temperature dependent width vanishes close to T_c and can therefore not help in resolving the crossings of the characteristic curves near the “phase transition”.

5 Improved quasiparticle models

5.1 An universal expression for the QPM entropy density

The entropy density contributions in eq. (2.44) are intrinsically linked with each other. While the Θ -terms describe the quasiparticles with infinite lifetime and mean free path, the arctan- and ReIm -terms give the damping and width corrections. Consequently, eq. (2.44) can be reformulated to give an universal expression for the entropy density. For the sake of brevity this is shown here for transverse gluons as symmetries allow for a compact presentation of the formulas. Nevertheless, these symmetries are not necessary: the calculation can be performed as well without using them.

We start from the transverse gluon entropy density (2.44) and use the symmetries of propagator (see Figure 2.5) and self-energy (eq. 2.28, see Figure 2.3) to simplify the energy integration. For convenience, the integrals, the sign function $\varepsilon(\text{Im}\Pi_{\text{T}}) = -\varepsilon(\omega)$ and $\text{Re}D_{\text{T}}$ are exhibited explicitly:

$$s_{g,\text{T}} = \frac{d_g}{\pi^2} \int_0^\infty dk k^2 \int_0^\infty \frac{d\omega}{\pi} \frac{\partial n_{\text{B}}}{\partial T} \left\{ -\pi\varepsilon(\text{Im}\Pi_{\text{T}})\Theta(-\text{Re}D_{\text{T}}^{-1}) \right. \\ \left. - \arctan \frac{\text{Im}\Pi_{\text{T}}}{\text{Re}D_{\text{T}}^{-1}} + \frac{\text{Re}D_{\text{T}}^{-1}\text{Im}\Pi_{\text{T}}}{\text{Re}^2D_{\text{T}}^{-1} + \text{Im}^2\Pi_{\text{T}}} \right\}. \quad (5.1)$$

The derivative of the bosonic distribution function is now substituted by the derivative of σ_{B} from section 3.1 with respect to ω (cf. eq. (3.3)). In order to perform an integration by parts we need the derivative of the curly bracket. Using the derivatives of the arc tangent and the Heaviside and sign functions from Appendix B.2 we find

$$\frac{\partial\{\}}{\partial\omega} = \left(\pi\varepsilon(\omega)\delta(\text{Re}D_{\text{T}}^{-1}) - \pi\varepsilon(\omega)\delta(\text{Re}D_{\text{T}}^{-1}) + \frac{2\text{Im}^3\Pi_{\text{T}}}{(\text{Re}^2D_{\text{T}}^{-1} + \text{Im}^2\Pi_{\text{T}})^2} \right) \frac{\partial\text{Re}D_{\text{T}}^{-1}}{\partial\omega} \\ + \left(-2\pi\delta(\text{Im}\Pi_{\text{T}})\Theta(-\text{Re}D_{\text{T}}^{-1}) - \frac{2\text{Re}D_{\text{T}}^{-1}\text{Im}^2\Pi_{\text{T}}}{(\text{Re}^2D_{\text{T}}^{-1} + \text{Im}^2\Pi_{\text{T}})^2} \right) \frac{\partial\text{Im}\Pi_{\text{T}}}{\partial\omega}.$$

The Dirac delta distributions arising from the Θ -function and the arc tangent exactly cancel. The term $-2\pi\delta(\text{Im}\Pi_{\text{T}})\Theta(-\text{Re}D_{\text{T}}^{-1})$ does not contribute, as the sign change of $\text{Im}\Pi_{\text{T}}$ is at $\omega = 0$, where $\text{Re}D_{\text{T}}^{-1}$ is positive (see Figure 2.5). Introducing a new variable $\xi_{g,\text{T}} := \text{Im}\Pi_{\text{T}}/\text{Re}D_{\text{T}}^{-1}$ allows to further compactify the expression and define the distribution function $F_{g,\text{T}}$:

$$\frac{\partial\{\}}{\partial\omega} = -2 \frac{\xi_{g,\text{T}}^2}{(1 + \xi_{g,\text{T}}^2)^2} \frac{\partial\xi_{g,\text{T}}}{\partial\omega} =: \pi F_{g,\text{T}}(\xi). \quad (5.2)$$

Now, performing the integration by parts gives

$$s_{g,\text{T}} = \frac{d_g}{\pi^2} \int_0^\infty d\omega \int_0^\infty dk k^2 \sigma_{\text{B}}(\omega) F_{g,\text{T}}(\xi(\omega)) + [C(\omega)]_0^\infty \quad (5.3)$$

with

$$C(\omega) = \frac{d_g}{\pi^2} \int_0^\infty dk k^2 \sigma_B(\omega) \left\{ \right\}, \quad (5.4)$$

where $C(0)$ vanishes for the transverse gluons since the expression within the curly bracket is antisymmetric. Due to $\sigma(\omega \rightarrow \infty) = 0$ and the curly bracket being finite at positive infinity, $C(\infty)$ is zero, too.

This derivation can also be done by integrating eq. (2.41) by parts. Use of $\text{Im} \ln z = \text{Arg} z$ and eq. (B.10) gives (5.3) in a straightforward way without the need to use the delta distribution at all. This can be interpreted as a hint for some ambiguity in the decomposition into quasiparticle pole and damping contributions.

Expression (5.3) is not limited to transverse gluons or the HTL self-energies themselves. Performing the derivation for particles with nonzero chemical potential (e.g. quarks) without the use of special symmetries and taking into account the antiparticle contributions we find the general form of the entropy density s_i for particle species i

$$s_i = \frac{d_i}{2\pi^2} \int_0^\infty d\omega \int_0^\infty dk k^2 (\sigma_F + \sigma_F^A) F(\xi_i) - [C(\xi_i(\omega))]_0^\infty \quad (5.5)$$

with

$$F(\xi_i) := -\frac{1}{\pi} \left(\frac{\xi_i^2(\omega)}{(1 + \xi_i^2(\omega))^2} \frac{\partial \xi_i(\omega)}{\partial \omega} - \frac{\xi_i^2(-\omega)}{(1 + \xi_i^2(-\omega))^2} \frac{\partial \xi_i(-\omega)}{\partial \omega} \right). \quad (5.6)$$

The ξ_i for longitudinal gluons and the normal and abnormal quark (or (anti)quark and plasmino) branches are, analogously to $\xi_{g,T}$, defined as quotients of the imaginary part of the corresponding self-energy and the real part of the respective inverse propagator. The expressions for σ_F and σ_F^A can be found in section 3.1.

If ξ_i is symmetric, its derivatives are equal up to the sign and $F(\xi_i)$ simplifies as for the transverse gluons. The analogously extended expression for $C(\omega)$ vanishes at zero and infinity as long as the real part of the propagator and the imaginary part of the self-energy are (and therefore ξ_i is) continuous at $\omega = 0$ and do not diverge for $\omega \rightarrow \infty$.

Using this general expression, two ways of including widths and damping effects into the QPM are investigated.

5.2 Lorentz widths improved quasiparticle model

The eQP can heuristically be extended to include Lorentz widths [Pes04, Pes05]. We are going to verify these results using eq. (5.5), e.g. for transverse gluons, by using the ansatz $\text{Im}\Pi_T = 2\gamma\omega$ and $\text{Re}\Pi_T = m_{g,\infty}^2$ instead of the more involved HTL expression. The resulting spectral function $\varrho = 2\text{Im}D(\omega + i\varepsilon)$ (see Appendix A) is

$$\varrho_{Ltz} = \frac{\gamma}{\omega_k} \left(\frac{1}{(\omega - \omega_k)^2 + \gamma^2} - \frac{1}{(\omega + \omega_k)^2 + \gamma^2} \right) \quad (5.7)$$

as opposed to quasiparticle poles $\varrho_D(\omega) = \frac{2\pi}{2\omega_k} [\delta(\omega + \omega_k) - \delta(\omega - \omega_k)]$ (see footnote 3 in Appendix A), where ω_k is the dispersion relation of particle family k . Consequently, the parameter γ of the Lorentz widths improved QPM (iQP) is a width measure.

Starting from

$$\xi_{g,T}^{Ltz} = \frac{2\gamma\omega}{-\omega^2 + k^2 + m_{g,\infty}^2} \quad (5.8)$$

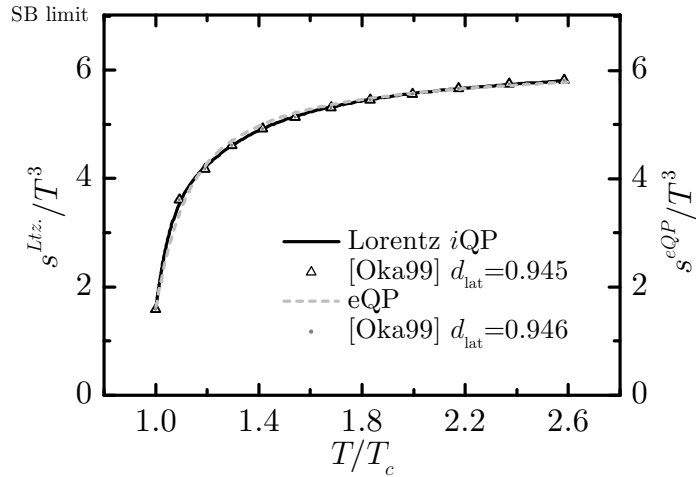


Figure 5.1: The ansatz of uniform Lorentz widths at truncated 2-loop order of the effective coupling G^2 visibly improves the possibility to adjust the QPM. Shown are the best possible adjustments of Lorentz iQP ($T_s = -0.273T_c$, $\lambda = 2.164$ and $\gamma = 4.27T$ with $d_{lat} = 0.945$ - $\chi_s^2/T^3/N = 0.47 \times 10^{-3}$) and eQP ($T_s = -0.543T_c$, $\lambda = 3.08$ with $d_{lat} = 0.946$ - $\chi_s^2/T^3/N = 7.10 \times 10^{-3}$) to lattice data from [CPP99] for the pure SU(3) plasma.

we arrive at

$$F_{g,T}^{Ltz} = \frac{16\gamma^3\omega^2(\omega^2 + \omega_T^2(k))}{\pi\left((\omega^2 - \omega_T^2(k))^2 + 4\gamma^2\omega^2\right)^2}. \quad (5.9)$$

Performing an integration by parts in reverse order of the previous chapter, we recover the entropy density expression given in [Pes04]. While F^{Ltz} is not normalized, the integral $\int d\omega F^{Ltz} \rightarrow 1$ and $\int d\omega f(\omega)F^{Ltz} \rightarrow f(\omega_T)$ for $\gamma \rightarrow 0$, so that $F^{Ltz} \rightarrow \delta(\omega - \omega_T)$ for vanishing γ . Consequently the eQP is found in the limit $\gamma \rightarrow 0$.

Figure 5.1 shows the adjustment of the Lorentz width iQP in comparison with the adjustment of the eQP to lattice data for the pure gluon plasma entropy density from [CPP99]. Clearly the model improves the adjustment quality. This is due to a steeper incline close to the transition temperature.

Peshier has shown [Pes04] that the direct inclusion of quasiparticle widths in this way strictly increases the overall entropy density. Therefore, it is not suitable to remove the crossings of the characteristics of the flow equation (cf. section 3.3). However the Lorentz iQP provides us with strong support for the ansatz for quasiparticle widths used in chapter 4.

To this avail the distributed energies from the universal entropy density expression can be translated into distributed masses, giving the possibility to compare the Lorentz ansatz with the dQP

$$s_i^{Ltz} = \frac{d_i}{2\pi^2} \int_{-k^2}^{\infty} dM \int_0^{\infty} dk k^2 (\sigma(k^2 + M^2) + \sigma^A(k^2 + M^2)) F^{Ltz,M} \quad (5.10)$$

with

$$F^{Ltz,M} = \frac{16\gamma^3 M \sqrt{k^2 + M^2} (M^2 + 2k^2 + m_{i,\infty}^2)}{\pi \left((M^2 - m_{i,\infty}^2)^2 + 4\gamma^2 (k^2 + M^2) \right)^2}. \quad (5.11)$$

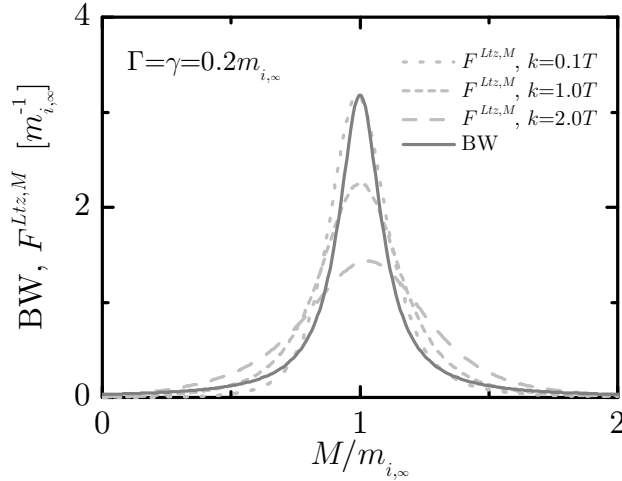


Figure 5.2: The two mass distribution functions of eqs. (5.11) and (4.2) as functions of $M/m_{i,\infty}$ for several values of the quasiparticle momentum and fixed width $\Gamma = \gamma = 0.2m_{i,\infty}$. For small momenta k , both are equal. For larger values of k , Lorentz widths lead to broader mass distributions.

This new entropy density expression exactly matches the dQP entropy density (4.6) up to a partial integration as performed for (3.8) and the substitution $BW \rightarrow F^{Ltz,M}$. The comparison of both mass distribution functions (see Figure 5.2) can therefore provide us with valuable information on the differences of both models.

While $F^{Ltz,M}$ is a function of k , there is no momentum dependence of the Breit-Wigner distribution. This leads a scale-dependence of the mass distribution functions. While both functions are virtually identical for small momenta $k < m_{i,\infty}$, the Lorentz mass distribution shows an increased peak width at full width half maximum (FWHM) at higher momentum scales. Yet, it is exactly at $k \sim m_{i,\infty}$ where thermodynamic momentum integrals have their main contributions. Consequently, both models show significant differences. For increasing widths, the dQP entropy density decreases, while the Lorentz entropy density grows. I therefore propose the study of the dQP with a momentum dependent width of the form

$$\Gamma(M, k) = \gamma \sqrt{k^2 + M^2} \quad (5.12)$$

modeling the momentum scale dependence of the Lorentz iQP in a straightforward way (see Figure 5.3).

Nevertheless, it is the special Lorentz width ansatz which leads to the momentum dependent mass widths. The general formulation of the quasiparticle entropy density of eq. (5.5) for itself provides a strong justification of the dQP treated in chapter 4.

5.3 Landau damping improved quasiparticle model

While the treatment of quasiparticle widths is essential, the damping contributions of the HTL self-energies are not connected to the poles of the spectral function. To be specific, the imaginary parts of the HTL self-energies are nonzero below the light cone only. As outlined in section 2.4 they are related to Landau damping.

While Landau damping contributions for transverse and collective longitudinal modes are separated, the collective quark modes and quark Landau damping contribution are interrelated in a complex way (see sections 2.4 and 2.5 as well as the

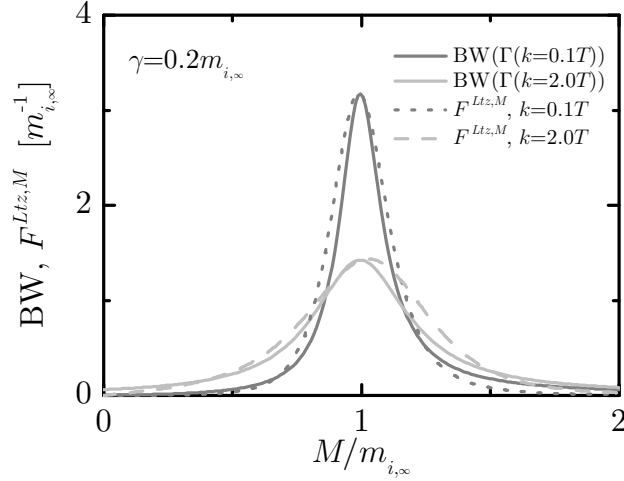


Figure 5.3: As Figure 5.2 but with the width parameter of the Breit-Wigner distribution Γ parametrized according to eq. (5.12). Using this parametrization the momentum dependence of the Lorentz mass distribution function can be modeled so that the dQP is a good approximation of the Lorentz iQP.

comment related to eq. (2.48)). It is therefore not straightforward how Landau damping can be implemented while neglecting plasminos.

One possibility is a correction term aimed at refining the eQP approximation (section 3.1). The LD iQP entropy density is then given by $s^{LD} = s^{eQP} + \Delta s^{LD}$, where s^{eQP} is the sum of eqs. (3.1) and (3.2) while the contributions to $\Delta s^{LD} = \sum \Delta s_i^{LD}$ with $i = \{g, T; q\}$ follow from eqs. (2.44) and (2.47). The entropy density correction terms read

$$\begin{aligned} \Delta s_{g,T}^{LD} &= 2d_g \int_{d^4k} \frac{\partial n_B}{\partial T} \left\{ \text{Re}D_T \text{Im}\Pi_T - \arctan \frac{\text{Im}\Pi_T}{\text{Re}D_T^{-1}} \right\}, \\ \Delta s_{q/s}^{LD} &= 2d_q \int_{d^4k} \left(\frac{\partial n_F}{\partial T} + \frac{\partial n_F^A}{\partial T} \right) \left\{ \text{Re}S_+ \text{Im}\Sigma_+ - \arctan \frac{\text{Im}\Sigma_+}{\text{Re}S_+^{-1}} \right\}. \end{aligned} \quad (5.13)$$

Note that the quantities $\Delta s_{q/s}^{LD}$ contain the full Landau damping contributions of both quarks and plasminos (and their respective antiparticles), while for the eQP quark entropy density s_q plasminos were neglected (eq. (3.1)). This is due to the fact that the Landau damping term within the quark self-energies Σ_{\pm} cannot be separated into quark and plasmino contributions in a straightforward manner.

Using the abbreviation ξ_i introduced in section 5.1 we can rewrite the terms within the curly brackets above. Since the resulting terms $\xi_i/(1 + \xi_i^2)$ and $\arctan \xi_i$, vanish at $\xi_i = 0$, the Heaviside function contained within the imaginary parts of the

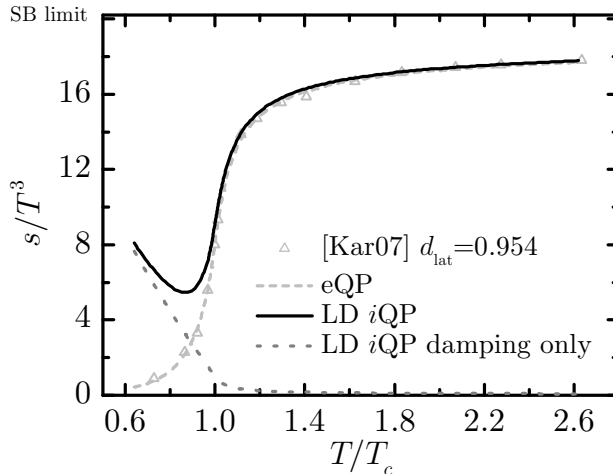


Figure 5.4: The eQP (light grey dashed) and LD iQP (solid black) scaled entropy densities s/T^3 are shown as function of the scaled temperature T/T_c for equal parameter values (specifically $T_s = -0.738T_c$, $\lambda = 5.93$ and $\alpha = 0.941$ with $d_{\text{lat}} = 0.954$ from the adjustment of the eQP to the given lattice data [Kar07]). The grey dotted line is the difference of both models, i.e. it gives the LD iQP entropy density correction. It is most notable in the region $T < T_c$ with vanishing impact for temperatures clearly above T_c and seems to correlate with the effective coupling G^2 .

HTL self-energies can be applied to the integral limits.¹ We have

$$\begin{aligned} \Delta s_{g,T}^{LD} &= 2d_g \int_{d^3k} \int_{-k}^k \frac{d\omega}{2\pi} \frac{\partial n_B}{\partial T} \left\{ \frac{\xi_{g,T}}{1 + \xi_{g,T}^2} - \arctan \xi_{g,T} \right\}, \\ \Delta s_{q/s}^{LD} &= 2d_q \int_{d^3k} \int_{-k}^k \frac{d\omega}{2\pi} \left(\frac{\partial n_F}{\partial T} + \frac{\partial n_F^A}{\partial T} \right) \left\{ \frac{\xi_{q,+}}{1 + \xi_{q,+}^2} - \arctan \xi_{q,+} \right\}. \end{aligned} \quad (5.14)$$

The effect of the correction terms can be seen in Figure 5.4. It is extremely large in the area below and at the pseudocritical temperature while vanishing for temperatures clearly above T_c , seemingly correlating with the effective coupling G^2 . Therefore, the linear IR cutoff of G^2 for temperatures below the pseudocritical temperature (cf. section 3.5) is not successful for the LD iQP: it causes a substantial increase of the entropy density below T_c . Even using a quadratic cutoff of the effective coupling below T_c (eq. 3.24) at quite extreme parameters ($a = -950$ and $b = 1479$) cannot significantly reduce the entropy density.

The LD iQP is therefore adjusted to lattice data above T_c only (see Figure 5.5). We find that for $T > T_c$ the inclusion of the Landau damping contributions to the entropy density does not improve the quality of the adjustment, however it does not worsen either. It seems the eQP can absorb the effects of Landau damping into a small change of the parameters T_s and λ . This is a strong argument for the neglect of Landau damping as done in the derivation of the eQP (section 3.1).

Extending the LD iQP to nonzero chemical potential does not promise improvement in the issue of crossing characteristics. This is due to the fact, that the positive

¹Consider functions $f(x)$, $g(x)$ and $h(x)$ with $f(0) = 0$, $g(x) \neq 0$ and $h(x) \in \mathbb{R}$.

Then $f(g(x)\Theta(h(x))) = \begin{cases} h(x) \geq 0 : f(g(x) \cdot 1) = f(g(x)) = f(g(x)) \cdot 1 \\ h(x) < 0 : f(g(x) \cdot 0) = f(0) = 0 = f(g(x)) \cdot 0 \end{cases} = f(g(x)) \cdot \Theta(h(x))$.

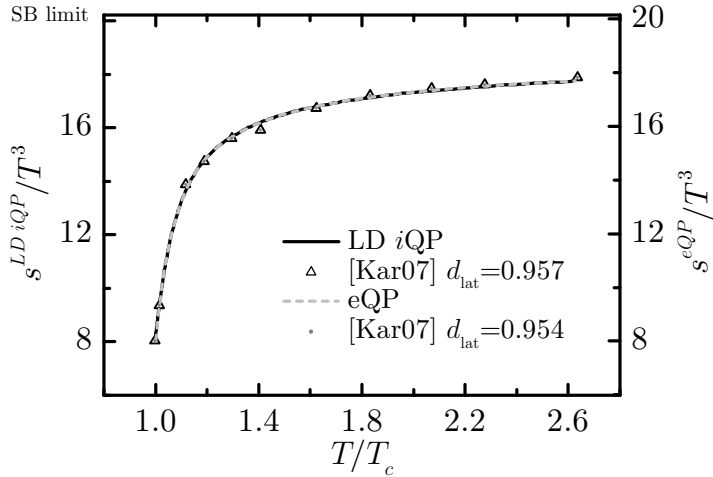


Figure 5.5: The Figure shows the scaled entropy density of the LD iQP adjustment ($T_s = -0.737$ and $\lambda = 5.66$ with $d_{\text{lat}} = 0.957$ resulting in $\chi_s^2/T^3/N = 0.0195$) compared to the scaled entropy density of the eQP adjustment ($T_s = -0.738T_c$ and $\lambda = 5.93$ with $d_{\text{lat}} = 0.954$ giving $\chi_s^2/T^3/N = 0.0171$) to lattice data from [Kar07] as functions of the scaled temperature T/T_c . There is no improvement by taking into account Landau damping.

LD entropy density correction leads to an increased effective coupling G^2 in the adjustment of the LD iQP to lattice data and thus adversely effects the characteristics (cf. section 3.3).²

²Due to the inclusion of the complete Landau damping contribution of quarks and plasminos while neglecting the quasiparticle contribution of the latter as well as the use of the asymptotic dispersion relation for the quasiparticle contribution of quarks and gluons as opposed to the damping contributions with exact propagators and self-energies, the extension to nonzero chemical potential even proves problematic. The characteristics do not display the usual behavior of perpendicular incidence to the T and μ axes as the coefficients of the resulting LD iQP flow equation have different limits than the ones given in section 3.3.

6 Full HTL quasiparticle model

6.1 Outline of the model

After investigating several approximations we now return to the full HTL entropy density expression derived in chapter 2. While the previous model ansätze made use of the asymptotic dispersion relations, the exact dispersion relations are employed within the full HTL QP model. As a consequence, quark rest masses are not included. This is not a major obstacle, as the lattice data used here to adjust the model features rather small lattice rest masses.

As in the eQP and dQP case, we use an ansatz for the pressure which gives the full HTL entropy density expression (eqs. (2.40), (2.44) and (2.47)) after partial differentiation with respect to the temperature at constant μ :

$$p = p_{g,T} + p_{g,L} + \sum_{i=q,s} p_i - B(\Pi_T, \Pi_L, \Sigma_{\pm}), \quad (6.1)$$

$$\begin{aligned} p_{g,T} &= +2d_g \int_{d^4k} n_B \left\{ \pi \varepsilon(\omega) \Theta(-\text{Re}D_T^{-1}) - \arctan \frac{\text{Im}\Pi_T}{\text{Re}D_T^{-1}} + \text{Re}D_T \text{Im}\Pi_T \right\}, \\ p_{g,L} &= -d_g \int_{d^4k} n_B \left\{ \pi \varepsilon(\omega) \Theta(+\text{Re}D_L^{-1}) - \arctan \frac{\text{Im}\Pi_L}{\text{Re}D_L^{-1}} + \text{Re}D_L \text{Im}\Pi_L \right\}, \\ p_{q/s} &= 2d_{q/s} \int_{d^4k} (n_F + n_F^A) \left\{ \pi \Theta(-\text{Re}S_+^{-1}) - \arctan \frac{\text{Im}\Sigma_+}{\text{Re}S_+^{-1}} + \text{Re}S_+ \text{Im}\Sigma_+ \right\}. \end{aligned} \quad (6.2)$$

The quantity B again ensures self-consistent thermodynamics by fulfilling the integrability conditions

$$\frac{\partial B}{\partial \Pi_i} = \frac{\partial p}{\partial \Pi_i} \quad \text{and} \quad \frac{\partial B}{\partial \Sigma_{\pm}} = \frac{\partial p}{\partial \Sigma_{\pm}}. \quad (6.3)$$

This is entirely analogous to eq. (3.12). Note that the plasma frequency within the s -quark pressure differs from the plasma frequency within p_q as $\mu_s = 0$.

The particle density follows by differentiation with respect to the chemical potential at constant temperature. The Bose-Einstein distribution function n_B does not depend on μ and strange quarks are included into the model with manifest zero net particle density, therefore $n_{g,T} = n_{g,L} = n_s = 0$. Due to the integrability condition, the terms containing the derivatives of the self-energies with respect to μ vanish, so that

$$n = n_q = 2d_q \int_{d^4k} \left(\frac{\partial n_F}{\partial \mu} + \frac{\partial n_F^A}{\partial \mu} \right) \left\{ \pi \Theta(-\text{Re}S_+^{-1}) - \arctan \frac{\text{Im}\Sigma_+}{\text{Re}S_+^{-1}} + \text{Re}S_+ \text{Im}\Sigma_+ \right\}. \quad (6.4)$$

As required, the density goes to zero for $\mu \rightarrow 0$ as the sum of the partial derivatives of the statistical distribution functions with respect to the chemical potential vanishes.

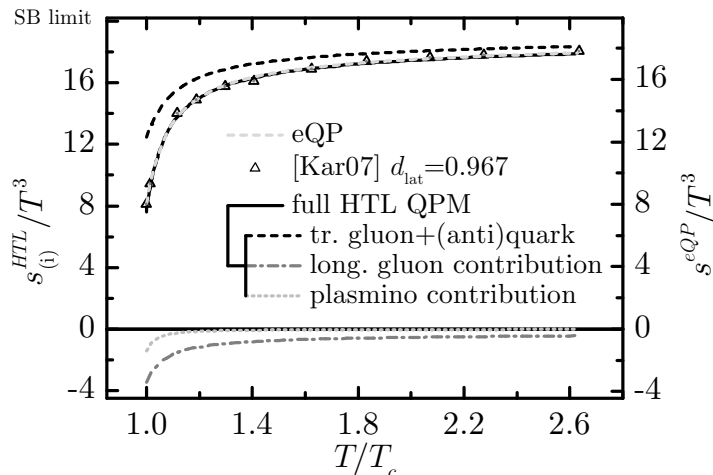


Figure 6.1: The scaled entropy densities s/T^3 of the full HTL QPM (solid black; $T_s = -0.749T_c$ and $\lambda = 6.53$ with $d_{\text{lat}} = 0.967$) and the eQP (dashed grey; $T_s = -0.738T_c$ and $\lambda = 5.93$ with $d_{\text{lat}} = 0.954$) adjusted to lattice data for $N_f = 2 + 1$ from [Kar07] are shown as functions of the scaled temperature T/T_c . The single parts of s^{HTL} (including their respective LD contributions) are given by the dashed black, dash-dotted and dotted grey lines as indicated in the legend.

6.2 Comparison with lattice data at $\mu = 0$

When evaluating the entropy density contributions of the full HTL QPM we find the longitudinal gluon entropy density $s_{g,L}$ (eq. (2.44)) and the (anti)plasmino entropy density $s_{q,P1}$ (eq. (2.48)) to be negative. This is due to fact that both represent collective phenomena of the QGP resulting in correlations not present in a noninteracting medium. As a consequence, the transverse gluon and (anti)quark entropy density contributions have to increase compared to the eQP in order for the entropy density to describe the same lattice data as the eQP (see Figure 6.1). This proves to have a positive impact on the extension to nonzero chemical potential (cf. Appendix 6.3). Note that as another consequence of the negative collective contributions the pure quasiparticle entropy density is closer to the Stefan-Boltzmann limit than for the eQP.

For $T > T_c$ and $N_f = 2$ the full HTL model has been shown to give adjustments to lattice data equal to the eQP ([Rom04] for data from [CPP01]). This can be reproduced. Using the given extension to include a heavy quark flavor this can also be shown for $N_f = 2 + 1$ (see figs. 6.1 and 6.3).

The extension to $T < T_c$, on the other hand, is not straightforward. Using the usual linear IR regulator of the effective coupling, problems arise from the additional contributions. In order to compensate for the negative terms, the linear slope parameter α can be chosen much smaller. However, the contributions also cause a different overall behavior of the entropy density below T_c so that an adjustment using this simple parametrization is not possible (see Figure 6.2). Using the quadratic IR regulator introduced in section 3.6 this can in fact be remedied, as Figure 6.3 shows.

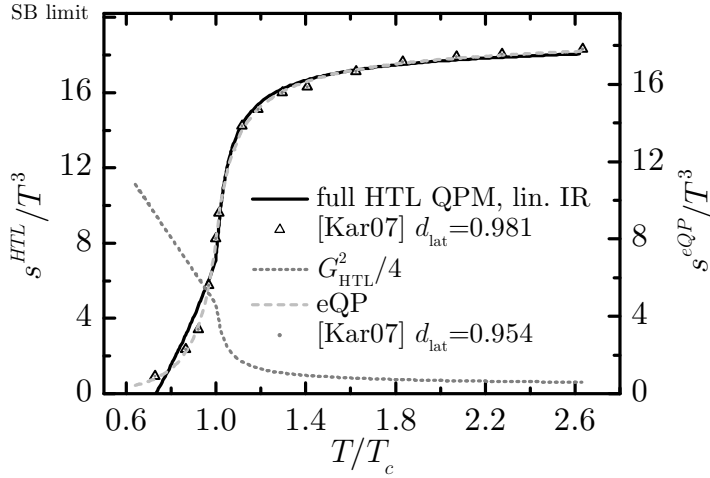


Figure 6.2: The scaled entropy densities s/T^3 of the full HTL QPM with linear ($T_s = -0.806T_c$, $\lambda = 8.34$ and $\alpha = 0.789$ with $d_{\text{lat}} = 0.981$) IR regulator and the eQP ($T_s = -0.738T_c$, $\lambda = 5.93$, $\alpha = 0.941$ with $d_{\text{lat}} = 0.954$) adjusted to lattice data from [Kar07] are shown as functions of the scaled temperature T/T_c . The dotted line indicates the coupling of the full HTL QPM at a scale of 4 to the left ordinate. The adjustment below the pseudocritical temperature is not satisfactory while the adjustment above is also subpar due to the connection of the parametrizations above and below T_c through $G^2(T_c)$.

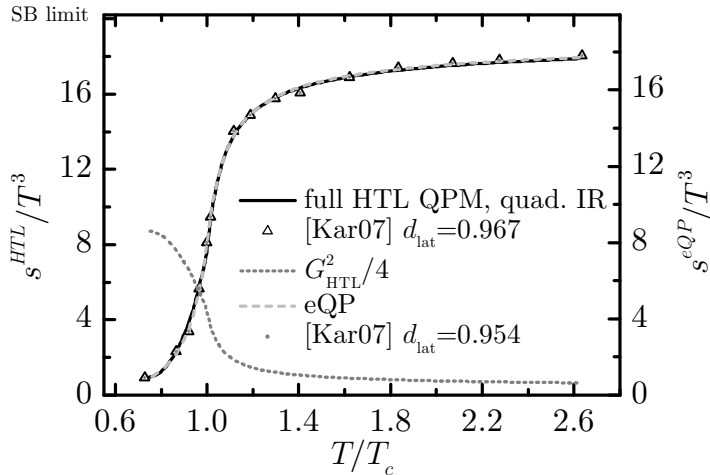


Figure 6.3: As Figure 6.2 but using a quadratic (bottom; $T_s = -0.749T_c$, $\lambda = 6.53$, $a = -245$ and $b = 361$ with $d_{\text{lat}} = 0.967$) IR regulator for the full HTL QPM. The adjustment quality to lattice data is comparable to the eQP.

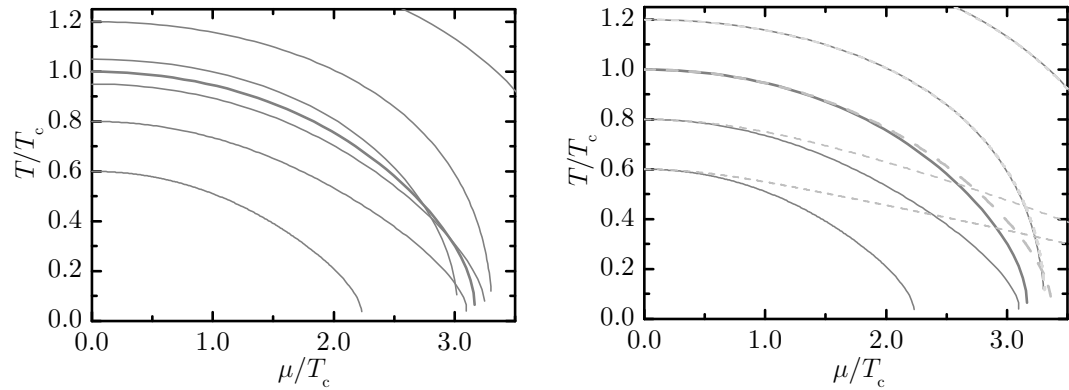


Figure 6.4: The solid curves in both graphs show several characteristics of the eQP flow equation (3.16) using parameters found from the adjustment of the full HTL QPM to lattice data shown in Figure 6.3 ($T_s = -0.749T_c$, $\lambda = 6.53$, $a = -245$ and $b = 361$). While not all crossings can be avoided (left panel), the situation improves significantly in comparison to the characteristics of the eQP (Figure 4.5, top left panel, here shown as dashed grey curves in the right panel). Note that characteristics above the immediate transition region are barely affected by the change in parameters.

6.3 Extension of the full HTL QPM to nonzero chemical potential

Approximate solution

We can find an approximate extension of the full HTL QPM to $\mu \neq 0$ by applying its adjusted parameters to the eQP flow equation (3.16). As might be expected from the discussion in section 3.3 the increased entropy density does indeed remove some of the crossing of the characteristics (Figure 6.4).

While not all crossings vanish, this is a first sign that plasmons and plasminos are the relevant degrees of freedom necessary to remove the ambiguities in the solutions of the flow equation.

Exact solution

In his Ph.D. thesis [Rom04], Romatschke claims to have solved the flow equation for the full HTL quasiparticle model at $N_f = 2$ as outlined in [BIR01]. His solution suggests that, as a consequence of the inclusion of all medium effects (plasmons and plasminos additionally to Landau damping), the ambiguities caused by crossing characteristic curves near the phase transition vanish for two massless quark flavors. However, it is not entirely obvious how this result was obtained. Additionally, the only equation given by him exhibits obvious mistakes (see footnote 2 in Appendix D).

In order to verify the results from [Rom04], the full HTL flow equation was rederived. As this is quite extensive, the details are - in a very condensed way -

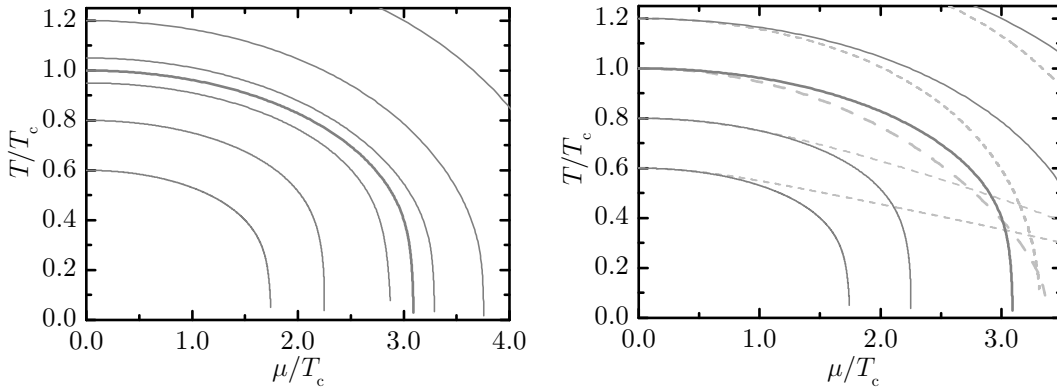


Figure 6.5: The solid curves in both graphs are several characteristics of the full HTL flow equation (D.34) for $2 + 1$ quark flavors using parameters from the adjustment of the full HTL QPM to lattice data shown in Figure 6.3 ($T_s = -0.749T_c$, $\lambda = 6.53$, $a = -245$ and $b = 361$). All crossings have disappeared (left panel). For comparison the right panel shows the characteristics of the eQP (Figure 4.5, top left panel) as dashed curves.

given in Appendix D. The inaccurate terms within the results of Romatschke are pointed out.

In addition to his work, the obtained flow equation is then also extended to $N_f = 2 + 1$ as well as to temperatures below the pseudocritical temperature T_c . This allows a comparison to the results obtained for the other models investigated within this thesis.

The flow equation (D.34) is then solved for $N_f = 2 + 1$ using the method of characteristics as in the preceding chapters. Indeed, the crossings of the characteristics vanish above and also below the pseudocritical temperature as can be seen in Figure 6.5. Also a more pronounced change of direction of the full HTL characteristics compared to the eQP characteristics (shown as dashed lines in the right panel) is observable.

Interestingly, in the flow equation, it is not the plasmon or plasmino term which accounts for the vanishing of the crossings still present in the approximate solution. This can be shown by neglecting both contributions in the coefficients a_T , a_μ and b , i.e. disregarding the second term in the square bracket of the energy integration in eq. (D.24) and the respective last term in the round parentheses of the momentum integrations in eqs. (D.24), (D.30) and (D.32).¹

While this causes the characteristics to deform and meet with the μ axis at smaller μ , no crossings appear. However, neglecting the Landau damping terms, i.e. the energy integrals, immediately leads to crossing characteristics (cf. Figure 6.6).

Therefore both, collective excitations (in order to obtain a reasonably small coupling G^2 , cf. section 3.3) and Landau damping (in order to ultimately remove the crossings), are necessary to obtain a flow equation with unique solutions. Using this flow equation, it is possible to find an EOS for cold and dense matter.

¹As for the LD iQP, the quark Landau damping is in its entirety attributed to the (anti)particles.

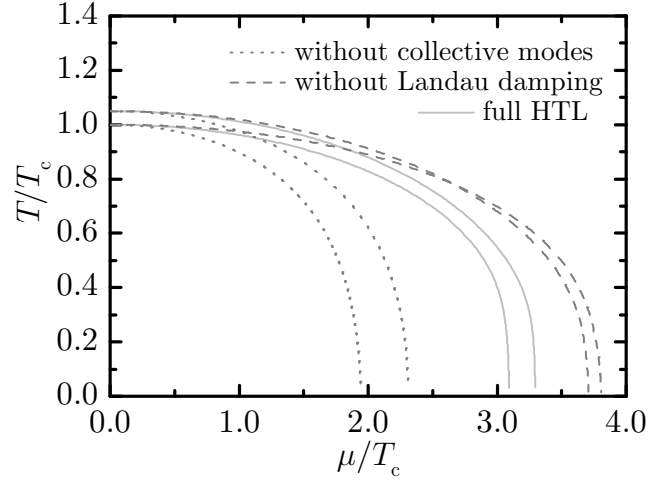


Figure 6.6: As Figure 6.5, but here neglecting the contributions of collective excitations (dotted lines) and the Landau damping contributions (dashed lines) to the coefficients of the flow equation (eq. (D.35) in Appendix D). For reference, the characteristics of the full HTL model (Figure 6.5) are shown as solid grey lines. It is in fact the Landau damping contribution which removes the crossings.

7 Conclusion and Outlook

Conclusion

The goal of this work was to find a quasiparticle description of the EOS of strongly interacting matter taking into account particle widths and damping effects. This goal was successfully achieved. Several methods in doing so were investigated. In addition, collective modes such as plasmons and plasminos could be implemented. As common starting point the full Hard Thermal Loop (HTL) quasiparticle model was derived from 2-loop QCD using the Cornwall-Jackiw-Tomboulis formalism and an effective coupling G^2 .

Applying several additional approximations to the full HTL quasiparticle model yields the existing effective quasiparticle model (eQP) which was investigated in detail in chapter 3. The problem of crossing characteristics which lead to ambiguities in the solutions of the extension to nonzero chemical potential μ and its reason (an increased effective coupling G^2 due to the severe approximations) were pointed out. In addition, some alternative parametrizations of the effective coupling were considered but did not provide significant improvement for the eQP. Propagators and self-energies rely consequently on 1-loop QCD expressions.

As one possibility to allow for quasiparticle widths, a model with Breit-Wigner distributed masses was proposed in chapter 4. The model was tested thoroughly with all its quantities giving their eQP equivalents in the limit of vanishing width. While the extension of the model to finite μ is able to remove the crossings due to an overall decrease of entropy and thus G^2 when adjusting the model to lattice data, this is only the case for rather large quasiparticle widths which are not consistent with data for $\mu = 0$. As a slight modification of the ansatz, temperature and particle dependent widths were then examined, providing excellent agreement with lattice data but showing vanishing widths for the region $T \approx T_c$, where the crossings appear. Consequently, these width parametrizations cannot remove the ambiguities introduced by the crossings.

Therefore, it proved necessary to return to the exact 1-loop entropy density expression. In chapter 5 the expression was transformed in order to allow for arbitrary imaginary parts of the self-energies, i.e. widths and damping effects. Using the obtained expression, a proposal by Peshier to include Lorentz widths could be verified and reformulated in a new concise way. While Lorentz widths increase the overall entropy and are therefore not suited to remove the crossings, a comparison of the Lorentz widths improved quasiparticle model to the distributed quasiparticle model from chapter 4 did provide us with a strong foundation for the latter.

As a second application of the new entropy expression, it was applied to the imaginary parts of the HTL self-energies which contain Landau damping but no particle widths. By including the damping effect the agreement with lattice data at $\mu = 0$ improved only slightly. The overall effect of the inclusion of Landau damping turned out to be an increase in entropy density which again meant that the damping effect (alone) cannot contribute in removing the crossings of characteristics and in obtaining unique solutions.

As it turns out in chapter 6, it is the combination of Landau damping and collective modes, i.e. plasmons and plasminos, which leads to unique solutions in the extension to $\mu > 0$. In other words, only the complete HTL quasiparticle model is fully consistent in contrast to some of the approximations considered within this thesis. This confirms a statement by Romatschke whose work was still restricted to $T > T_c$ and $N_f = 2$ only. While several inaccuracies within his work were found, they could be corrected and his findings still hold. They were even extended to $N_f = 2 + 1$ quark flavors and below the pseudocritical temperature. Finding that the linear IR cutoff of the effective coupling G^2 cannot be used when extending the model below T_c , one of the alternative parametrizations - a quadratic cutoff - from chapter 3 was successfully applied.

Outlook

With the crossings removed, the ambiguities in the solution of the flow equation vanish, i.e. the solutions of the flow equation are now unique. Therefore, the calculation of an EOS for regions in the $T - \mu$ plane which are of interest for future Heavy Ion Collision experiments is now possible. For instance providing the EOS in a tabulated form based on this thesis is subject of future investigations. Using the EOS in turn within hydrodynamic calculations, predictions e.g. for the elliptic flow can be made. The treatment of quasiparticle widths and damping effects within this work provides the key to the calculation of transport coefficients.

Another interesting field of application for the EOS, moving further along the characteristics to even lower temperatures and towards very dense matter into the field of astrophysics, are neutron stars or, even further, possible quark stars. Notably, the extension of the model to include strange quarks is especially important for astrophysics, as there is still much debate about possible strange stars (for a review see [Web05]).

Appendix A Evaluation of Matsubara sums

Considering an arbitrary function $f(p_0 = i\omega_n)$ which is to be summed over all bosonic Matsubara frequencies $i\omega_n = 2n\pi T$ one defines a quantity

$$M := T \sum_{n=-\infty}^{+\infty} f(p_0 = i\omega_n). \quad (\text{A.1})$$

The factor T in front of the sum will turn out to be very helpful in performing the sum.

We start by examining the bosonic distribution function for imaginary frequencies $n_B(p_0 = i\omega) = (e^{i\beta\omega} - 1)^{-1}$. It has poles at the bosonic Matsubara frequencies with residuum¹ T

$$\text{Res}_{i\omega_n} n_B = \text{Res}_{i\omega_n} \frac{1}{e^{\beta p_0} - 1} = \frac{T}{e^{\beta i\omega_n} - 1} = T, \quad (\text{A.3})$$

so M can be written as

$$M = \sum_n f(i\omega_n) \text{Res}[n_B(p_0 = i\omega_n)]. \quad (\text{A.4})$$

We now require $f(i\omega)$ to be analytic at the poles of the bosonic distribution function n_B and n_B to be analytic at the poles of $f(i\omega)$. Thus the set of poles of the product $f(i\omega) n_B(i\omega)$ is equal to the union of the two sets of poles of $f(i\omega)$ and $n_B(i\omega)$:

$$\{i\omega_m\} = \{i\omega_n\} + \{i\omega_l\}. \quad (\text{A.5})$$

Here m counts the poles of the product and l and n those of $f(i\omega)$ and $n_B(i\omega)$, respectively. This implies the relation

$$\sum_m \text{Res}[n_B(i\omega_m) f(i\omega_m)] = \sum_l \text{Res}[f(i\omega_l)] n_B(i\omega_l) + \underbrace{\sum_n f(i\omega_n) \text{Res}[n_B(i\omega_n)]}_{=M}. \quad (\text{A.6})$$

Each of these terms can be translated back into a contour integral encircling the respective poles. In particular, the first integral then represents the contour integral containing all poles. Its contour can be moved to infinity, where the integral vanishes as long as $f(i\omega)$ is a monotonically decreasing function going to zero for $\omega \rightarrow \pm\infty$.² This leaves us with

¹For functions $f(z)$ with a pole of first order at $z = a$ we find

$$\text{Res}_a \frac{1}{f(z)} = \lim_{z \rightarrow a} (z - a) \frac{1}{f(z)} \stackrel{f(a)=0}{=} \lim_{z \rightarrow a} \frac{z - a}{f(z) - f(a)} =: \frac{1}{f'(a)}. \quad (\text{A.2})$$

²While the expression is Boltzmann suppressed by $n_B(i\omega)$ for $\omega \rightarrow \pm\infty$, since $n_B(i\omega) \xrightarrow{i\omega \rightarrow \pm\infty} e^{\mp\beta\omega}$, it is purely oscillatory for $\omega \rightarrow \pm\infty$ and does not interfere with the asymptotics of $f(i\omega)$.

$$M = - \sum_l \text{Res} [f(i\omega_l)] n_B(\omega = i\omega_l). \quad (\text{A.7})$$

We reintroduce an energy integration, thus constructively complicating the expression by using the definition of the Dirac delta distribution $\int dx' f(x') \delta(x - x') = f(x)$:

$$M = -\frac{1}{2\pi} \int_{-i\infty}^{+i\infty} d(i\omega') \sum_l 2\pi\delta(i\omega' - i\omega_l) \text{Res}[f(i\omega')] n_B(i\omega'). \quad (\text{A.8})$$

After substituting $i\omega' \rightarrow \omega$ we find the well-known structure of a spectral density $\varrho_f(\omega) := \sum_l 2\pi\delta(\omega - \omega_l) \text{Res}_{\omega_l} f(\omega)$

$$M = -\frac{1}{2\pi} \int_{-\infty}^{+\infty} d\omega \underbrace{\sum_l 2\pi\delta(\omega - \omega_l) \text{Res} [f(\omega)] n_B(\omega)}_{=: \varrho_f(\omega) = 2\text{Im} f(\omega + i\varepsilon)} \quad (\text{A.9})$$

which can be replaced by the imaginary part of the retarded expression³ for f , finally yielding

$$M = - \int_{-\infty}^{+\infty} \frac{d\omega}{\pi} n_B(\omega) \text{Im}(f(\omega + i\varepsilon)). \quad (\text{A.10})$$

For a sum over all fermionic Matsubara frequencies, one replaces n_B by the Fermi-Dirac distribution function n_F with poles at $i\omega_n = (2n + 1)i\pi T + \mu$ and $\text{Res}_{i\omega_n} n_F = T$ in eq. (A.4). Since the remaining steps are independent of the explicit form of the distribution function, the result is found in an analogous way.

³As an example, this is shown for a bosonic propagator $f(\omega) = D(\omega) = -(\omega^2 - \omega_k^2)^{-1}$. The expression

$$\text{Res}_{\pm\omega_k} D(\omega) = \lim_{\omega \rightarrow \pm\omega_k} \frac{-(\omega \mp \omega_k)}{(\omega + \omega_k)(\omega - \omega_k)} = \lim_{\omega \rightarrow \pm\omega_k} \frac{-1}{\omega \pm \omega_k} = \mp \frac{1}{2\omega_k}$$

leads to $\varrho_D(\omega) = \frac{2\pi}{2\omega_k} [\delta(\omega + \omega_k) - \delta(\omega - \omega_k)]$. Using $(A + i\varepsilon)^{-1} = PA^{-1} - i\pi\delta(A)$, where P denotes the principle value, we obtain the same result for

$$\begin{aligned} 2\text{Im} D(\omega + i\varepsilon) &= -2\text{Im} \frac{1}{\omega^2 + 2i\varepsilon\omega - \omega_k^2} \\ &= 2\pi\delta(\omega^2 - \omega_k^2) = \frac{2\pi}{2\omega_k} [\delta(\omega + \omega_k) - \delta(\omega - \omega_k)] \end{aligned}$$

In fact, this simple example can be expanded to a rigorous proof by treating an arbitrary spectral function as infinite sum of delta distributions (convolution integral) and calculating its propagator using the Lehmann representation.

Appendix B Mathematical relations

B.1 Imaginary part of the logarithm

The imaginary part of the logarithm of a complex quantity z (e.g. an inverse propagator) equals the argument of z :

$$\begin{aligned} \text{Im} \ln(z) &= \text{Im} \ln \left(|z| e^{i \text{Arg}(z)} \right) \\ &= \text{Im} \left(\underbrace{\ln |z|}_{\in \mathbb{R}} + i \text{Arg}(z) \right) \\ &= \text{Arg}(z). \end{aligned} \tag{B.1}$$

Therefore, z is allowed to have a dimension, e.g. in the inverse of $z = D_{\text{T}}^{-1}$ a squared energy dimension, even though the logarithm itself is defined for dimensionless numbers only. For explicit calculations, the dimension has to be removed:

$$\text{Im} \ln D_{\text{T}}^{-1} = \text{Im} \left(\ln \frac{D_{\text{T}}^{-1}}{T^2} + \underbrace{2 \ln T}_{\in \mathbb{R}} \right) = \text{Im} \ln \frac{D_{\text{T}}^{-1}}{T^2}. \tag{B.2}$$

This is not an ambiguity since, as long as the dimension is well-behaved, it has no influence on the argument of D_{T}^{-1} .

The argument can be calculated using the arc tangent. Compensating for quadrant relations it is given by

$$\text{Im} \ln(z) = \text{Arg}(z) = \arctan \frac{\text{Im}z}{\text{Re}z} + \pi \varepsilon(\text{Im}z) \Theta(-\text{Re}z) \tag{B.3}$$

and, if the argument is $-z$,

$$\text{Im} \ln(-z) = \text{Arg}(-z) = \arctan \frac{\text{Im}z}{\text{Re}z} - \pi \varepsilon(\text{Im}z) \Theta(\text{Re}z). \tag{B.4}$$

Note that the step function Θ is defined for dimensionless quantities only too, so implicitly it is always to be divided by a reference quantity (e.g. again a power of the temperature if z is an inverse propagator).

B.2 Derivative of Arg and arctan

As a prerequisite, we need the derivative of the Heaviside function¹

$$\frac{\partial}{\partial x} \Theta \left(\frac{x}{a} \right) = \frac{1}{a} \delta \left(\frac{x}{a} \right) = \frac{|a|}{a} \delta(x) = \varepsilon(a) \delta(x) \tag{B.5}$$

¹At several points of this thesis we use the Dirac delta distribution $\delta(x)$. Even though it is a (singular) distribution, the integral sign is used for simplicity reasons. It has to be understood as a symbol for the bilinear form associated to the dual pair $\langle \mathcal{E}, \mathcal{E}' \rangle$ where $\mathcal{E} = C^\infty(\Omega)$ with $\Omega \subset \mathbb{R}^n$ chosen appropriately and \mathcal{E}' is the space of distributions with compact support.

In some situations we use the Delta distribution without even the integral sign, knowing that it is always part of a thermodynamic integral.

and as a consequence the derivative of the sign function $\varepsilon(x) := \Theta(x) - \Theta(-x)$

$$\frac{\partial}{\partial x} \varepsilon\left(\frac{x}{a}\right) = 2\varepsilon(a)\delta(x). \quad (\text{B.6})$$

Using a symmetry relation and the derivative of the arc tangent (cf. [TBM01])

$$\arctan\left(\frac{a}{x}\right) = -\arctan\left(\frac{x}{a}\right) + \pi\Theta\left(\frac{x}{a}\right) - \frac{\pi}{2}, \quad (\text{B.7})$$

$$\frac{\partial}{\partial x} \arctan\left(\frac{x}{a}\right) = \frac{a}{a^2 + x^2} \quad (\text{B.8})$$

we find

$$\frac{\partial}{\partial x} \arctan\left(\frac{a}{x}\right) = -\frac{a}{a^2 + x^2} + \pi\varepsilon(a)\delta(x). \quad (\text{B.9})$$

Applying this relation to the argument $\text{Arg } z = \arctan \frac{\text{Im } z}{\text{Re } z} + \pi\varepsilon(\text{Im } z)\Theta(-\text{Re } z)$ of a complex quantity z (e.g. an inverse propagator) we find

$$\frac{\partial}{\partial \text{Re } z} \text{Arg } z = \frac{-\text{Im } z}{\text{Im}^2 z + \text{Re}^2 z}, \quad (\text{B.10})$$

$$\frac{\partial}{\partial \text{Im } z} \text{Arg } z = \frac{\text{Re } z}{\text{Im}^2 z + \text{Re}^2 z} + 2\pi\delta(\text{Im } z)\Theta(-\text{Re } z). \quad (\text{B.11})$$

The two emerging Dirac delta distributions of the derivative with respect to the real part of z exactly cancel.

Appendix C List of derivatives

C.1 Derivatives of the HTL thermal masses

Effective and distributed quasiparticle models

The derivatives of the asymptotic masses $\tilde{m}_{i,\infty}$ with temperature dependent rest-masses $m_{q,s} = a_{q,s}T$ as defined in eq. (2.35) are given here. The derivatives of the asymptotic masses $m_{i,\infty}$ without restmasses can be found by taking the limit $a \rightarrow 0$. For gluons $\tilde{m}_g = m_g$, as defined in section 2.5, $\mu_q = \mu$ and $\mu_s = 0$. We obtain

$$\frac{\partial \tilde{m}_{g,\infty}^2}{\partial T} = \frac{C_b}{3} T G^2 + \tilde{C}_b \frac{\partial G^2}{\partial T}, \quad (\text{C.1})$$

$$\frac{\partial^2 \tilde{m}_{g,\infty}^2}{\partial T^2} = \frac{C_b}{3} G^2 + 2 \frac{C_b}{3} T \frac{\partial G^2}{\partial T} + \tilde{C}_b \frac{\partial^2 G^2}{\partial T^2}, \quad (\text{C.2})$$

$$\tilde{C}_b := \frac{1}{6} \left\{ C_b T^2 + \frac{N_c N_q}{2\pi^2} \mu^2 \right\} \quad (\text{C.3})$$

$$\frac{\partial \hat{M}_{q,s}^2}{\partial T} = \frac{C_f}{4} T G^2 + \frac{C_f}{8} \left(T^2 + \frac{\mu_{q,s}^2}{\pi^2} \right) \frac{\partial G^2}{\partial T} \quad (\text{C.4})$$

$$\frac{\partial \tilde{m}_{q/s,\infty}^2}{\partial T} = \left(2a_{q,s}T + 2\hat{M}_{q,s} \right) a_{q,s} + \left(\frac{a_{q,s}T}{\hat{M}_{q,s}} + 2 \right) \frac{\partial \hat{M}_{q,s}^2}{\partial T} \quad (\text{C.5})$$

$$= \underbrace{\left(2a_{q,s}T + 2\hat{M}_{q,s} \right) a_{q,s} + \left(\frac{a_{q,s}T}{\hat{M}_{q,s}} + 2 \right) \frac{C_f}{4} T G^2}_{(I)} + \underbrace{\left(\frac{a_{q,s}T}{\hat{M}_{q,s}} + 2 \right) \frac{C_f}{8} \left(T^2 + \frac{\mu_{q,s}^2}{\pi^2} \right)}_{(1)} \frac{\partial G^2}{\partial T}, \quad (\text{C.6})$$

$$\frac{\partial^2 \tilde{m}_{q/s,\infty}^2}{\partial T^2} = \left(2a_{q,s} + \frac{1}{\hat{M}_{q,s}} \frac{\partial \hat{M}_{q,s}^2}{\partial T} \right) a_{q,s} + \left(\frac{a_{q,s}}{\hat{M}_{q,s}} - \frac{a_{q,s}T}{2\hat{M}_{q,s}^3} \frac{\partial \hat{M}_{q,s}^2}{\partial T} \right) \frac{\partial \hat{M}_{q,s}^2}{\partial T} + \left(\frac{a_{q,s}T}{\hat{M}_{q,s}} + 2 \right) \frac{\partial^2 \hat{M}_{q,s}^2}{\partial T^2}, \quad (\text{C.7})$$

$$\frac{\partial^2 \hat{M}_{q,s}^2}{\partial T^2} = \frac{C_f}{8} \left(2G^2 + 4T \frac{\partial G^2}{\partial T} + \left(T^2 + \frac{\mu_{q,s}^2}{\pi^2} \right) \frac{\partial^2 G^2}{\partial T^2} \right), \quad (\text{C.8})$$

$$\frac{\partial \tilde{m}_{g,\infty}^2}{\partial \mu} = \underbrace{\frac{N_q \mu}{2\pi^2} G^2}_{(III)} + \underbrace{\frac{\tilde{C}_b}{6}}_{(C)} \frac{\partial G^2}{\partial \mu}, \quad (C.9)$$

$$\frac{\partial \tilde{m}_{q,\infty}^2}{\partial \mu} = \underbrace{\left(\frac{m_q}{\hat{M}_q} + 2 \right) \frac{C_f \mu}{4\pi^2} G^2}_{(II)} + \underbrace{\left(\frac{m_q}{\hat{M}_q} + 2 \right) \frac{C_f}{8} \left(T^2 + \frac{\mu^2}{\pi^2} \right)}_{(A)} \frac{\partial G^2}{\partial \mu}, \quad (C.10)$$

$$\frac{\partial \tilde{m}_{s,\infty}^2}{\partial \mu} = \underbrace{\left(\frac{m_s}{\hat{M}_s} + 2 \right) \frac{C_f T^2}{8}}_{(B)} \frac{\partial G^2}{\partial \mu}, \quad (C.11)$$

$$\frac{\partial^2 \tilde{m}_{q,\infty}^2}{\partial \mu^2} = -\frac{m_q}{2\hat{M}_q^3} \frac{\partial \hat{M}_q^2}{\partial \mu} + \left(\frac{m_q}{\hat{M}_q} + 2 \right) \frac{\partial^2 \hat{M}_q^2}{\partial \mu^2}, \quad (C.12)$$

$$\frac{\partial \hat{M}_q^2}{\partial \mu} = \frac{C_f \mu}{4\pi^2} G^2 + \frac{C_f}{8} \left(T^2 + \frac{\mu^2}{\pi^2} \right) \frac{\partial G^2}{\partial \mu}, \quad (C.13)$$

$$\frac{\partial^2 \hat{M}_q^2}{\partial \mu^2} = \frac{C_f}{8} \left(\frac{2}{\pi} G^2 + \frac{4\mu}{\pi^2} \frac{\partial G^2}{\partial \mu} + \left(T^2 + \frac{\mu^2}{\pi^2} \right) \frac{\partial^2 G^2}{\partial \mu^2} \right). \quad (C.14)$$

C.2 Derivatives of the Breit-Wigner distribution

This appendix lists the derivatives of the Breit-Wigner distribution $\text{BW}(m_i, M, \Gamma)$ as defined in section 4.1 with respect to the chemical potential μ . They are given by

$$\frac{\partial \text{BW}_i}{\partial \mu} = N_i \frac{\partial \widetilde{\text{BW}}_i}{\partial m_i^2} \frac{\partial m_i^2}{\partial \mu} - \widetilde{\text{BW}}_i \frac{\partial N_i}{\partial \mu}, \quad (C.15)$$

$$\frac{\partial^2 \text{BW}_i}{\partial \mu^2} = 2 \frac{\partial N_i}{\partial \mu} \frac{\partial \widetilde{\text{BW}}_i}{\partial m_i^2} \frac{\partial m_i^2}{\partial \mu} + N_i \frac{\partial^2 \widetilde{\text{BW}}_i}{(\partial m_i^2)^2} \left(\frac{\partial m_i^2}{\partial \mu} \right)^2 + N_i \frac{\partial \widetilde{\text{BW}}_i}{\partial m_i^2} \frac{\partial^2 m_i^2}{\partial \mu^2} + \widetilde{\text{BW}}_i \frac{\partial^2 N_i}{\partial \mu^2}, \quad (C.16)$$

where

$$\frac{\partial N_i}{\partial \mu} = -\frac{N_i}{2m_i} \frac{\partial N^{-1}}{\partial m_i} \frac{\partial m_i^2}{\partial \mu}, \quad (C.17)$$

$$\frac{\partial^2 N_i}{\partial \mu^2} = \frac{2}{N_i} \left(\frac{\partial N_i^2}{\partial \mu} \right)^2 - \frac{N_i^2}{2m_i} \frac{\partial^2 N_i^{-1}}{(\partial m_i)^2} \left(\frac{\partial m_i^2}{\partial \mu} \right)^2 + \frac{N_i^2}{4m_i^3} \frac{\partial N_i^{-1}}{\partial m_i} \left(\frac{\partial m_i^2}{\partial \mu} \right)^2 - \frac{N_i^2}{2m_i} \frac{\partial N_i^{-1}}{\partial m_i} \frac{\partial^2 m_i^2}{\partial \mu^2} \quad (C.18)$$

and

$$\frac{\partial \widetilde{\text{BW}}_i}{\partial m_i^2} = \frac{(M - m_i) \widetilde{\text{BW}}_i^2}{\Gamma m_i}, \quad (C.19)$$

$$\frac{\partial^2 \widetilde{\text{BW}}_i}{(\partial m_i)^2} = -\frac{M}{2\Gamma m_i^3} \widetilde{\text{BW}}_i^2 + \frac{(M - m_i)^2}{\Gamma m_i^2} 2\widetilde{\text{BW}}_i^3, \quad (C.20)$$

$$\frac{\partial N^{-1}}{\partial m_i} = \frac{4}{\Gamma} \left(\frac{1}{1 + 4m_i^2/\Gamma^2} - \frac{1}{1 + 4(M_{\max} - m_i)^2/\Gamma^2} \right), \quad (C.21)$$

$$\frac{\partial^2 N_i^{-1}}{(\partial m_i)^2} = -\frac{16}{\Gamma^3} \left(\frac{m_i}{(1 + 4m_i^2/\Gamma^2)^2} + \frac{M_{\max} - m_i}{(1 + (2(M_{\max} - m_i)/\Gamma)^2)^2} \right). \quad (C.22)$$

Appendix D Coefficients of the flow equations

D.1 Effective and distributed quasiparticle models

Using the abbreviations from Appendix C.1 and denoting the asymptotic masses $\hat{m}_{i,\infty}$ by m_i , the coefficients of the eQP and dQP flow equation are found to be

$$\begin{aligned} a_T &= -(1) \frac{\partial n_q}{\partial m_q^2}, \\ a_\mu &= (A) \frac{\partial s_q}{\partial m_q^2} + (B) \frac{\partial s_s}{\partial m_s^2} + (C) \frac{\partial s_g}{\partial m_g^2}, \\ b &= (I) \frac{\partial n_q}{\partial m_q^2} - (II) \frac{\partial s_q}{\partial m_q^2} - (III) \frac{\partial s_g}{\partial m_g^2}, \end{aligned} \quad (\text{D.1})$$

where for the eQP

$$\frac{\partial n_q^{eQP}}{\partial m_q^2} = \frac{d_q}{4\pi^2 T} \int_0^\infty dk \frac{k^2}{\omega_{\text{TL}}(k)} [e^+ f_-^2 - e^- f_+^2], \quad (\text{D.2})$$

$$\frac{\partial s_i^{eQP}}{\partial m_i^2} = \frac{d_i}{4\pi^2 T^2} \int_0^\infty dk k^2 \left\{ -[e^- f_+^2 + e^+ f_-^2] + \frac{\mu}{\omega_{\text{TL}}(k)} [e^- f_+^2 + e^+ f_-^2] \right\}, \quad (\text{D.3})$$

while for the dQP the derivative with respect to the asymptotic mass solely acts on the Breit-Wigner distribution

$$\frac{\partial n_q^{dQP}}{\partial m_q^2} = \frac{d_q}{2\pi^2} \int_0^\infty dM dk k^2 [f_+ - f_-] \frac{\partial \text{BW}}{\partial m_q^2}, \quad (\text{D.4})$$

$$\frac{\partial s_i^{dQP}}{\partial m_i^2} = \frac{d_i}{2\pi^2 T} \int_0^\infty dM dk k^2 \left\{ \frac{\frac{4}{3}k^2 + M^2}{\omega_i(k)} [f_+ + f_-] - \mu_i [f_+ - f_-] \right\} \frac{\partial \text{BW}}{\partial m_i^2} \quad (\text{D.5})$$

with

$$\frac{\partial \text{BW}_i}{\partial m_i^2} = \frac{\left(\frac{M}{m_i} - 1\right)}{\Gamma} N_i \widetilde{\text{BW}}_i^2 - \frac{N_i^2}{2m_i} \widetilde{\text{BW}}_i \left(\widetilde{\text{BW}}_i \Big|_{M=0} - \widetilde{\text{BW}}_i \Big|_{M=M_{\text{max}}} \right). \quad (\text{D.6})$$

The derivatives of the coefficients at vanishing chemical potential are

$$\frac{\partial b}{\partial \mu} \Big|_{\mu=0} = (I) \frac{\partial^2 n_q}{\partial \mu \partial m_q^2} \Big|_{\mu=0} - \frac{\partial(II)}{\partial \mu} \frac{\partial s_q}{\partial m_q^2} \Big|_{\mu=0} - \frac{\partial(III)}{\partial \mu} \frac{\partial s_g}{\partial m_g^2} \Big|_{\mu=0}, \quad (\text{D.7})$$

$$\frac{\partial a_T}{\partial \mu} \Big|_{\mu=0} = -(1) \frac{\partial^2 n_q}{\partial \mu \partial m_q^2} \Big|_{\mu=0} \quad (\text{D.8})$$

with

$$\left. \frac{\partial(II)}{\partial\mu} \right|_{\mu=0} = \left(\frac{m_q}{\omega_{\text{TL}}} + 2 \right) \frac{C_f}{4\pi^2} G^2|_{\mu=0}, \quad (\text{D.9})$$

$$\left. \frac{\partial(III)}{\partial\mu} \right|_{\mu=0} = \frac{3N_q}{6\pi^2} G^2|_{\mu=0} \quad (\text{D.10})$$

and

$$\left. \frac{\partial^2 n_q^{eQP}}{\partial\mu \partial m_q^2} \right|_{\mu=0} = \frac{d_q}{2\pi^2 T} \int_0^\infty dk \frac{k^2}{\omega_{\text{TL}}(k)} [ef^2 - 2e^2 f^3], \quad (\text{D.11})$$

$$\left. \frac{\partial^2 n_q^{dQP}}{\partial\mu \partial m_q^2} \right|_{\mu=0} = \frac{d_q}{2\pi^2 T} \int_0^\infty dM \int_0^\infty dk k^2 2ef^2 \left. \frac{\partial \text{BW}}{\partial m_q^2} \right|_{\mu=0}. \quad (\text{D.12})$$

D.2 Full HTL model

Note that in the following the abbreviations (1), (I), (A), etc. are defined differently than for the eQP/dQP. This is due to a different structure of the derivatives of entropy density and particle density with respect to μ and T , respectively, since the full HTL QPM uses the full dispersion relations as opposed to the asymptotic dispersion relations of eQP and dQP.

As in the chapters above we start from the Maxwell relation (3.14) and have in turn to calculate the derivatives of the entropy density with respect to μ and the particle density with respect to T .

Gluons

As first part of the Maxwell relation, the derivative of the full HTL gluon entropy density $s_g = s_{g,T} + s_{g,L}$ with partial gluon entropy densities (2.44) with respect to μ at constant T has to be calculated. For gluons there is no explicit dependence of the entropy density on the chemical potential, so that only the self-energies and propagators depend on μ due to the contained Debye mass. Consequently, there are four contributions to the derivative

$$\frac{\partial s_g}{\partial\mu} = \left(\frac{\partial s_g}{\partial\mu} \right)_{\text{Re}D_T^{-1}} + \left(\frac{\partial s_g}{\partial\mu} \right)_{\text{Im}\Pi_T} + \left(\frac{\partial s_g}{\partial\mu} \right)_{\text{Re}D_L^{-1}} + \left(\frac{\partial s_g}{\partial\mu} \right)_{\text{Im}\Pi_L}, \quad (\text{D.13})$$

where the index on the bracket indicates the considered dependence.

For the first term we find

$$\begin{aligned} \left(\frac{\partial s_g}{\partial\mu} \right)_{\text{Re}D_T^{-1}} &= - \frac{2d_g}{\pi m_D^2} \frac{\partial m_D^2}{\partial\mu} \int_{d^3k} \int_0^\infty d\omega \frac{\partial n_B}{\partial T} \\ &\times \left\{ - \frac{\text{Re}\Pi_T \text{Im}\Pi_T}{\text{Re}^2 D_T^{-1} + \text{Im}^2 \Pi_T} + \text{Re}\Pi_T \text{Im}\Pi_T \frac{\text{Re}^2 D_T^{-1} - \text{Im}^2 \Pi_T}{(\text{Re}^2 D_T^{-1} + \text{Im}^2 \Pi_T)^2} \right\}, \end{aligned} \quad (\text{D.14})$$

where the derivative of the quasiparticle pole term $\pi\Theta()$ is canceled by the term $\pi\delta()$ arising from the derivative of the arc tangent quite similar to the cancellation in section 5.1. We split the energy integration at the light cone. For $\omega > k$ the

imaginary part of the transverse gluon self-energy is equal to $\eta\varepsilon(\text{Im}\Pi_{\text{T}})$, where $\eta \rightarrow 0$ due to retardation (cf. eqs. 2.30). Leaving aside the prefactor $-\text{Re}\Pi_{\text{T}}$ and after multiplication by $\varepsilon(\text{Im}\Pi_{\text{T}})/\pi$ to assure a positive width $\Gamma := 2|\text{Im}\Pi_{\text{T}}|$ and normalization, the first term of the curly bracket corresponds to a Breit-Wigner distribution of a quantity $x = \text{Re}D_{\text{T}}^{-1}$:

$$\frac{1}{\pi} \frac{|\text{Im}\Pi_{\text{T}}|}{\text{Re}^2 D_{\text{T}}^{-1} + \text{Im}^2 \Pi_{\text{T}}} \longleftrightarrow \frac{1}{2\pi} \frac{\Gamma}{x^2 + \Gamma^2/4}. \quad (\text{D.15})$$

The normalization of the distribution to 2π instead of the exact expression (4.4) is justified in the limit of vanishing width considered here. The Breit-Wigner distribution is a representation of the Dirac delta distribution, therefore

$$\frac{\varepsilon(\text{Im}\Pi_{\text{T}})}{\pi} \frac{\text{Im}\Pi_{\text{T}}}{\text{Re}^2 D_{\text{T}}^{-1} + \text{Im}^2 \Pi_{\text{T}}} \xrightarrow{\text{Im}\Pi_{\text{T}} \rightarrow 0} \delta(\text{Re}D_{\text{T}}^{-1}) \quad (\text{D.16})$$

in the region $\omega > k$. Consequently, for $\omega > k$, the first term in the curly bracket equals $-\pi\varepsilon(\text{Im}\Pi_{\text{T}})\delta(\text{Re}D_{\text{T}}^{-1})\text{Re}\Pi_{\text{T}}$. The dispersion relation is valid for $\omega_{\text{T},k}$ so that

$$\begin{aligned} \delta(\text{Re}D_{\text{T}}^{-1}) &= \sum_{\text{zeroes } i \text{ of } \text{Re}D_{\text{T}}^{-1}} \delta(\omega - \omega_i) / \left| \frac{\partial \text{Re}D_{\text{T}}^{-1}}{\partial \omega} \right|_{\omega_i} \\ &= \delta(\omega - \omega_{\text{T},k}) / \left| \frac{\partial \text{Re}D_{\text{T}}^{-1}}{\partial \omega} \right|_{\omega_{\text{T},k}}. \end{aligned} \quad (\text{D.17})$$

The derivative of the real part of the inverse transverse gluon propagator with respect to ω is found to be

$$\frac{\partial \text{Re}D_{\text{T}}^{-1}}{\partial \omega} = -2\omega + \frac{m_D^2}{2} \left(\frac{3\omega}{k} - \frac{3\omega - k}{2k^3} \ln \left| \frac{\omega + k}{\omega - k} \right| \right). \quad (\text{D.18})$$

After substitution of the logarithmic term with $\text{Re}\Pi_{\text{T}}$ and evaluation at the dispersion relation ($\text{Re}\Pi_{\text{T}}(\omega_{\text{T},k}) = \omega_{\text{T},k}^2 - k^2$) the energy integration of the first term of the curly bracket can be executed:

$$\begin{aligned} -\pi \int_k^\infty d\omega \frac{\partial n_{\text{B}}}{\partial T} \varepsilon(\text{Im}\Pi_{\text{T}}) \text{Re}\Pi_{\text{T}} \delta(\omega - \omega_{\text{T},k}) / \left| \frac{\partial \text{Re}D_{\text{T}}^{-1}}{\partial \omega} \right|_{\omega_{\text{T},k}} &= \\ + \pi \frac{\partial n_{\text{B}}}{\partial T} \Big|_{\omega_{\text{T},k}} \omega_{\text{T},k} \frac{(\omega_{\text{T},k}^2 - k^2)^2}{|(\omega_{\text{T},k}^2 - k^2)^2 - m_D^2 \omega_{\text{T},k}^2|}. \end{aligned} \quad (\text{D.19})$$

The energy integral of the second term in the curly bracket vanishes for $\text{Im}\Pi_{\text{T}} \rightarrow 0$. Consequently, it does not contribute for $\omega > k$.

For $\omega < k$ the imaginary part of the self-energy Π_{T} is nonzero except for $\omega = 0$. However, at $\omega = 0$ the real part of the inverse transverse gluon propagator D_{T}^{-1} is generally nonzero so that no special treatment is necessary. The terms of the curly bracket can be simplified and the final expression for the derivative of the entropy density with respect to μ within $\text{Re}D_{\text{T}}^{-1}$ becomes

$$\begin{aligned} \left(\frac{\partial s_g}{\partial \mu} \right)_{\text{Re}D_{\text{T}}^{-1}} &= + \frac{d_g}{\pi^3 m_D^2} \frac{\partial m_D^2}{\partial \mu} \int_0^\infty dk k^2 \\ &\times \left(\int_0^k d\omega \left[\frac{\partial n_{\text{B}}}{\partial T} \frac{2\text{Re}\Pi_{\text{T}}\text{Im}^3 \Pi_{\text{T}}}{(\text{Re}^2 D_{\text{T}}^{-1} + \text{Im}^2 \Pi_{\text{T}})^2} \right] - \pi \frac{\partial n_{\text{B}}}{\partial T} \Big|_{\omega_{\text{T},k}} \frac{\omega_{\text{T},k}(\omega_{\text{T},k}^2 - k^2)^2}{|(\omega_{\text{T},k}^2 - k^2)^2 - m_D^2 \omega_{\text{T},k}^2|} \right). \end{aligned} \quad (\text{D.20})$$

Analogously we find

$$\begin{aligned} \left(\frac{\partial s_g}{\partial \mu}\right)_{\text{Re}D_L^{-1}} &= + \frac{d_g}{2\pi^3 m_D^2} \frac{\partial m_D^2}{\partial \mu} \int_0^\infty dk k^2 \\ &\times \left(\int_0^k d\omega \left[\frac{\partial n_B}{\partial T} \frac{2\text{Re}\Pi_L \text{Im}^3 \Pi_L}{(\text{Re}^2 D_L^{-1} + \text{Im}^2 \Pi_L)^2} \right] - \pi \frac{\partial n_B}{\partial T} \Big|_{\omega_{L,k}} \frac{\omega_{L,k}(\omega_{L,k}^2 - k^2)}{|\omega_{L,k}^2 - k^2 - m_D^2|} \right). \end{aligned} \quad (\text{D.21})$$

The derivatives of the gluon entropy density with respect to μ within the imaginary parts of the self-energies are straightforward. The Dirac delta distributions arising from the the sign functions within the quasiparticle pole contributions $\pi \varepsilon(\text{Im}\Pi_i) \Theta(\mp \text{Re}D_i^{-1})$ vanish due to the prefactor $\text{Im}\Pi_i/m_D^2$ from the chain rule. We are left with

$$\left(\frac{\partial s_g}{\partial \mu}\right)_{\text{Im}\Pi_T} = - \frac{d_g}{\pi^3 m_D^2} \frac{\partial m_D^2}{\partial \mu} \int_0^\infty dk k^2 \int_0^\infty d\omega \frac{\partial n_B}{\partial T} \frac{2\text{Re}D_T^{-1} \text{Im}^3 \Pi_T}{(\text{Re}^2 D_T^{-1} + \text{Im}^2 \Pi_T)^2}, \quad (\text{D.22})$$

$$\left(\frac{\partial s_g}{\partial \mu}\right)_{\text{Im}\Pi_L} = + \frac{d_g}{2\pi^3 m_D^2} \frac{\partial m_D^2}{\partial \mu} \int_0^\infty dk k^2 \int_0^\infty d\omega \frac{\partial n_B}{\partial T} \frac{2\text{Re}D_L^{-1} \text{Im}^3 \Pi_L}{(\text{Re}^2 D_L^{-1} + \text{Im}^2 \Pi_L)^2}. \quad (\text{D.23})$$

Putting things together and substituting $\text{Re}\Pi_T - \text{Re}D_T^{-1} = \omega^2 - k^2$ and $\text{Re}\Pi_L + \text{Re}D_L^{-1} = -k^2$ we have

$$\begin{aligned} \frac{\partial s_g}{\partial \mu} &= \frac{\partial m_D^2}{\partial \mu} \left\{ \frac{d_g}{2\pi^3 m_D^2} \int_0^\infty dk k^2 \right. \\ &\times \left(\int_0^k d\omega \left[\frac{\partial n_B}{\partial T} \frac{4(\omega^2 - k^2) \text{Im}^3 \Pi_T}{(\text{Re}^2 D_T^{-1} + \text{Im}^2 \Pi_T)^2} - \frac{\partial n_B}{\partial T} \frac{2k^2 \text{Im}^3 \Pi_L}{(\text{Re}^2 D_L^{-1} + \text{Im}^2 \Pi_L)^2} \right] \right. \\ &\left. \left. - \pi \frac{\omega_{T,k}(\omega_{T,k}^2 - k^2)^2}{|(\omega_{T,k}^2 - k^2)^2 - m_D^2 \omega_{T,k}^2|} \frac{\partial n_B}{\partial T} \Big|_{\omega_{T,k}} - \pi \frac{\omega_{L,k}(\omega_{L,k}^2 - k^2)}{|\omega_{L,k}^2 - k^2 - m_D^2|} \frac{\partial n_B}{\partial T} \Big|_{\omega_{L,k}} \right) \right\}_{(1)} \end{aligned} \quad (\text{D.24})$$

as final expression for the gluons with the derivative of the Debye mass with respect the μ given in Appendix C.1. The numbered curly bracket is used as abbreviation below.

Quarks

The derivative of the quark entropy density with respect to μ is done in a similar fashion. Due to the dependence of the Fermi-Dirac distribution function n_F on the chemical potential explicit derivatives emerge, however, in the Maxwell relation these are canceled by explicit derivatives from the derivative of the particle density with respect to the temperature due to Schwarz's theorem, as for the models above. For convenience starting from eq. (2.47) only the dependencies of $\text{Re}S_+^{-1}$ and $\text{Im}\Sigma_+$ on μ have to be taken into account:

$$\frac{\partial s_q}{\partial \mu} = \left(\frac{\partial s_q}{\partial \mu}\right)_{\text{Re}S_+^{-1}} + \left(\frac{\partial s_q}{\partial \mu}\right)_{\text{Im}\Sigma_+} + \left(\frac{\partial s_q}{\partial \mu}\right)_{n_F^{(A)}}. \quad (\text{D.25})$$

The third term is the explicit term which is given by eq. (2.47) with the substitution $\partial n_F^{(A)}/\partial T \rightarrow \partial^2 n_F^{(A)}/\partial \mu \partial T$. While the derivative of s_q with respect to μ within

$\text{Im}\Sigma_+$ is entirely equivalent to the transverse gluon case, the derivative of s_q with respect to μ within $\text{Re}S_+^{-1}$ differs due to the two dispersion relations $\omega_{\text{TL},k}$ and $\omega_{\text{Pl},k}$ and the different derivative of the real part of the inverse propagator with respect to ω .

For the case¹ $|\omega| > k$ we have

$$\delta(\text{Re}S_+^{-1}) = \delta(\omega - \omega_{\text{TL},k}) / \left. \left| \frac{\partial \text{Re}S_+^{-1}}{\partial \omega} \right| \right|_{\omega_{\text{TL},k}} + \delta(\omega - \omega_{\text{Pl},k}) / \left. \left| \frac{\partial \text{Re}S_+^{-1}}{\partial \omega} \right| \right|_{\omega_{\text{Pl},k}}, \quad (\text{D.26})$$

where

$$\frac{\partial \text{Re}S_+^{-1}}{\partial \omega} = -1 + \frac{\text{Re}\Sigma_+}{\omega - k} - \frac{2\hat{M}^2}{\omega^2 - k^2}. \quad (\text{D.27})$$

The integral over the first term of the curly bracket times $\pi\varepsilon(\text{Im}\Sigma_+)$ which, up to the different propagators/self-energies, is analogous to the transverse gluon case (cf. eqs. (D.14) and (D.19)) then reads

$$\pi \frac{\omega_{\text{TL},k}^2 - k^2}{2\hat{M}^2} (\omega_{\text{TL},k} - k) (+)|_{\omega_{\text{TL},k}} - \pi \frac{\omega_{\text{Pl},k}^2 - k^2}{2\hat{M}^2} (\omega_{\text{Pl},k} + k) (+)|_{\omega_{\text{Pl},k}}, \quad (\text{D.28})$$

where

$$(+):= \left(\frac{\partial n_{\text{F}}}{\partial T} + \frac{\partial n_{\text{F}}^A}{\partial T} \right). \quad (\text{D.29})$$

The energy integral of second term of the curly bracket again vanishes for $\text{Im}\Sigma_+ \rightarrow 0$ and thus does not contribute for $|\omega| > k$.

For $|\omega| < k$ there is no difference to the transverse gluon expression except for the different propagators and self-energies so that the final quark expression reads

$$\begin{aligned} \frac{\partial s_q}{\partial \mu} &= \frac{\partial \hat{M}^2}{\partial \mu} \left\{ \frac{d_q}{2\pi^3 \hat{M}^2} \int_0^\infty dk k^2 \left(\int_{-k}^k d\omega \left[(+) \frac{2(\omega - k) \text{Im}^3 \Sigma_+}{(\text{Re}^2 S_+^{-1} + \text{Im}^2 \Sigma_+)^2} \right. \right. \right. \\ &\quad \left. \left. \left. - \pi \frac{\omega_{\text{TL},k}^2 - k^2}{2\hat{M}^2} (\omega_{\text{TL},k} - k) (+)|_{\omega_{\text{TL},k}} - \pi \frac{\omega_{\text{Pl},k}^2 - k^2}{2\hat{M}^2} (\omega_{\text{Pl},k} + k) (+)|_{\omega_{\text{Pl},k}} \right] \right) \right\}_{(I)} \end{aligned} \quad (\text{D.30})$$

with (I) indicating the brackets for quarks. The derivative of \hat{M}^2 with respect to μ is also found in Appendix C.1, eq. (C.13).

The strange quark contribution to the Maxwell relation equals the quark expression at vanishing chemical potential

$$\frac{\partial s_s}{\partial \mu} = \frac{\partial s_q}{\partial \mu} \Big|_{\mu=0} \quad (\text{D.31})$$

with curly brackets $\{\}_{(II)} := \{\}_{(I)}|_{\mu=0}$ and $\partial \hat{M}^2 / \partial \mu \rightarrow \partial \hat{M}_s^2 / \partial \mu = (\partial \hat{M}^2 / \partial \mu)|_{\mu=0}$.

¹Note that the energy integral limits for both quark contributions are $(-\infty \dots \infty)$ as opposed to the gluons with $(0 \dots \infty)$.

Particle density

The last step towards the flow equation is the derivative of the particle density with respect to the temperature. The calculation mirrors the calculation for $\partial s_q/\partial\mu$ with the derivatives $\partial/\partial\mu$ and $\partial/\partial T$ being exchanged. Due to $\partial^2 n_F^{(A)}/\partial\mu\partial T = \partial^2 n_F^{(A)}/\partial T\partial\mu$ it is clear that the explicit derivatives of both cases are equal and cancel within the flow equation. They are, therefore, again omitted. We find

$$\begin{aligned} \frac{\partial n_q}{\partial T} = & \frac{\partial \hat{M}^2}{\partial T} \left\{ \frac{d_q}{2\pi^3 \hat{M}^2} \int_0^\infty dk k^2 \left(\int_{-k}^k d\omega \left[(\tilde{\dagger}) \frac{2(\omega - k) \text{Im}^3 \Sigma_+}{(\text{Re}^2 S_+^{-1} + \text{Im}^2 \Sigma_+)^2} \right] \right. \right. \\ & \left. \left. - \pi \frac{\omega_{\text{TL},k}^2 - k^2}{2\hat{M}^2} (\omega_{\text{TL},k} - k) (\tilde{\dagger})|_{\omega_{\text{TL},k}} - \pi \frac{\omega_{\text{P1},k}^2 - k^2}{2\hat{M}^2} (\omega_{\text{P1},k} + k) (\tilde{\dagger})|_{\omega_{\text{P1},k}} \right) \right\}_{(A)} \end{aligned} \quad (\text{D.32})$$

with

$$(\tilde{\dagger}) := \left(\frac{\partial n_F}{\partial \mu} + \frac{\partial n_F^A}{\partial \mu} \right) \quad (\text{D.33})$$

and $\partial \hat{M}^2/\partial T$ given by eq. (C.4). For the heavy quark flavor and gluons $(\tilde{\dagger})$ and thus $\partial n_{g,s}/\partial T$ vanishes as a consequence of $\mu_{g,s} = 0$.

The flow equation

Using the results above and the derivatives of the gluon/fermion mass parameters from Appendix C.1 the Maxwell relation becomes a flow equation of the form

$$a_T \frac{\partial G^2}{\partial T} + a_\mu \frac{\partial G^2}{\partial \mu} = b \quad (\text{D.34})$$

as partial differential equation for the effective coupling G^2 with the coefficients²

$$\begin{aligned} a_T &= -\tilde{C}_f \{ \}_{(A)}, \\ a_\mu &= 2\tilde{C}_b \{ \}_{(1)} + \tilde{C}_f \{ \}_{(I)} + \frac{C_f}{8} T^2 \{ \}_{(II)}, \\ b &= \frac{C_f}{4} T G^2 \{ \}_{(A)} - \frac{N_c N_l}{3\pi^2} \mu G^2 \{ \}_{(1)} - \frac{C_f}{4\pi^2} \mu G^2 \{ \}_{(I)}. \end{aligned} \quad (\text{D.35})$$

²Comparing these coefficients to the results from [Rom04] (eqs. (B.1) to (B.5)) several differences are noticeable:

1. The expression $(\omega_{\text{T},k}^2 - k^2)$ in the numerator of $\frac{\omega_{\text{T},k}(\omega_{\text{T},k}^2 - k^2)^2}{|(\omega_{\text{T},k}^2 - k^2)^2 - m_D^2 \omega_{\text{T},k}^2|}$ within bracket $\{ \}_{(1)}$ (eq. D.24) is not squared. This is incorrect, as the dimension of the term thus differs from the terms it is being added to.
2. The terms $\frac{\omega_{i,k}^2 - k^2}{2\hat{M}^2}$ within $-\pi \frac{\omega_{i,k}^2 - k^2}{2\hat{M}^2} (\omega_{i,k} - k) (\tilde{\dagger})|_{\omega_{i,k}}$ in bracket $\{ \}_{(A)}$ (eq. D.32) are missing. This is most probably a typographical error, as the neglect of the term leads to an increased a_T and thus to characteristics reaching $T = 0$ at very small values of the chemical potential.
3. The coefficient b from eq. (D.35) and the same coefficient found by Romatschke are related by $b^{\text{Rom}} = -b/G^2$. As a consequence the coupling G^2 from [Rom04] would decrease for $\mu \gtrsim 0$ as opposed to any of the other models. Therefore, we believe this to be incorrect, too.

As a consequence, the results obtained for $N_f = 2$ within [Rom04] are not reproducible.

Glossary of abbreviations

BW	Breit-Wigner
CJT	Cornwall-Jackiw-Tomboulis
dQP	distributed QPM
EOS	equation of state
eQP	effective (simple) QPM
FWHM	full width at half maximum
HIC	Heavy Ion Collisions
HTL	Hard Thermal Loops
iQP	improved QPM
IR	infrared
LD	Landau damping
LW	Luttinger-Ward
QCD	Quantum Chromodynamics
QED	Quantum Electrodynamics
QGP	quark-gluon plasma
QPM	quasiparticle model
UV	ultraviolet

Bibliography

- [All03] C. R. Allton et al., *Equation of state for two flavor QCD at nonzero chemical potential*. Phys. Rev. D **68**, 014507 (2003), doi:10.1103/PhysRevD.68.014507, arXiv:hep-lat/0305007.
- [And06] A. Andronic, P. Braun-Munzinger, J. Stachel, *Hadron production in central nucleus nucleus collisions at chemical freeze-out*. Nucl. Phys. A **772**, 167 (2006), doi:10.1016/j.nuclphysa.2006.03.012, arXiv:nucl-th/0511071.
- [Bay62] G. Baym, *Self-Consistent Approximations in Many-Body Systems*. Phys. Rev. **127**, 1391 (1962), doi:10.1103/PhysRev.127.1391.
- [BB04] D. B. Blaschke, K. A. Bugaev, *Hadronic correlations above the chiral / deconfinement transition*. Fizika B **13**, 491 (2004), arXiv:nucl-th/0311021, http://fizika.phy.hr/fizika_b/bv04/b13p491.htm.
- [Bec05] W. C. Beckmann, *Self-consistent Calculations of Hadron Properties at Non-zero Temperature*. Ph.D. thesis, University of Frankfurt a. M. (2005), <http://deposit.ddb.de/cgi-bin/dokserv?idn=979509920>.
- [Ber04] J. Berges, *n-Particle irreducible effective action techniques for gauge theories*. Phys. Rev. D **70**, 105010 (2004), doi:10.1103/PhysRevD.70.105010, arXiv:hep-ph/0401172.
- [BIR01] J.-P. Blaizot, E. Iancu, A. Rebhan, *Approximately self-consistent resummations for the thermodynamics of the quark-gluon plasma: Entropy and density*. Phys. Rev. D **63**, 065003 (2001), doi:10.1103/PhysRevD.63.065003, arXiv:hep-ph/0005003.
- [Bir06] T. S. Biró, P. Lévai, P. Ván, J. Zimányi, *Equation of state for distributed mass quark matter*. J. Phys. G **32**, S205 (2006), doi:10.1088/0954-3899/32/12/S26, arXiv:hep-ph/0605274.
- [BK61] G. Baym, L. P. Kadanoff, *Conservation Laws and Correlation Functions*. Phys. Rev. **124**, 287 (1961), doi:10.1103/PhysRev.124.287.
- [BKS06] M. Bluhm, B. Kämpfer, R. Schulze, D. Seipt, *Isentropic Equation of State of Two-Flavour QCD in a Quasi-Particle Model*. Acta Phys. Hung. A **27**, 397 (2006), doi:10.1556/APH.27.2006.4.2, arXiv:hep-ph/0608052.
- [BKS07a] M. Bluhm, B. Kämpfer, R. Schulze, D. Seipt, *Quasi-particle description of strongly interacting matter: Towards a foundation*. Eur. Phys. J. C **49**, 205 (2007), doi:10.1140/epjc/s10052-006-0056-y, arXiv:hep-ph/0608053.
- [BKS07b] M. Bluhm, B. Kämpfer, R. Schulze, D. Seipt, U. Heinz, *A family of equations of state based on lattice QCD: Impact on flow in ultrarelativistic heavy-ion collisions* (2007), arXiv:hep-ph/0705.0397.

- [Blu04] M. Bluhm, *On the equation of state of strongly interacting matter - A quasi-particle description*. Diploma thesis, Technical University Dresden (2004).
- [BP90a] E. Braaten, R. D. Pisarski, *Resummation and gauge invariance of the gluon damping rate in hot QCD*. Phys. Rev. Lett. **64**, 1338 (1990), doi:10.1103/PhysRevLett.64.1338.
- [BP90b] E. Braaten, R. D. Pisarski, *Soft amplitudes in hot gauge theories: A general analysis*. Nucl. Phys. B **337**, 569 (1990), doi:10.1016/0550-3213(90)90508-B.
- [Bra03] P. Braun-Munzinger, K. Redlich, J. Stachel, *Particle production in heavy ion collisions*. in *Quark Gluon Plasma*, edited by R. Hwa, X.-N. Wang, pp. 491–599 (World Scientific, 2003), ISBN 9812380779, arXiv:nucl-th/0304013.
- [Bro92] L. S. Brown, *Quantum Field Theory* (Cambridge University Press, 1992), ISBN 0521469465.
- [Car04] M. E. Carrington, *The 4PI effective action for ϕ^4 theory*. Eur. Phys. J. C **35**, 383 (2004), doi:10.1140/epjc/s2004-01849-6, arXiv:hep-ph/0401123.
- [CH98] S. Chiku, T. Hatsuda, *Optimized perturbation theory at finite temperature*. Phys. Rev. D **58**, 076001 (1998), doi:10.1103/PhysRevD.58.076001.
- [CJT74] J. M. Cornwall, R. Jackiw, E. Tomboulis, *Effective action for composite operators*. Phys. Rev. D **10**, 2428 (1974), doi:10.1103/PhysRevD.10.2428.
- [CP75] G. M. Carneiro, C. J. Pethick, *Specific heat of a normal Fermi liquid. II. Microscopic approach*. Phys. Rev. B **11**, 1106 (1975), doi:10.1103/PhysRevB.11.1106.
- [CPP01] A. Ali Khan et al., *Equation of state in finite-temperature QCD with two flavors of improved Wilson quarks*. Phys. Rev. D **64**, 074510 (2001), doi:10.1103/PhysRevD.64.074510, arXiv:hep-lat/0103028.
- [CPP99] M. Okamoto et al., *Equation of state for pure SU(3) gauge theory with renormalization group improved action*. Phys. Rev. D **60**, 094510 (1999), doi:10.1103/PhysRevD.60.094510, arXiv:hep-lat/9905005.
- [dDM64] C. De Dominicis, P. C. Martin, *Stationary Entropy Principle and Renormalization in Normal and Superfluid Systems. I. Algebraic Formulation*. J. Math. Phys. **5**, 14 (1964), doi:10.1063/1.1704062.
- [DJ67] H. D. Dahmen, G. Jona-Lasinio, *Variational Formulation of Quantum Field Theory. - I*. Nuovo Cimento **A52**, 807 (1967).
- [DJ69] H. D. Dahmen, G. Jona-Lasinio, *Variational Formulation of Quantum Field Theory. - II. A study of a Functional Derivative Equation Related to the gA^3 Theory*. Nuovo Cimento **A62**, 889 (1969).
- [DJT72] H. D. Dahmen, G. Jona-Lasinio, J. Tarski, *The method of characteristics for functional-derivative equations*. Nuovo Cimento **A10**, 513 (1972).

-
- [FW71] P. Fulde, H. Wagner, *Low-Temperature Specific Heat and Thermal Conductivity of Noncrystalline Solids*. Phys. Rev. Lett. **27**, 1280 (1971), doi:10.1103/PhysRevLett.27.1280.
- [GTP11] W. Greiner, S. Schramm, E. Stein, *Quantum Chromodynamics*, vol. 11 of *Classical Theoretical Physics* (Springer, 2002), 2nd edn., ISBN 3540666109.
- [GW65] W. Götze, H. Wagner, *On the T^3 -law for the specific heat of bose liquids*. Physica **31**, 475 (1965), doi:10.1016/0031-8914(65)90074-1.
- [GY95] M. I. Gorenstein, S. N. Yang, *Gluon plasma with a medium-dependent dispersion relation*. Phys. Rev. D **52**, 5206 (1995), doi:10.1103/PhysRevD.52.5206.
- [Hei27] W. Heisenberg, *Über den anschaulichen Inhalt der quantentheoretischen Kinematik und Mechanik*. Z. Phys. A **43**, 172 (1927), doi:10.1007/BF01397280.
- [Jon64] G. Jona-Lasinio, *Relativistic Field Theories with Symmetry-Breaking Solutions*. Nuovo Cimento **34**, 1790 (1964).
- [Kap89] J. I. Kapusta, *Finite-Temperature Field Theory* (Cambridge University Press, 1989), ISBN 0521449456.
- [Kar07] F. Karsch, *Transition temperature in QCD with physical light and strange quark masses* (2007), arXiv:hep-ph/0701210.
- [KBS06] B. Kämpfer, M. Bluhm, R. Schulze, D. Seipt, U. Heinz, *QCD matter within a quasi-particle model and the critical end point*. Nucl. Phys. A **774**, 757 (2006), doi:10.1016/j.nuclphysa.2006.06.131, arXiv:hep-ph/0509146.
- [Kle82] H. Kleinert, *Higher effective actions for bose systems*. Fortsch. Phys. **30**, 187 (1982), doi:10.1002/prop.19820300402.
- [KLP00] F. Karsch, E. Laermann, A. Peikert, *The Pressure in 2, 2+1 and 3 Flavour QCD*. Phys. Lett. B **478**, 447 (2000), doi:10.1016/S0370-2693(00)00292-6, arXiv:hep-lat/0002003.
- [KSS06] R. Klanner, T. Schörner-Sadenius, *Verstehen wir die starke Kraft?* Phys. J. **5**, 41 (2006), <http://www.pro-physik.de/Phy/pdfstart.do?recordid=23604>.
- [LeB96] M. L. Bellac, *Thermal Field Theory* (Cambridge University Press, 1996), ISBN 0521654777.
- [LFK98] C. Lobban, J. L. Finney, W. F. Kuhs, *The structure of a new phase of ice*. Nature **391**, 268 (1998), doi:10.1038/34622.
- [LL06] L. D. Landau, E. M. Lifshitz, *Fluid mechanics*, vol. 6 of *Course of Theoretical Physics* (Pergamon, 1987), 2nd edn.
- [LW60] J. M. Luttinger, J. C. Ward, *Ground-State Energy of a Many-Fermion System. II*. Phys. Rev. **118**, 1417 (1960), doi:10.1103/PhysRev.118.1417.

- [LY60b] T. D. Lee, C. N. Yang, *Many-Body Problem in Quantum Statistical Mechanics. IV. Formulation in Terms of Average Occupation Number in Momentum Space*. Phys. Rev. **117**, 22 (1960), doi:10.1103/PhysRev.117.22.
- [NC75] R. E. Norton, J. M. Cornwall, *On the formalism of relativistic many body theory*. Ann. Phys. **91**, 106 (1975), doi:10.1016/0003-4916(75)90281-X.
- [ONC99] T. M. O'Neil, F. V. Coroniti, *The collisionless nature of high-temperature plasmas*. Rev. Mod. Phys. **71**, S404 (1999), doi:10.1103/RevModPhys.71.S404.
- [PDG06] W.-M. Yao et al., *Review of Particle Physics*. J. Phys. G **33**, 1 (2006), doi:10.1088/0954-3899/33/1/001, <http://pdg.lbl.gov>.
- [Pei00] A. Peikert, *QCD thermodynamics with 2+1 flavours in lattice simulations*. Ph.D. thesis, University of Bielefeld (2000), <http://www.physik.uni-bielefeld.de/theory/e6/publicphd.html>.
- [Pes00] A. Peshier, B. Kämpfer, G. Soff, *Equation of state of deconfined matter at finite chemical potential in a quasiparticle description*. Phys. Rev. C **61**, 045203 (2000), doi:10.1103/PhysRevC.61.045203, arXiv:hep-ph/9911474.
- [Pes01] A. Peshier, *Hard thermal loop resummation of the thermodynamic potential*. Phys. Rev. D **63**, 105004 (2001), doi:10.1103/PhysRevD.63.105004, arXiv:hep-ph/0011250.
- [Pes02] A. Peshier, B. Kämpfer, G. Soff, *From QCD lattice calculations to the equation of state of quark matter*. Phys. Rev. D **66**, 094003 (2002), doi:10.1103/PhysRevD.66.094003, arXiv:hep-ph/0206229.
- [Pes04] A. Peshier, *Hard gluon damping in hot QCD*. Phys. Rev. D **70**, 034016 (2004), doi:10.1103/PhysRevD.70.034016, arXiv:hep-ph/0403225.
- [Pes05] A. Peshier, *Hard parton damping in hot QCD*. J. Phys. G **31**, 371 (2005), doi:10.1088/0954-3899/31/4/046, arXiv:hep-ph/0409270.
- [Pes98] A. Peshier, *Zur Zustandsgleichung heißer stark wechselwirkender Materie- konsistente Beschreibungen stark gekoppelter Quantensysteme*. Ph.D. thesis, Technical University Dresden (1998), <http://www.physik.tu-dresden.de/publik/habildiss.htm>.
- [Pis89b] R. D. Pisarski, *Renormalized fermion propagator in hot gauge theories*. Nucl. Phys. A **498**, 423 (1989), doi:10.1016/0375-9474(89)90620-9.
- [Pis93] R. D. Pisarski, *Damping rates for moving particles in hot QCD*. Phys. Rev. D **47**, 5589 (1993), doi:10.1103/PhysRevD.47.5589.
- [PS95] M. E. Peskin, D. V. Schroeder, *An Introduction to Quantum Field Theory* (Perseus Books, 1995), ISBN 0201503972.
- [Ris03] D. H. Rischke, *The quark-gluon plasma in equilibrium*. Prog. Part. Nucl. Phys. **52**, 197 (2004), doi:10.1016/j.ppnp.2003.09.002, arXiv:nucl-th/0305030.

-
- [Riv88] R. J. Rivers, *Path integral methods in quantum field theory* (Cambridge University Press, 1988), 1st edn., ISBN 0521368707.
- [Roe05] D. Röder, *Selfconsistent calculations of mesonic properties at nonzero temperature*. Ph.D. thesis, University of Frankfurt a. M. (2005), arXiv:hep-ph/0601146, <http://deposit.ddb.de/cgi-bin/dokserv?idn=978020219>.
- [Rom04] P. Romatschke, *Quasiparticle description of the hot and dense quark-gluon plasma*. Ph.D. thesis, Technical University Vienna (2004), arXiv:hep-ph/0312152.
- [RW00] K. Rajagopal, F. Wilczek, *The Condensed Matter Physics of QCD*. in *At the Frontier of Particle Physics: Handbook of QCD*, edited by M. Shifman, chap. 35 (World Scientific, 2000), ISBN 9812380280, arXiv:hep-ph/0011333.
- [Sei07] D. Seipt, *Quark Mass Dependence of One-Loop Self-Energies in Hot QCD*. Diploma thesis, Technical University Dresden (2007).
- [TBM01] I. N. Bronstein, K. A. Semendjajew, *Taschenbuch der Mathematik*, vol. 1 (Teubner Verlagsgesellschaft Leipzig, 1996).
- [TL97] B. T. Tsurutani, G. S. Lakhina, *Some basic concepts of wave-particle interactions in collisionless plasmas*. *Rev. Geo.* **35**, 491 (1997), doi:10.1029/97RG02200.
- [VB98] B. Vanderheyden, G. Baym, *Self-Consistent Approximations in Relativistic Plasmas: Quasiparticle Analysis of the Thermodynamic Properties*. *J. Stat. Phys.* **93**, 843 (1998), doi:10.1023/B:JOSS.0000033166.37520.ae.
- [VK72] A. N. Vasil'ev, A. K. Kazanskii, *Legendre transforms of the generating functionals in quantum field theory*. *Teor. Mat. Fiz.* **12**, 352 (1972), doi:10.1007/BF01035606.
- [VK73a] A. N. Vasil'ev, A. K. Kazanskii, *Equations of motion for a Legendre transform of arbitrary order*. *Teor. Mat. Fiz.* **14**, 289 (1973), doi:10.1007/BF01029302.
- [VK73b] A. N. Vasil'ev, A. K. Kazanskii, *Convexity properties of Legendre transformations (variational methods in quantum field theory)*. *Teor. Mat. Fiz.* **15**, 43 (1973), doi:10.1007/BF01028262.
- [Web05] F. Weber, *Strange quark matter and compact stars*. *Prog. Part. Nucl. Phys.* **54**, 193 (2005), doi:10.1016/j.pnpnp.2004.07.001, arXiv:astro-ph/0407155.
- [YHM95] K. Yagi, T. Hatsuda, Y. Miake, *Finite-Temperature Field Theory* (Cambridge University Press, 2005), ISBN 0521561086.

Acknowledgments

First I would like to thank Prof. Dr. R. Schmidt for accepting me as diploma student in the Institute for Theoretical Physics. Prof. B. Kämpfer is gratefully acknowledged for providing me with an interesting topic and his encouraging assistance in elaborating this thesis. I also would like to thank M. Bluhm for extensive and helpful discussions and my other colleagues D. Seipt, R. Thomas, H. Schade and T. Hilger for many fruitful discussions. The excellent working conditions which are due to the Institute of Theoretical Physics and the Research Center Dresden-Rossendorf are gratefully acknowledged.

I owe thanks to C. Richter, T. Kluge and S. Ruck who were constant companions during my studies. Without their continuous collaboration and support, I could not have succeeded. Most of all, I would like to thank my parents for supporting every step of my studies and Constanze for her love.

Declaration/Selbständigkeitserklärung

Hiermit versichere ich, dass die vorliegende Diplomarbeit von mir selbständig und ohne die unzulässige Hilfe Dritter angefertigt worden ist. Dabei wurden lediglich die von mir explizit angegebenen Hilfsmittel verwendet. Wissen, welches von mir direkt oder indirekt aus fremden Quellen übernommen wurde, ist als solches kenntlich gemacht und in das Literaturverzeichnis aufgenommen worden. Die Diplomarbeit wurde bisher weder im Inland noch im Ausland in gleicher oder ähnlicher Form bei einer anderen Prüfungsbehörde eingereicht.

I declare, that I have written this diploma thesis on my own without undue help of others. External work used directly or indirectly is explicitly referenced. This diploma thesis has not been submitted for any other qualification.

Dresden, den 29.6.2007

Robert Schulze